OPTICAL MILLIMETER-WAVE SIGNAL GENERATION, TRANSMISSION AND PROCESSING FOR SYMMETRIC SUPER-BROADBAND OPTICAL-WIRELESS ACCESS NETWORKS

A Thesis
Presented to
The Academic Faculty

by

Zhensheng Jia

In Partial Fulfillment
of the Requirements for the Degree
Doctor of Philosophy in the
School of Electrical and Computer Engineering

Georgia Institute of Technology
August 2008

OPTICAL MILLIMETER-WAVE SIGNAL GENERATION, TRANSMISSION AND PROCESSING FOR SYMMETRIC SUPER-BROADBAND OPTICAL-WIRELESS ACCESS NETWORKS

Approved by:

Dr. Gee-Kung Chang, advisor
School of Electrical and Computer Engineering
Georgia Institute of Technology

Dr. Jianjun Yu, co-advisor
School of Electrical and Computer Engineering
Georgia Institute of Technology

Dr. John A Buck
School of Electrical and Computer Engineering
Georgia Institute of Technology

Dr. Joy Laskar
School of Electrical and Computer Engineering
Georgia Institute of Technology

Dr. Ye (Gefforey) Li
School of Electrical and Computer Engineering
Georgia Institute of Technology

Dr. Umakishore Ramachandran
College of Computing
Georgia Institute of Technology

Date Approved: 25 June 2008

To my parents and my beloved wife

ACKNOWLEDGEMENTS

My PhD life was like undertaking a four-year challenging and exciting journey with so much memorable experience. I would like to express my heartfelt gratitude for all the people who accompanied me to reach this point.

First of all, I am heartily grateful to my advisor, Prof. Gee-Kung Chang, for his support, encouragement, guidance, and vision to my research work. I am so fortunate to have such a great advisor who not only taught me how to identify and solve research problems, but showed me how to be a pioneer researcher with excellent personality. I was deeply touched for his extraordinary thoughtfulness and kindness to me on my future career. I learned a tremendous amount about the way he conducts the research and the way he lives the real life. I will forever remember the belief he has passed on me. He is my role model.

Another person I am also deeply indebted to is Dr. Jianjun Yu. In addition to his fantabulous experimental skill, his endless energy, enthusiasm, patience, and idea creation to research always motivate and inspire me. Much experimental work would not have been done without his help in the in-depth suggestions and experimental preparation.

The next thanks go to my thesis committee members Dr. John Buck, Dr. Ye (Geoffrey) Li, Dr. Joy Laskar, and Dr. Umakishore Ramachandran for their valuable time, suggestions, and approval of my research work.

I am also grateful to all my colleagues from Optical Networking Research Group for their discussions and help. Thanks to Jerome Vasseur, David Boivin, Arshad Chowdhury, Yong-Kee Yeo, Chunpeng Xiao, Yin-Jung Chang, Oladeji Akanbi, Muhammad Haris, Ming-Fang Huang, Hung-Chang Chien, Claudio Estevez, Lingbing Kong, and Yu-Ting Hsueh. It has been a real privilege to work among such a talented group.

I would like to thank all my friends who helped me in many ways during my graduate life in Atlanta. Special thanks go to Bo Pan, Gang Huang, Tony, Rongqiang Hu, Ye Luo, Lihui Wang, Qiang Fu, and Yuan Li. We had so much fun in Georgia Tech!

Finally, I owe thanks to my family. My parents, Sixian Jia and Jinglan Wang, always have faith in me and helped me become the person I am today. My older sisters spent a huge amount of time taking care of our family during my study in America. Thanks to my lovely wife, Rui Feng, for her love, support, and inspiration. We have shared together through thick and thin!

TABLE OF CONTENTS

LIST OF TABLES

LIST OF FIGURES

LIST OF SYMBOLS AND ABBREVIATIONS

3G	third generation
3R	reamplification, reshaping, and retiming
ADSL	asymmetric digital subscriber loop
APD	avalanche photodiode
APON	asynchronous-transfer-mode passive optical network
ASE	amplified spontaneous emission
AWG	arrayed waveguide Grating
BER	bit error rate
BPON	broadband passive optical network
BS	base station
B-t-B	back-to-back
BW	bandwidth
CO	central office
CSR	carrier to sideband ratio
CW	continuous wave
dB	decibel
dBm	the measured power referenced to one milliwatt
DC	direct current
DCF	dispersion compensation fiber
DFB-LD	distributed feedback laser diode
DPSK	differential phase-shift keying
DSB	double sideband
EA	electrical amplifier
EAM	electro-absorption modulator
EDFA	erbium-doped fiber amplifiers

EPON	Ethernet passive optical network
f	center frequency
FBG	fiber Bragg Grating
FD	frequency doubler
FM	frequency multiplier
FTTH/P	fiber-to-the-home/premise
FWM	four-wave mixing
Gb/s	gigabit per second = 10^9 bits per second
GHz	gigahertz = 10^9 cycles per second
GPON	gigabit passive optical network
HDTV	high-definition television
HNL-DSF	highly nonlinear dispersion-shifted fiber
IM	intensity modulation
km	kilometer = 10^3 meters
LN-MZM	LiNbO3 Mach-Zehnder modulator
LO	local oscillator
LPF	low-pass filter
MZDI	Mach-Zehnder delay interferometer
NOLM	nonlinear optical loop mirror
OC	optical coupler
OCS	optical carrier suppression
O/E	opto-electrical
OF	optical filter
OFDM	orthogonal frequency division multiplexing
OL	optical interleaver
OLT	optical line terminal
ONU	optical network unit
OOK	ON-OFF Keying
PC	polarization controller

PIN	positive-intrinsic-negative
PM	phase modulation
PON	passive optical network
PRBS	pseudo-random bit sequence
PS	power splitter
QAM	quadrature-amplitude modulation
RF	radio frequency
ROADM	reconfigurable optical add/drop multiplexer
ROF	radio-over-fiber
SCM	subcarrier multiplexing
SDTV	standard-definition television
SMF	single mode fiber
SMF-28	single mode fiber (corning)
SOA	semiconductor optical amplifier
SSB	single sideband
TDM	time-division multiplexing
TL	tunable laser
TOF	tunable optical filter
VPI	virtual photonics Inc. (simulation software manufacturer)
VSB	vestigial sideband
ω	angle frequency
WDM	wavelength division multiplexing
WiFi	wireless fidelity
WiMAX	worldwide interoperability for microwave access
WLAN	wireless local area network
WSS	wavelength selective switch
XAM	cross-absorption modulation
XPM	cross-phase modulation

SUMMARY

Access bandwidth requirements for delivering high-speed data and video services are expected to grow to gigabits/second in future wired and wireless access networks. Today's wired networks, based on passive optical network (PON) access technologies, have the capability of providing huge bandwidth to end users using optical fiber, but are not flexible enough to allow convenient roaming connections. On the other hand, wireless-based access solutions offer portability and flexibility to users, but do not possess abundant bandwidth to meet the ultimate demand for multi-channel video services with high-definition (HD) quality. To exploit the benefits of both wired and wireless technologies, carriers and service provides are actively seeking a convergent network architecture to deliver multiple services to serve both fixed and mobile users. In this regard, optical-wireless access technologies have been considered the most promising solution to increase the capacity, coverage, bandwidth, and mobility in environments such as conference centers, airports, hotels, shopping malls - and ultimately to homes and small offices.

The objective of this research is to develop the enabling technologies for delivering future super-broadband (> 1 Gb/s) wireless services over optical fibers and air links in radio-over-fiber (ROF)-based optical-wireless access networks. The integration of optical and wireless means the convergence of two conventional technology field - radio frequency (RF) for wireless access and optical fiber for wired transmission. Long-range links are provided by optical fiber and the last tens of meters are accomplished by wireless. The requirement of more wireless bandwidth leads to spectral congestion at lower microwave frequencies in current wireless access networks. Millimeter-wave systems have the unique potential to resolve the scarcity of access bandwidth and the spectral congestion. Therefore, this thesis investigates the key technologies of novel ROF systems operating at the millimeter-wave band for the provision of future super-broadband services and applications.

Optical millimeter-wave signal generation and up-conversion with low-cost approaches

are vital to future real deployment in access networks. Several all-optical techniques for millimeter-wave signal up-conversion or mixing are proposed and experimentally demonstrated in this thesis. These include the methods based on four-wave mixing (FWM) or cross-phase modulation (XPM) effects in highly nonlinear dispersion-shifted fiber (HNL-DSF), the method based on cross-absorption modulation (XAM) in an electro-absorption modulator (EAM), and the method based on optical carrier suppression (OCS) or subcarrier multiplexing (SCM) modulation in the external intensity modulation. The generation using phase modulator and optical filtering is another developed scheme for millimeter-wave signal generation through frequency modulation (FM) to amplitude modulation (AM) conversion. The advantages and disadvantages of these up-conversion techniques are analyzed and compared based on experimental results. The experimental results suggest that the up-conversion method based on the external modulation (intensity and phase modulation) scheme shows practical advantages in terms of the low cost, simplicity of system configuration, and performance over long-distance transmission. These schemes of optical millimeter-wave signal generation and up-conversion pave the way for future-proof access networks using all-optical technologies.

The network architecture consisting of a single light source at the central office (CO) and the reuse of the downstream wavelength at the base station (BS) is an attractive solution for consolidated bidirectional connection as it requires no additional light source and wavelength management at the BS. Three different implementations are developed and experimentally demonstrated in this thesis. Among them, the system using one colorless semiconductor optical amplifier (SOA) as both the amplifier and the modulator for the upstream signal shows practical advantages in terms of low cost, reliability, and ease of maintenance. The performance of super-broadband wireless signals at 60-GHz band over a single span of fiber is also investigated for both direction transmissions. We also design and demonstrate three novel techniques for simultaneously delivering wired and wireless services over an optical fiber and an air link in a single transport platform. Our efficient techniques for generating dual- or multi-band signals do not require expensive high-frequency electrical components. Moreover, baseband and millimeter-wave signals can be easily separated and distributed at

the users' premises.

The transport feasibility in metro and wide-area access networks with multiple reconfigurable optical add-drop multiplexers (ROADMs) nodes is explored for 40-GHz and 60-GHz optical millimeter-wave signals. The use of wavelength selective switch (WSS)-based ROADM aims at dynamically allocating wireless capacity to meet instantaneous traffic load on demand. Additionally, the optical-wireless systems using the orthogonal frequency division multiplexing (OFDM) modulation format are analytically and experimentally demonstrated to mitigate the chromatic dispersion in optical fiber, and overcome multi-path delay spread and frequency-dependent channel distortion in the air links. Bandwidth record of radio signals on optical carriers is achieved in the thesis. These results represent a pioneering contribution to the optical-wireless field.

This thesis also successfully implements the testbed trial for the delivery of uncompressed 270-Mb/s standard-definition television (SDTV) and 1.485-Gb/s high-definition television (HDTV) video signals over optical fiber and air links. The demonstration represents the first ever reported real applications over hybrid wired and wireless access networks, showing that our developed up-conversion schemes and designed architectures are highly suitable for super-broadband applications in next-generation optical-wireless access networks.

CHAPTER I

INTRODUCTION

1.1 Background

The high-speed broadband penetration and ongoing growth of the Internet traffic among residential and business customers have been placing a huge bandwidth demand on the underlying telecommunications infrastructure. In March 2008, broadband penetration among active Internet users in US homes grew 0.43 percentage points to 88.82%, up from 88.39% in February [1]. According to the forecast [2] [3], as shown in Fig. 1.1, global IP traffic in 2007 stands at more than 6 exabytes per month, more than quadrupling to reach 29 exabytes per month in 2011. Meanwhile, traffic patterns have been propelled from voice- and text-based services to user-generated interactive video services [4]. As an inset in Fig. 1.1, Internet video streaming and downloads will grow from 9 percent of all consumer internet traffic in 2006 to 30 percent in 2010. Peer-to-peer (P2P)traffic is still the largest share of internet traffic today, but approximately 70 percent of P2P traffic is due to the exchange of video files. YouTube is just the beginning, real-time video communications and dynamic video content will ultimately test the network more than pre-recorded video content.

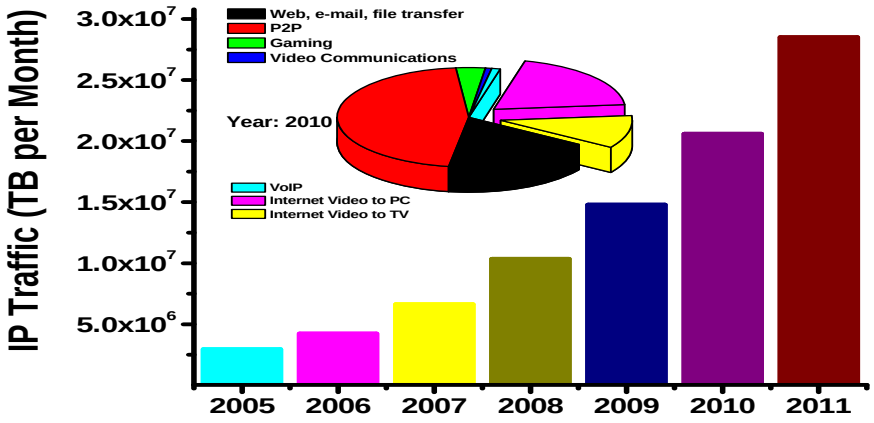

Figure 1.1: Global IP traffic growth and global consumer internet traffic by sub-segment at 2010. Source: Cisco Systems, Global IP Traffic Forecast and Methodology, 2005-2011.

In response to this remarkable development, the metro and core networks of the telecommunication infrastructure have experienced a tremendous growth in bandwidth and capacity with the wide deployment of fiber-optic technology in the past decade [5]. As shown in Fig. 1.2, data speeds in metro and long-haul systems are evolving from 10 Gbps to 40 Gbps transmission, 100 Gbps per wavelength channel system is taking shape as next step for core and metro networks [6].

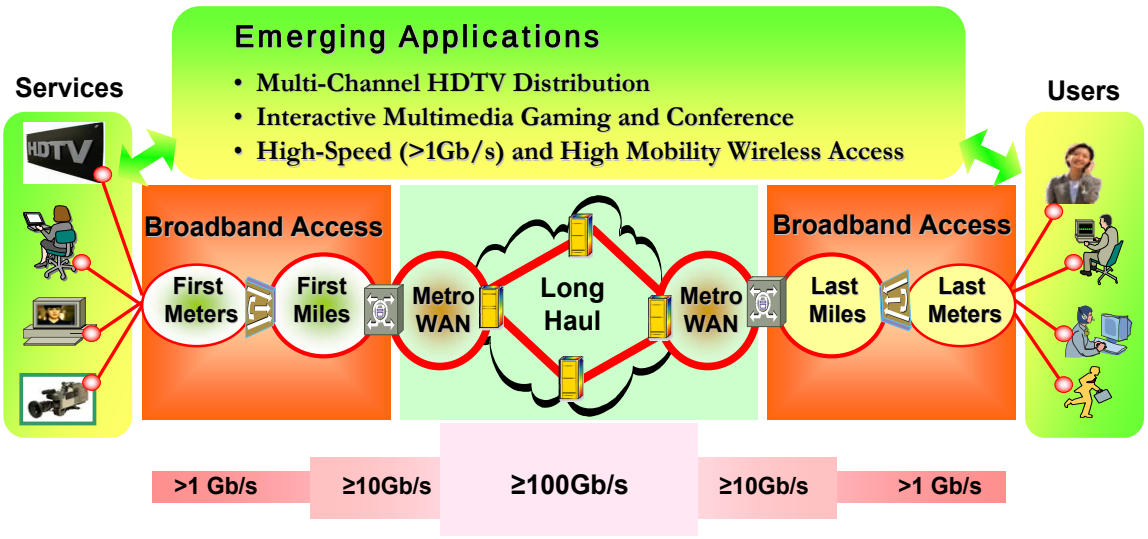

Figure 1.2: Emerging broadband applications and future network requirements.

Access bandwidth requirements for delivering multi-channel high-definition television (HDTV) signals and online gaming services are expected to grow to gigabits/second in the near future. However, the current subscriber access networks have not been scaled up commensurately. To avoid being the bottleneck in the last miles and last meters, and exploit the benefits of both wired and wireless technologies, carriers and service provides are actively seeking a convergent network architecture to deliver multiple services to serve both fixed and mobile users. In this regard, optical-wireless access technologies have been considered the most promising solution to increase the capacity, coverage, bandwidth, and mobility in environments such as conference centers, airports, hotels, shopping malls - and ultimately to homes and small offices.

This introductory chapter starts with a synopsis of the current trend in broadband wired and wireless access networks development in section 1.2 and 1.3. Then, section 1.4 discusses the convergence of optical and wireless technologies. Finally, the research objectives and the scope of this thesis are outlined in section 1.5.

1.2 Broadband wired access networks

It is well known that there are various technology options for broadband wired access providing high-speed Internet access and triple-play services including data, voice, and video. Most well-established broadband access solutions now are digital subscriber line (DSL) technologies deployed by telephone companies and the cable modem-based services from the Cable TV companies. These conventional access network infrastructures are having a hard time to keep up with traffic demands, especially for future video services with high-definition quality. At data rates of 100 Mb/s, the transmission distance is limited to about 100 m and requires the use of highly sophisticated transmission technologies [7]. To overcome this limitation, it is essential to use single-mode fiber (SMF) as the transmission media in future access networks. SMF provides essentially unlimited transmission bandwidth over extremely long distances. The end goal is to provide an optical fiber to each customer premise or home. This type of network is commonly referred to as Fiber to the Home/Premise (FTTH/P). Currently, the FTTH/P networks using passive optical network (PON) are highly recognized as the most promising candidates for next generation access systems because of low cost, simple maintenance and operation, and high-bandwidth provision [8].

1.2.1 Copper-based access networks

DSL technology is a modem technology that uses existing twisted-pair telephone lines to transport high-bandwidth data to service subscribers. Typically, DSL connections work by dividing the frequencies used in a single phone line into two primary transmission bands. The data is carried over the high-frequency band (25 kHz and above) whereas the voice is carried over the lower-frequency band (4 kHz and below). Multilevel-transmission methods, such as quadrature-amplitude modulation (QAM) and discrete multitone (DMT), have been

used to mitigate the bandwidth limitations of the twisted-pair copper lines. These relatively complex transmission technologies are generally described by the term x digital subscriber loop (xDSL). Although highly sophisticated technologies are used, the transmission distances are still quite limited. For distance under 1.5 km, asymmetric digital subscriber loop (ADSL) can deliver about 8 Mb/s while the latest very-high-speed digital subscriber loop (VDSL) technology can deliver up to 26 Mb/s for distances under 1 km [9]. A figure of merit for the bit-rate-times-distance product of twisted-pair copper cable is about 10 Mb/s ·km. This means that a 100-Mb/s signal can be transmitted only over a distance of about 100 m, which greatly limits its use in high-speed access networks.

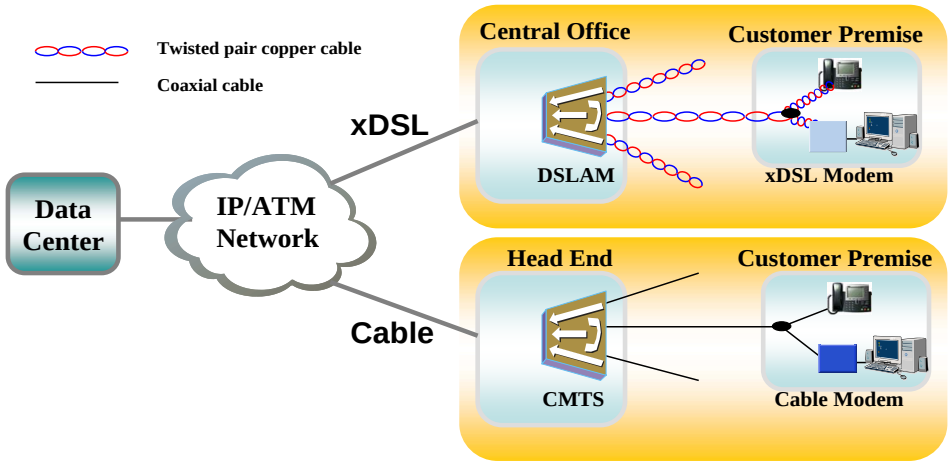

Figure 1.3: Copper-based broadband access systems: xDSL and Cable Modem.

The other most popularly deployed technology is coaxial copper cable access layered on top of the existing network infrastructure used for cable television similar to how xDSL uses the existing telephone network. Coax cable can deliver much larger bandwidths than twisted-pair wire since the electrical signal is guided between an inner conductor and a grounded outer shield conductor. Recently, 64/256-QAM modulation technologies have been introduced to send digital video and data through a coaxial cable. The home equipment that terminates the QAM signals is called a cable modem (CM), while the corresponding equipment located at the CO or head end is called the cable-modem termination system (CMTS). Figure 1.3 shows the generic architecture for xDSL and cable modem access

systems. Data-Over-Cable Service Interface Specifications (DOCSIS) defines the communications and operation support interface requirements for a data over the cable system. DOCSIS 3.0 is the newest version issued by CableLabs to offer downstream data rates of 160 Mbps or higher and upstream data rates of 120 Mbps or higher [10].

To extend the transmission distance limited by the required signal-to-noise ratio (SNR) in pure cable access system, SMF is used to realize the hybrid of fiber and coax (HFC) for feeding multiple analog and digital TV signals. In this network, a maximum downstream data rate of 2.8 Gb/s (450 –870 MHz) and upstream bandwidth of 150 Mb/s (5 –42 MHz) can be achieved. However, since multiple subscribers share the bandwidth within a cell, the guaranteed bandwidth per subscriber is only 2.8 –5.6 Mb/s for the downstream signal and 0.15 –0.3 Mb/s for the upstream signal. This is comparable with the bandwidth offered by xDSL over twisted-pair copper.

In summary, the major advantage of the above xDSL solution for twisted-pair wire and the HFC solution for coax cable is that they leverage the existing legacy infrastructure to deliver digital data. As bandwidth demands increase, trying to squeeze increasing data rates out of this bandwidth-limited legacy medium becomes increasingly expensive. Another main drawback of these two approaches is that they both require electrical-powered equipment in the field, except for customers close to the CO. This leads to high-operational costs associated with powering, maintaining, and managing this remotely located active equipment. It is quite clear that these existing solutions have limited lifetimes, and eventually, fiber connections will have to be provided to each home.

1.2.2 Optical fiber access networks

The unique properties of optical SMF, being its low loss and extremely wide inherent bandwidth, make it the ideal candidate to meet the capacity challenges for now and the foreseeable future. SMF has already been adopted in long-haul and metro transport networks, and it is increasingly penetrating the access domain as well.

There are two important types of systems that make FTTH broadband connections possible. The straightforward way, albeit perhaps the most expensive one, is with active

point-to-point Ethernet technologies. Active optical networks rely on some sort of electrically powered equipment to distribute the signal, such as a switch, router, or multiplexer. Such networks are identical to the ethernet computer networks used in businesses and academic institutions, except that their purpose is to connect homes and buildings to a central office (CO) rather than to connect computers and printers within a campus. The main drawbacks are high cost of installing and maintaining powered equipment cabinets.

A PON is an important alternative approach. The term PON means that there are no active elements between the CO and the customer premises [11]. A PON is a point-to-multipoint network architecture in which unpowered optical splitters are used to enable a single optical fiber to serve multiple premises, typically 32 –128. A PON configuration reduces the required amount of fiber and CO equipment compared with active architectures. Because of its point-to-multipoint architecture, multiplexing techniques are required in a PON to offer multiple access capability. These multiplexing schemes can be generally categorized as time-division multiple access (TDMA), wavelength-division multiple access (WDMA), subcarrier-division multiple access (SCMA), and code-division multiple access (CDMA). Among them, the TDM-PON and WDM-PON systems are expected to be most promising candidates for widespread use [12] [13]. Most of research work and standization effort towards next-generation optical access networks have focused on these two PON systems.

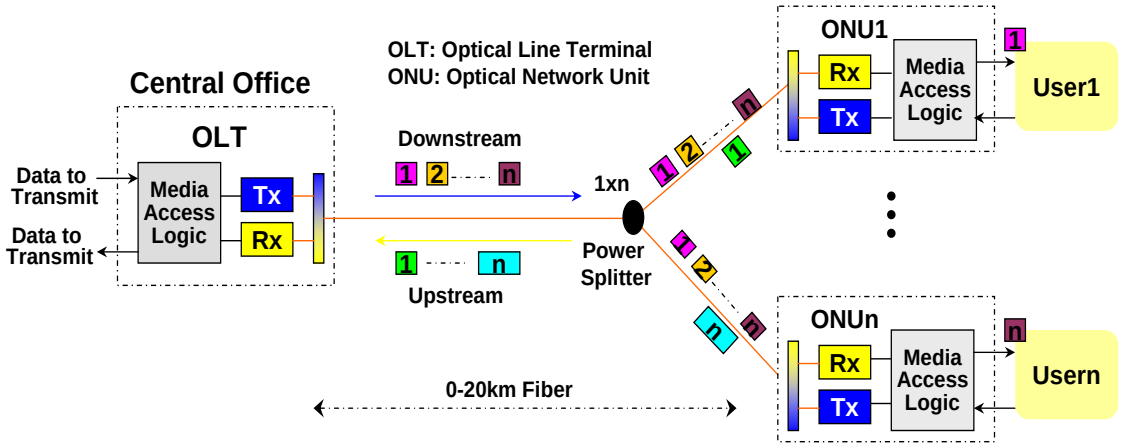

Figure 1.4: TDM-PON architecture.

TDM-PON is currently the most popular FTTP approach and is starting to see significant deployments in various regions of the world [14]. A typical TDM-PON system is shown in Fig. 1.4. Separate lightwaves at 1.55, 1.49, and 1.3 nm are used to carry the traffic for downstream video, downstream data, and upstream, respectively. A TDM-PON consists of an optical line termination (OLT) at the service provider's CO, optical feeder fiber, and a number of optical network units (ONUs) near end users. A passive optical splitter is used to split the downstream signals to multiple end users. The OLT broadcasts the downstream traffic to all ONUs in continuous mode, and each ONU selects the packets destined to it and discards the packets addressed to other ONUs. The OLT is also responsible for the allocation of time slots for the upstream connection of each ONU. Because of ONU's burst transmission nature, burst-mode receivers are required for upstream transmission [15].

To make a TDM-PON cost effective and practical for widespread deployment, standardization of the algorithms and protocols must be established. The two main standardization bodies that have developed TDM-PON standards are the full service access network (FSAN)/ITU-T group and the IEEE [16] [17] [18] [19]. Currently, there have been many standards established, and they are summarized in Table 1.1.

Table 1.1: TDM-PON comparison

Item	BPON	EPON	GPON
Standard	ITU G.983	IEEE 802.3ah	ITU G.984
Framing	ATM cell	Ethernet frame	GEM frame
Bit Rate	622Mb/s (down) 155Mb/s (up)	1.25Gb/s (up & down)	2.5Gb/s (down) 1.25Gb/s (up)
Users/PON	32	16	64

To enhance the speed and capacity for keeping up with the increased bandwidth demand, the research and development on next-generation PON focus on 10G-PON systems [20]. Several technical difficulties are faced to upgrade current PON systems to 10G such as higher receiver sensitivity, higher power split number, extended transmission distance, and burst-mode receiver with wide dynamic range to handle the asynchronous bursts with varying optical power levers. It is expected that 10G-PON systems will reach final market readiness by the year 2009 [21].

However, 10G-PON system is not the end game of PON access systems. As mentioned in the previous section, WDM-PON systems are the other important solutions for guaranteeing high bandwidth and quality of service (QoS) to each subscriber [22]. WDM-PON systems can eliminate the complicated time-sharing issues in TDM-PON systems by providing virtual point-to-point optical connectivity to multiple end users through a dedicated pair of wavelengths. In addition to the advantages of high scalability and flexibility, longer transmission distance can be achieved because of the efficient use of optical power at the remote node. The architecture of a WDM-PON system is shown in Fig. 1.5. The big difference in the outside-fiber plant is replacing the optical-power splitter in a TDM-PON with an array waveguide Grating (AWG) to demultiplex the downstream wavelengths and multiplex the upstream wavelengths.

Cost is the final factor to limit the commercial deployment of WDM-PON systems. To reduce the cost, many research have been conducted on colorless ONUs based on centralized light sources using amplified spontaneous emission (ASE)-injected Fabry-Perot laser diodes (FPLDs), ASE-seeded reflective semiconductor optical amplifiers (RSOAs), and spectrum-sliced RSOAs [23] [24]. Other efforts have been carried out on the reduction of Rayleigh noise for longer transmission distance, protection and restoration scheme, architecture design, and wavelength management. Trials of the technology are already underway in Korea, but costs have not yet been reduced to the point where mass deployments would be feasible.

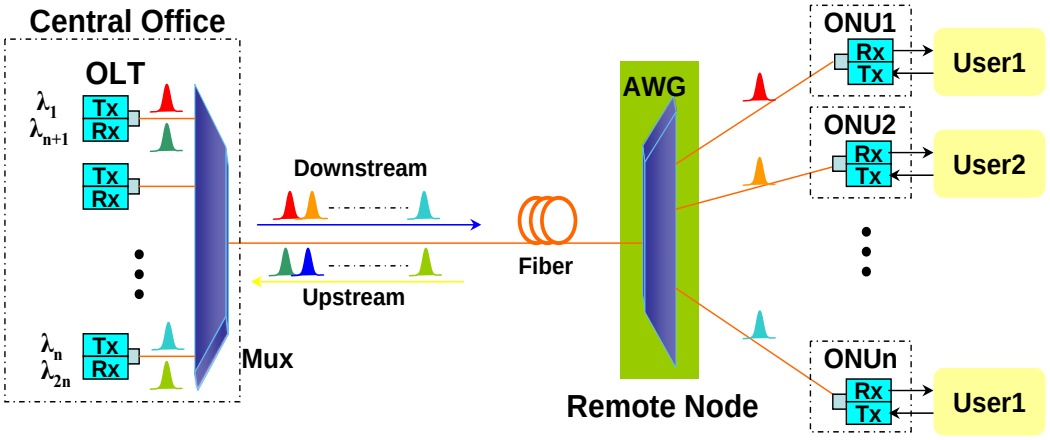

Figure 1.5: WDM-PON architecture.

The author believes that a TDM-PON appears to be a satisfactory solution for current bandwidth demands. With the cost drop of optical components for WDM systems, a WDM-PON will become the preferred solution for a future-proof fiber-based access network.

1.3 Broadband wireless access networks

In recent years, wireless networks are becoming more pervasive. This tremendous growth is mainly accelerated by advanced wireless communication technologies, inexpensive wireless equipment, and broader access availability. These networks are transforming the way people use computers and other personal electronic devices at work, home, and when traveling. There are many wireless communication technologies that can be differentiated by frequency, bandwidth, range, and applications (Fig. 1.6). These categories range from wireless wide area networks (WWANs), which cover the widest geographic area, to wireless personal area networks (WPANs), which cover less than 10 meters [25]. End-users and service providers are deploying diverse types of wireless networks to complement and substitute for wired infrastructure. All of these wireless technologies are changing the landscape for broadband access.

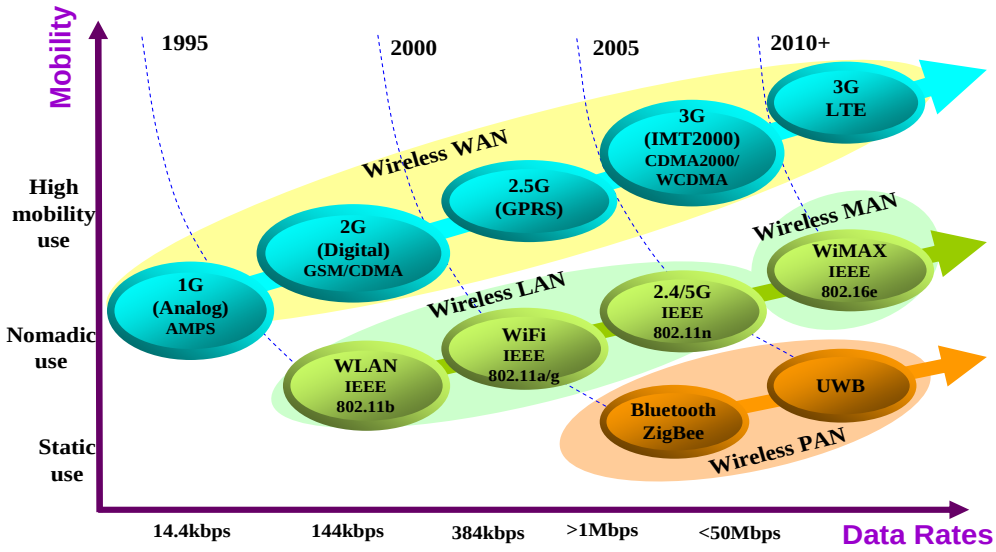

Figure 1.6: Current wireless access technologies.

1.3.1 Wireless networks from personal areas to wide areas

A WPAN defines wireless networks that have a maximal signal range of 10 meters, and these networks are used for the connection of consumer electronic devices with each other such as personal digital assistants (PDAs) or mobile phones. The ad-hoc mode connection is an advantage of these networks. Bluetooth, standardized in IEEE 802.15.1 [26], enables the wireless connection of mobile devices, computer peripherals, and electronic appliances with data rates up to 3 Mb/s. The other typical representatives are High Data Rate WPAN - Ultra Wide Band (UWB) in accordance with the IEEE 802.15.3a standard [27], and Low Data Rate WPAN - ZigBee in accordance with the IEEE 802.15.4 standard [28]. Using a wide range of frequency band without interfering with the original technologies and low-power consumption are the basic principles of the UWB technology. In the USA, this system was permitted in 2004 in the frequency band of 3.1 GHz - 10.6 GHz with the -42.3 dbm/MHz power signal and up to 0.5-Gb/s data rate. The UWB has found application in fast home networks for video or audio data transport, for digital camcorders, high-resolution printers, and so on. The ZigBee technology is designed low data rate (up to 250 kb/s) wireless sensor networks that has great possibilities in applications from home and building automation to industrial control.

Wireless local area network (WLAN) standard series (IEEE 802.11) are gained much popularity for their convenience, cost efficiency, and ease of integration with other networks in one room or maximally one building [29]. The signal range of WLAN is approximately 30 meters indoors and 100 meters outdoors. Although the terms of 802.11 and Wi-Fi are often used interchangeably, the Wi-Fi Alliance uses the term "Wi-Fi" to define a slightly different set of overlapping standards [30]. The majority of computers sold to consumers today come pre-equipped with all necessary WLAN technology. Operating in the RF spectrum of 2.4-GHz and 5-GHz bands and providing data rates up to 54 Mb/s, IEEE 802.11 a/b/g cover the specification of physical and data link layers in ad-hoc mode or access point for current wide use. IEEE 802.11n standard has the raw data rate of 248 Mb/s resulting from the Multiple Input Multiple Output (MIMO) function. In the present, the 802.11n is still not fully approved, it is expected in March 2009.

Wireless metro area network (WMAN) is the official name trademarked by the IEEE 802.16 Working Group on Broadband Wireless Access (BWA) [31] Standards for wireless metro area internet access [32]. The Worldwide Interoprability for Microwave Access (WiMAX, the expression from Industry Forum) works in the 10-66 GHz band with a line of sight (LOS) condition at 802.16 or in the band of 2 - 11 GHz with a non line of sight (NLOS) at 802.16d. In addition to support high data rates (75 Mb/s for fixed access and 30 Mb/s at speeds of 60 km/h) and high bandwidth efficiency (3 bps/Hz), WiMAX aims to support enhanced QoS, mobility and nomadic connectivity, and wide coverage up to 30 miles transmission for hot spots or rural areas. Equipment vendors, including Alvarion Ltd., Proxim Corp., Redline Communications Inc., and ZiMax Technologies Inc., all have announced agreements to use Intel silicon in products based on the IEEE 802.16-2004 standard. The next major step for WiMAX will be product certification and interoperability testing by the WiMax Forum [33], the industry body moving to commercialize 802.16 technology.

WWANs are digital cellular networks used for mobile phone and data service and operated by carriers. WWANs provide connectivity over a wide geographical area through handover mobility support and cell roaming. Two WWAN technologies - Global System for Mobile Communications (GSM) and Code Division Multiple Access (CDMA) - dominate WWAN deployments worldwide. These two technologies are expected to evolve to third generation (3G) mobile networks for providing increased bandwidth, enhanced packet-based QoS, improved spectrum efficiency and mobility. Europe standardized early on GSM [34]. Today, GSM and its associated wireless data capability, General Packet Radio Service (GPRS) and next-generation Enhanced Data GSM Evolution (EDGE), have about two-thirds of the worldwide market. CDMA technology dominates in the U.S. The CDMA2000 WWAN technology has seen strong deployments in North America, Japan, Korea, and China. The next-generation CDMA, 1xEvolution-Data Optimized (1xEV-DO), is currently deployed to support higher data rates and Voice over Internet Protocol (VoIP) calls.

Table 1.2 describes the main properties of individual technologies. A wide diversity of various networks will coexist in the future, and the only predictable trend is the continuing increase of the access data rate for all the technologies. Therefore, spectrum sensing, sharing,

and management enabled by cognitive radio are gaining much interest to communicate efficiently while avoiding interference in the ubiquitous wireless connectivity.

Table 1.2: Summary of broadband wireless networks

Name	Origin	Frequency band	Bit rate	Signal range
Bluetooth	2004	2.4 GHz	2.1 Mb/s	10 m
UWB	2007	3.1-10.6 GHz	500 Mb/s	10 m
ZigBee	2004	2.4 GHz	250 kb/s	10 m
802.11a	1999	5 GHz	54 Mb/s	100(outdoor)/30 m
802.11b	1999	2.4 GHz	11 Mb/s	110(outdoor)/35 m
802.11g	2003	2.4 GHz	54 Mb/s	110(outdoor)/35 m
802.11n	2006	2.4/5 GHz	150 Mb/s	160(outdoor)/70 m
802.16	2001	10-66 GHz	134 Mb/s	5 km
802.16a	2003	2-11 GHz	75 Mb/s	10 km
802.16d	2004	2-11 GHz	75 Mb/s	8 km
802.16e	2005	2-6 GHz	30 Mb/s	5 km
GSM	1992	900/1800 MHz	9.6 kb/s	35 km
GPRS	1997	900/1800 MHz	80 kb/s	35 km
EDGE	2004	900/1800 MHz	200/100 kb/s	30 km
UMTS	2000	873/1900 MHz	2048 kb/s	2 km
HSDPA	2004	900/1800 MHz	14.4 Mb/s	6 km

1.3.2 Millimeter-wave communications

Currently, there is a growing need in wireless applications for ultra-high data rate transfer, at speeds of 1 Gbps and up. Examples of high data transfer uses are transmission of uncompressed high-definition video content, PC to PC and server to server communications and backup, high-speed communication between space or airborne platforms, and temporary restoration of fiber-like communications infrastructure in a disaster recovery scenario. This requirement of more bandwidth allocation places heavy burden on the current operating radio spectrum (RF) and causes spectral congestion at lower microwave frequencies. Millimeter-wave communication system offers a unique way to resolve these problems [35]. Beside the huge and unexploited bandwidth availability and the perspective of multi-gigabit to terabit networks [36], the potential of the millimeter-wave spectrum has many others attributes: enabling densely packed communication link networks from very short range to

medium range, integrating high efficiency radiating elements at the millimeter scale, and leading to compact, adaptive and portable integrated systems [37].

In a very broad term, millimeter-wave can be classified as electromagnetic spectrum that spans between 30 GHz to 300 GHz, which corresponds to wavelengths from 10 mm to 1 mm. In 2001, the Federal Communications Commission (FCC) allocated 7 GHz in the 57 - 64 GHz band for unlicensed use [38]. The opening of that free spectrum, combined with the advances of low-cost fabrication technology and low-loss packaging material, has rekindled interest in this portion of wireless spectrum. Figure 1.7 illustrates the projected power consumption at pW/bit/m level. 60-GHz systems show excellent advantages for the future super-broadband data services delivery in terms of data rate and power consumption [39]. WirelessHD^{TM} [41] is an industry-led effort to define a specification for the next-generation wireless digital network interface specification for wireless high-definition signal transmission for consumer electronics products using 60-GHz band. The goal of the range for the first products will be in-room, point-to-point, NLOS at up to 10 meters.

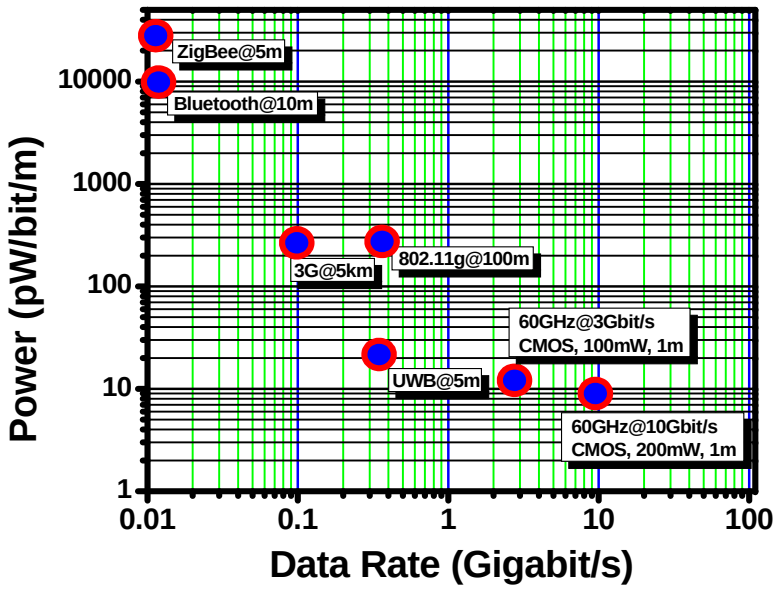

Figure 1.7: 60-GHz potentials for super-broadband communication.

Compared to lower bands, the radio signals in millimeter-wave band are extremely prone to atmospheric attenuation, making them of very little use over long distances [42].

In particular, signals in the 60-GHz region are subject to a resonance of the oxygen molecule and are severely attenuated (10-16 dB/km). In addition, the free space path loss increases quadratically with signal frequency, meaning that the free space attenuation on 60-GHz band is 21 dB higher than on 5 GHz. High propagation attenuation (Fig. 1.7) at 60-GHz band actually classifies a set of short-range applications, but it also means dense frequency reuse patterns [39]. Higher frequencies also lead to smaller sizes of RF components including antennas [40].

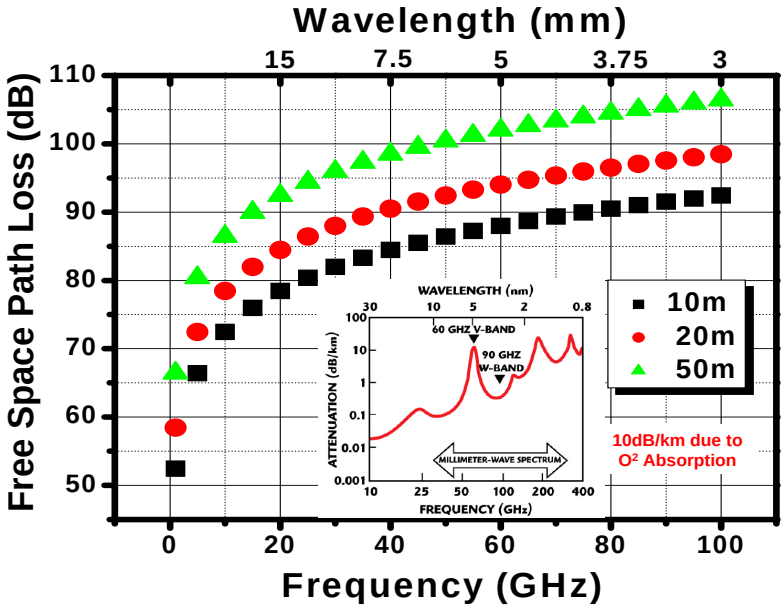

Figure 1.8: 60-GHz free-path loss and attenuation in the air.

There are two major problems with using 60-GHz band, however: the high directionality of the transmissions and the high cost of transceiver circuits, which make them difficult to use. The WirelessHD specification defines a novel wireless protocol that enables directional connections that adapt very rapidly to changes in the environment. This is accomplished by dynamically steering the antenna beam at the transmitter while at the same time focusing the receiver antenna in the direction of the incoming power from the transmitter. This dynamic beam forming and beam steering utilize not only the direct path, but allow the use of reflections and other indirect paths when the LOS connection is lost.

The cost concern is mainly related to the transceiver RF front-ends. Traditionally, the

expensive III-V semiconductors such as gallium arsenide (GaAs) are required for millimeter-wave radios. However, it is hard for GaAS to further lower cost. According to the reports about recent progress in developing the 60-GHz front-end chip sets, IBM engineers have demonstrated the first experimental 60-GHz transmitter and receiver chips using a high-speed alloy of silicon and germanium (SiGe). Meanwhile, researchers from Georgia Tech, UC Berkeley, and other universities or institutes are using a widely available and inexpensive complementary metal oxide semiconductor (CMOS) technology to build 60-GHz transceiver components. Another key driver in chipping the CMOS RF transceiver is SiBEAM Inc. of the US, a leader in the WirelessHD effort. Each of the two technologies has advantages and disadvantages. It is no doubt that the SiGe versus CMOS debate will continue.

1.4 Optical-wireless convergence

Today's wired networks, based on PON access technologies as discussed in Section 1.2, have the capability of providing huge bandwidth to end users using optical fiber, but they are not flexible enough to allow convenient roaming connections. On the other hand, wireless-based access solutions (in Section 1.3) offer portability and flexibility to users, but they do not possess abundant bandwidth at lower microwave frequencies or have the difficulties to transmit longer distance at the millimeter-wave frequencies because of high attenuation in the air. To make full use of the huge bandwidth offered by optical fiber and flexibility features presented via the wireless, radio-over-fiber (ROF)-based optical-wireless networks have been considered the most promising solution to increase the capacity, coverage, bandwidth, and mobility in environments such as conference centers, airports, hotels, shopping malls - and ultimately to homes and small offices [43] [44]. The expected evolution path of broadband access networks is shown in Fig. 1.9. The uses of photonic technologies in optical-wireless networks can significantly reduce the requirement of high-frequency electrical components for millimeter-wave signal processing. Meanwhile, relying on the efficient architecture design, simultaneous delivery of wired and wireless services can be achieved in a single platform to serve both fixed and mobile users.

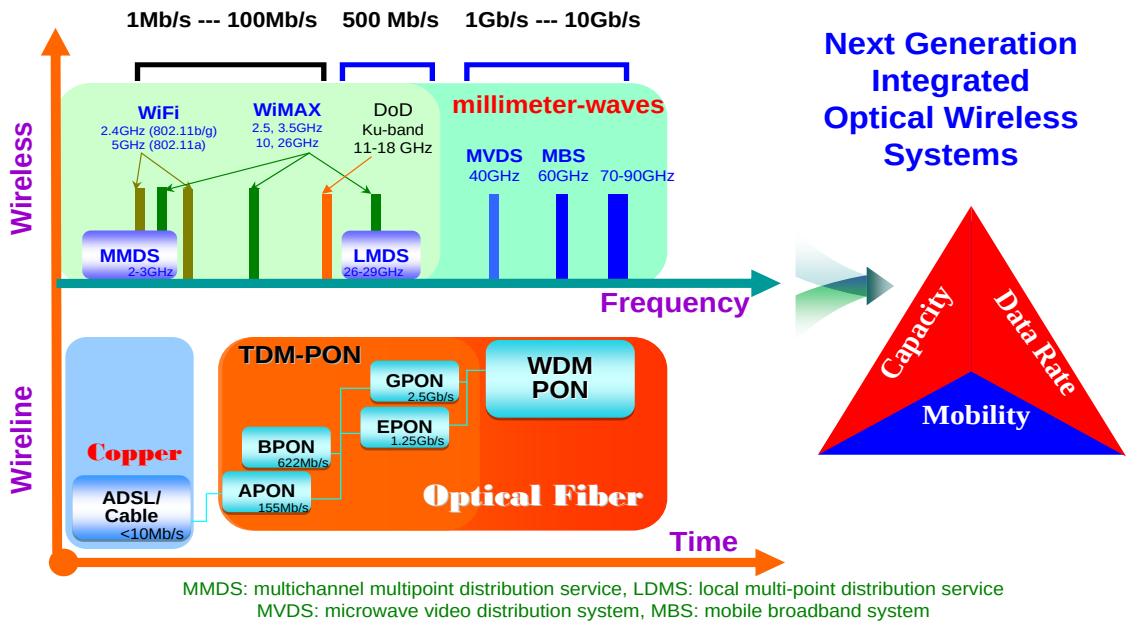

Figure 1.9: Convergence of broadband wireless and optical fiber access networks.

1.4.1 Radio-over-fiber systems

The concept of ROF refers to the merging use of two conventional technology worlds - radio frequency (RF) for wireless and optical fiber for wired transmission. Long-range metro or wide-area access links are provided by optical fiber and links to end users are accomplished by RF wireless [45]. As shown in Fig. 1.10, a typical ROF system consists of a CO, optical fiber network, remote passive node, and a large number of base stations (BSs). ROF systems perform all swithcing, multiplexing, signal generation and processing at the CO. An optical fiber network is used to transparently deliver the radio signals to multiple remote nodes (RN) and then to antenna BSs and end users. [46] The typical distances between the CO and the BSs are 10-25 km, where each of the BS serves a picocell covering the distances of tens of meters. The prime benefit of ROF systems is the super-broadband services provision with high flexibility. The capacity of millimter-wave fiber systems can be significantly increased by the integration with WDM-PON systems [47]. Each wavelength can carry one millimeter-wave channel, and it is optically routed at the RN. The use of optical fiber to distribute RF signals to the BSs also offer better coverage and higher transmission performance because of low loss and immunity to electromagnetic

interference of fiber.

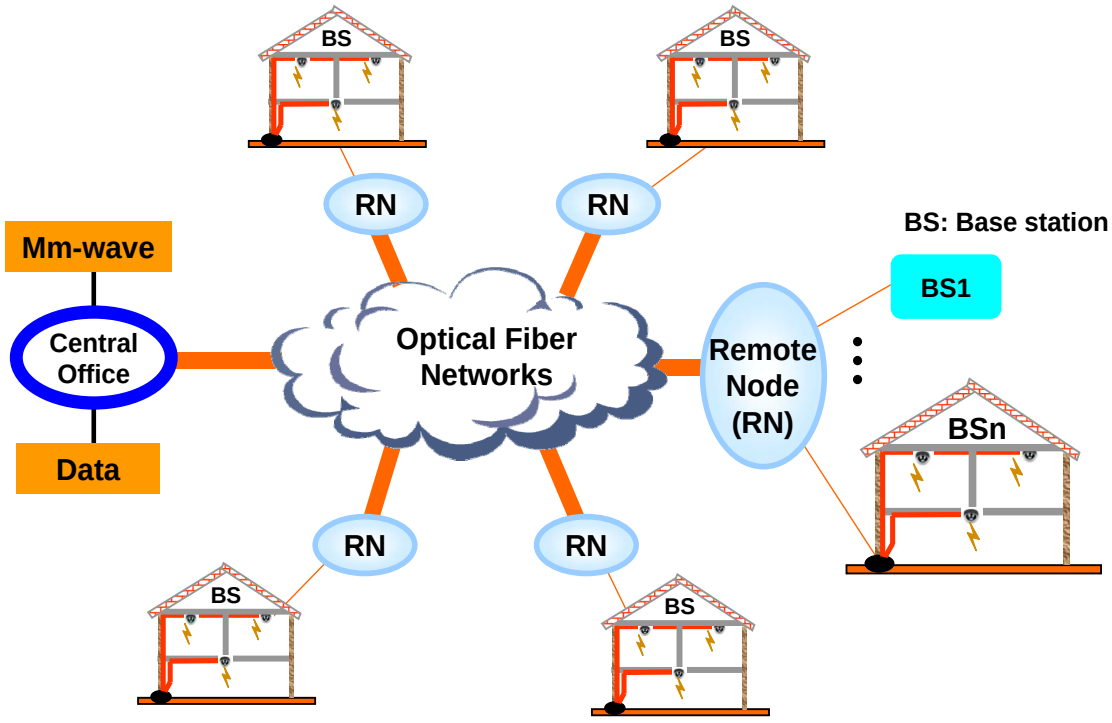

Figure 1.10: A schematic of a radio-over-fiber system.

1.4.2 Enabling technologies for millimeter-wave optical-wireless networks

In millimeter-wave fiber systems, numerous antenna BSs are needed because of high attenuation of millimeter-wave signals in the air. To make it economically viable, the BS architecture has to be simplified, consolidated, and cost effective. Therefore, it is critical for ROF systems to shift the complexity away from the RN and BS toward the CO, where the number of expensive millimeter-wave signal processing elements can be reduced greatly by sharing among multiple end users. Consolidating most of the expensive components at the CO also enables simple architecture, easier installation, and low-cost operation and maintenance [48]. Processing centralization at the CO also provides a number of system performance advantages like the feasibility of implementing efficient multiple input multiple output (MIMO) techniques and smart antennas array, centralized control of media access

layer, and radio sources management. The BS only needs to perform optoelectronic conversion, amplification and broadcast functions. In this context, Microwave Photonics [49] technologies are used to optically process millimeter-wave signals based on opto-electronic devices and all kinds of nonlinear effects [50].

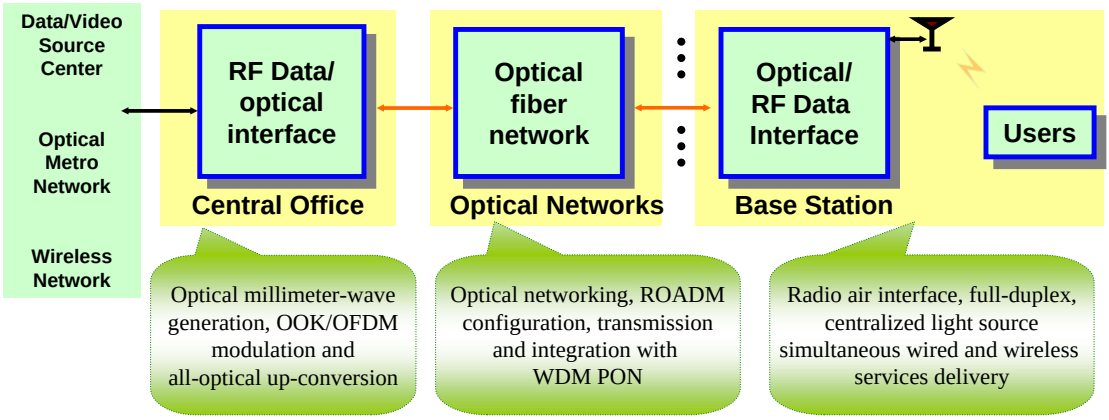

Figure 1.11: Key enabling technologies of optical-wireless networks.

Figure 1.11 depicts the block architecture of the optical-wireless system and the enabling technologies identified in this thesis for symmetric super-broadband optical-wireless networks. At the CO, optical millimeter-wave signals are generated and mixed with baseband digital signals using cost-efficient all-optical approaches. All-optical methods have the advantages on the use of low-frequency electronic devices and seamless integration with the deployed optical transmission systems. Optical networking technologies are leveraged to reach the longer transmission distance over SMF and realize flexible wavelength configuration. The major limitation is the RF signals fading effect induced by chromatic dispersion in optical fiber. The optical feeder networks act as an analogue transmission system that should deliver the radio signals with the best fidelity to the remote BSs. In this respect, futher efforts need to be given to overcome this dispersion effect.

Additionally, a low-cost and simple architecture is required for the BS design because of the need for numerous BSs as a result of shirinkage of a BS cell size. The full-duplex operation with centralized light sources in the CO is an attractive solution for overall architecture planning and implementation. Another goal for the architecture design is to

achieve simultaneous delivery of wired and multi-band wireless services to serve both fixed and mobile users in a unified platform. Besides the conventional intensity modulation, different modulation formats can be employed in the air interface to overcome the multi-path spreading interfence. These are all vital technologies for successful deployment in the real networks.

1.5 Objectives and organization of the thesis

The objective of this research is to develop the enabling technologies for delivering future super-broadband (> 1 Gb/s) wireless services over optical fibers and air links in ROF-based optical-wireless access networks. The thesis develops novel techniques for the optical millimeter-wave signal generation, up-conversion, and transmission using all-optical methods, which enable the developed systems compatible with current TDM/WDM-PON networks. Two significant parts of the thesis are devoted in designing the architecture for bidirectional connection with a centralized light source in the CO and simultaneous delivery of wired and wireless services in a single platform. The thesis also explores the transport feasiblity of WDM-ROF signals over multiple reconfigurable optical add-drop multiplexers (ROADMs) for flexible metro and wide-area access networks. The optical-wireless systems using the orthogonal frequency division multiplexing (OFDM) modulation format are investigated for the air interface. The developed techniques and overall systems are also verified by the super-broadband video applications.

The rest of this thesis is organized as follows. Chapter 2 focuses on optical millimeter-wave signals generation and up-conversion. Several all-optical schemes for millimeter-wave up-conversion or mixing have been proposed and experimentally demonstrated. These include the methods based on four-wave-mixing (FWM) and cross-phase modulation (XPM) in highly nonlinear dispersion-shifted fiber (HNL-DSF), the method based on cross-absorption modulation (XAM) in an electro-absorption modulator (EAM), the method based on optical carrier suppression (OCS) modulation in an external intensity modulator, and phase modulator plus optical filtering. The advantages and disadvantages of these generation and up-conversion technologies are compared based on extensive experimental results.

In Chapter 3, three schemes are reported for realizing full-duplex connection based on wavelength reuse to avoid the need for the light source at the BS. These include the system using up-converted differential phase-shift keyed (DPSK) signal for downstream and remodulated ON-OFF keying (OOK) signal for upstream, the system based on the OCS for downstream and reuse for upstream, and the system using phase modulator with subsequent filter for downstream and directly modulated semiconductor optical amplifier (SOA) for upstream. We also design and experimentally show the first demonstration of a 60-GHz ROF system simultaneously transmitting 2.5-Gb/s data for both directions over a single span of fiber.

In Chapter 4, three schemes are presented for simultaneously delivering both wired and wireless services. The first one uses cascaded optical modulations for separated baseband modulation and millimeter-wave up-conversion. The second scheme employs a single dual-arm intensity modulator for independent wired and wireless modulation. The third one is more advanced technology that utilizes vestigial sideband (VSB) filtering and alternate sub-carrier modulations to generate three frequency bands with increased dispersion tolerance.

Chapter 5 shows the transport feasibility of 40-GHz and 60-GHz optical millimeter-wave signals in metro and wide-area access networks with multiple ROADMs nodes. The record cascadability of straight-line ROADMs and transmission distance are successfully demonstrated in this chapter.

Chapter 6 investigates orthogonal frequency division multiplexing (OFDM) modulation adopted in the optical-wireless network. Because of high tolerance of chromatic dispersion and multi-path spreading effects, longer transmission distance and record-bandwidth signals are verified in the experiments.

Based on the develped technologies, Chapter 7 shows the integrated testbed for real applications. The uncompressed 270-Mb/s standard-definition television (SDTV) and 1.485-Gb/s high-definition television (HDTV) video signals are demonstrated over optical fiber and air links. The demonstration represents the first ever reported real applications over hybrid wired and wireless access networks.

Chapter 8 concludes the dissertation and envisiages future research directions.

CHAPTER II

OPTICAL MILLIMETER-WAVE SIGNALS GENERATION

This chapter is organized as follows. Section 2.1 presents the motivation and introduction of millimeter-wave signal generation and up-conversion using photonic technologies in optical-wireless access networks. Then, six developed technologies, classified into four categories, are presented in the following sections. In section 2.2, the generation methods based on optical nonlinear effect in the highly nonlinear dispersion-shifted fiber (HNL-DSF) and electro-absorption modulator (EAM) are investigated. The generation methods based on external intensity or phase modulation are carried out in sections 2.3 and 2.4, respectively. Then, the scheme using subcarrier multiplexing (SCM) and optical filtering is introduced in section 2.5. Finally, the pros and cons of all generation methods and the main conclusions of the chapter are given in section 2.6.

2.1 Introduction

An intermediate frequency (IF) or baseband signal can be transmitted over optical fiber to the base station (BS), where the baseband or IF signal are up-converted to millimeter-wave carriers for broadcasting in the air. In this way, the signal transmission over optical fiber is less severely affected by chromatic dispersion. However, this approach requires frequency up-conversion at the BS with a millimeter-wave mixer and a local oscillator (LO) signal [51] [52]. Generating millimeter-wave frequencies using electrical devices is challenging because of the bottleneck of high-speed electronic processing. Additionally, because of the requirement of numerous BSs in optical millimeter-wave access networks, this approach significantly increases the cost and complexity of the BS. The most promising solution is to use optical approaches for millimeter-wave signal generation at the central office (CO). Over the past few years, many groups have conducted research to develop optical millimeter-wave generation, up-conversion, and transmission techniques. Traditionally, four different methods have developed for the generation of millimeter-wave signals over optical

links with intensity modulation: direct intensity modulation, external modulation, optical heterodyning, and harmonics generation.

The most straightforward approach for optical transport of radio spectrum (RF) signals is to directly modulate the intensity of lasers with the RF signal itself and then to use direct detection at the phototdetector to recover the RF signal [53] [54]. Although this approach does not have the limitations of the linearity and carrier response of laser source for its application to current cellular and wireless local area systems (< 5 GHz), when moving to higher millimeter-wave bands, its major hurdles are the limited modulation bandwidth and transmission distance [55].

External intensity modulation is another simple way to direct transport of radio signals over optical fiber at the RF transmission carrier [56]. However, the generated double sideband (DSB) signals can not be transmitted longer distance because of the chromatic dispersion in the fiber [57]. To overcome the dispersion effect, optical single sideband (SSB) modulation has been reported, and it can be achieved using a single dual-arm Mach-Zehnder modulator (MZM), a hybrid intensity and phase modulation scheme or two electro-absorption modulators [58] [59] [60]. Nevertheless, the costly high-frequency optoelectronic devices (modulators and drivers with the RF bandwidth) are required, and the receiver sensitivity is low resulting from the high direct current (DC) components at center wavelength.

Optical heterodyning technology refers to the process where two optical lightwaves of different wavelengths beat each other at a photodetector to generate a millimeter-wave signal. This approach has the capability of generating the Teraherz signal, and it is only limited by the response of the photodetector. Since all the optical power contributes to the generated RF carrier, optical heterodyne can offer high RF power and high carrier-to-noise ratio. This technology can be achieved by two lasers that emit the light at wavelengths separated by the required millimeter-wave frequency. However, the performance is limited by the phase noise and frequency stability of the lasers. To obtain a high-quality carrier, phase control mechanisms, such as optical injection locking (OIL) [61] and optical phase-locked loops (OPLL) [62], are reported. OIL generates low phase noise signals, but the locking range is small because of instabilities occurring in the locking process above critical levels

of injection. OPLL exhibits a wider locking range but requires short loop propagation delay or lasers with narrow linewidth. Optical injection phase-locked loop (OIPLL) techniques combine the benefits of OIL and OPLL, allowing locking of wide linewidth lasers with wide locking range, even with considerable loop propagation delay [63]. However, OIPLL greatly adds the cost and complexity of the generation system.

The techniques based on harmonics generation by frequency-modulation to intensity-modulation (FM-IM) conversion have the advantage of generating high millimeter-wave signals with the use of a single laser source and low-frequency electrical devices [64]. These techniques utilize an optical phase modulator to produce an optical FM signal, which has frequency components at every multiple of the modulating RF carrier that drives the phase modulator. An FM-IM conversion is applied with an periodic optical bandpass filter prior to photodetection to extract the multiple-order harmonics of the modulating frequency. A delay interferometer or a Fabry-Perot etalon have been reported for the use of periodic optical filter [65]. In this case, the free spectral range of the periodic bandpass filter and its alignment with the optical carrier add two more degrees of flexibility to optimize the strength of the generated harmonics. However, they can not offer high detected power for one certain millimeter-wave carrier because the optical power is distributed to multiple RF carriers.

Recently, several approaches for all-optical up-conversion of radio signals using a semiconductor optical amplifier (SOA) have been reported. These techniques, based on the nonlinear effects in waveguide devices, exhibit low conversion efficiency and need very high input optical power [66]. The scheme based on cross-gain modulation (XGM) in an SOA [67] requires large input power to saturate the gain of the SOA. The scheme using cross-phase modulation (XPM) in an SOA Mach-Zehnder Interferometer (SOA-MZI) [68] loosens the requirement for the input power, however, nonlinear crosstalk among multiple channels and the complicated conversion structures are major hurdles that greatly limit the application in wavelength division multiplexed (WDM) systems for real optical-wireless networks.

2.2 Based on nonlinear effect

2.2.1 FWM in HNL-DSF

Four-wave mixing (FWM) is one of the important nonlinear effects to generate new waves or parametric amplification, especially for an effectively ultra-fast response using HNL-DSF [69]. Relying on the third-order electric susceptibility and beating process with the frequency phase-matching condition when the light of three or more different wavelengths is launched into HNL-DSF, it is possible to realize terahertz all-optical mixing or up-conversion, as shown in Fig. 2.1.

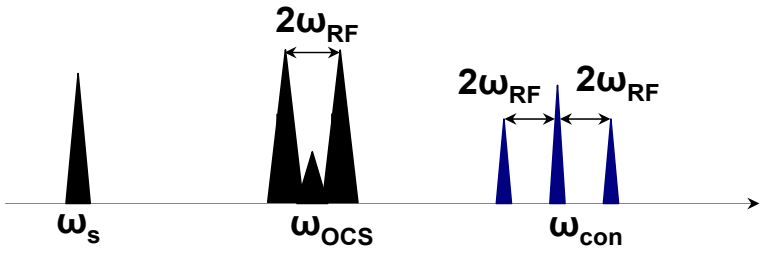

Figure 2.1: Schematic of FWM-based all-optical up-conversion.

Two pumping waves, $\omega_{OCS} - \omega_{RF}$ and $\omega_{OCS} + \omega_{RF}$, are generated by using optical carrier suppression (OCS) technologies, where ω_{RF} is the RF sinusoidal clock frequency. The converted signal ω_{con} may then be determined by

$$\omega_{con} = (\omega_{OCS} - \omega_{RF}) + (\omega_{OCS} + \omega_{RF}) - \omega_s = 2\omega_{OCS} - \omega_s, \tag{2.1}$$

where ω_s is the input signal frequency. The two pumping waves are set to coincide with the fiber zero-dispersion wavelength to effectively generate beating grating in HNL-DSF, which will modulate the input signal ω_s to produce two sideband waves with the frequency shift

$$\omega_{con} \pm |(\omega_{OCS} - \omega_{RF}) - (\omega_{OCS} + \omega_{RF})| = \omega_{con} \pm 2\omega_{RF}, \tag{2.2}$$

The power is determined by the third-order nonlinearity susceptibility $\chi_{(3)}$ and the fiber parameters [70]. FWM is independent of the signal bit rate and coding format. This property can be used to realize simultaneous up-conversion of multiple WDM signals and

easily integrated with passive optical access networks. In addition, the HNL-DSF has high Raman gain to assist the FWM process in terms of conversion efficiency and bandwidth [71]. Table 2.1 shows the transmission characteristics of the HNL-DSF used in these experiments [72]. The fiber was made by OFS Denmark and has a nonlinear coefficient γ of 10 $W^{-1}km^{-1}$ with a length of 1 km.

Table 2.1: Transmission parameters of HNL-DSF

Characteristics	Measured value
Attenuation coefficient	0.4 dB/km
Zero-dispersion wavelength	1561.0 nm
Dispersion slope (at zero-dispersion wavelength)	0.03 $ps/nm^2/km$
Nonlinear coefficient	$10W^{(-1)}km^{(-1)}$
Length	1 km
Raman gain	4 - 8.5 dB

The experimental setup for FWM-based optical millimeter-wave signal generation is shown in Fig. 2.2. Eight WDM signals with channel spacing of 3.2 nm are generated from eight DFB lasers and modulated by a LiNbO3 Mach-Zehnder (M-Z) modulator driven by 2.5-Gb/s baseband signals. The modulated WDM signals are then transmitted over 10-km SMF to decorrelate the signals before the up-conversion. The OCS modulation scheme is used to generate a 40-GHz optical local oscillator (LO) signal as the two FWM pumping signals. It is realized by driving a dual-arm M-Z modulator biased at V_π (minimum transmission point) with two complementary 20-GHz radio frequency sinusoid waveforms. The spectrum and waveform of the 40-GHz LO signal are inserted in Fig. 2.2 insets (i) and (ii). The OCS ratio (the ratio of the optical power in the first-order sideband to that of the optical carrier) is larger than 20 dB. Both the optical LO signal and the WDM signals are amplified by EDFAs before they are launched into the HNL-DSF. The signal power is 4 dBm/ch and the pump power is 14 dBm. To increase the FWM conversion efficiency and broaden the conversion bandwidth, we use a backward Raman pump LDs at 1440 nm with a total power of 750 mW. Two cascaded C/L band filters are used to filter out the LO signal and input WDM signals.

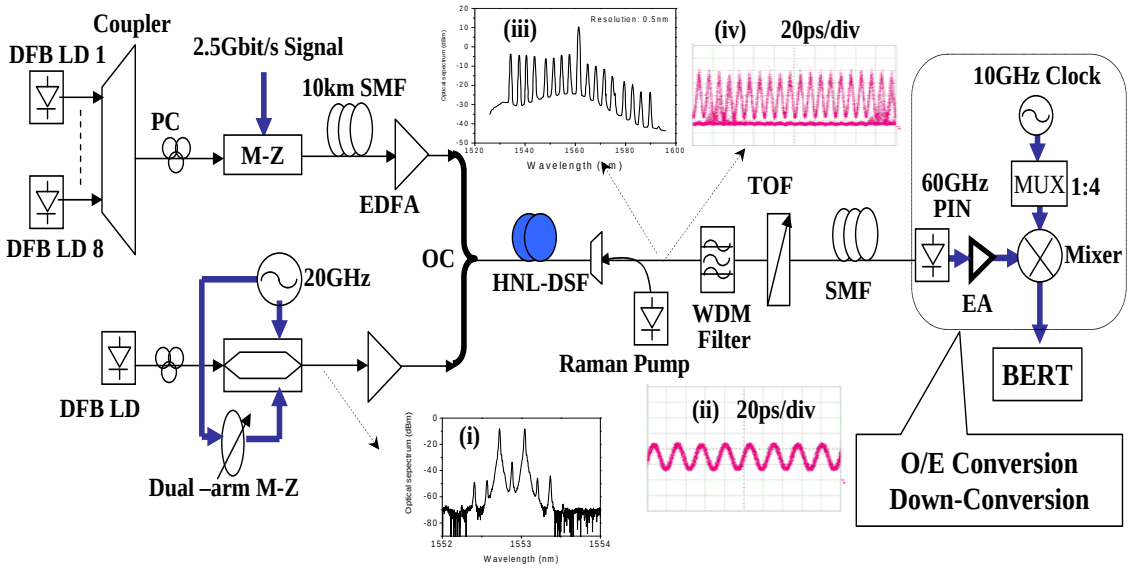

Figure 2.2: Experimental setup of FWM-based all-optical up-conversion.

Insets (iii) and (iv) in Fig. 2.2 show the optical spectrum and optical eye diagram at the output of the HNL-DSF. The optical signal-to-noise ratio (OSNR) of all up-converted channels is larger than 20 dB at a noise bandwidth of 0.1 nm. Since the Raman pump is optimized for C-band signal amplification, the up-converted signals with longer wavelengths have smaller gain. The Raman gains for the longest and shortest wavelengths are 8.5 dB and 4 dB, respectively. The power of each up-converted channel is larger than -24 dBm; it can be well amplified by an L-band EDFA. A tunable optical filter (TOF) with a 3-dB bandwidth of 0.5 nm is used to extract the desired channel. The extracted channel is then transmitted over a 5-km SMF before optical-to-electrical (O/E) conversion by a photo-detector (PIN) with a 3-dB bandwidth of 60 GHz. The converted electrical signals are amplified by a narrow band electrical amplifier (EA) with a bandwidth of 10 GHz centered at 40 GHz. An electrical LO signal at 40 GHz is generated by using a 1:4 frequency multiplier from 10 to 40 GHz. We use the LO signal and a 40-GHz electrical mixer to down-convert the millimeter-wave signal to its baseband form.

The power penalty is around 2.5 dB after a 12-km transmission. We then offset the center frequency of the optical filter by 30 GHz to realize the vestigial sideband (VSB)

filtering, as shown in Fig. 2.3 (left). The down-converted 2.5-Gb/s electrical eye diagrams are also shown in Fig. 2.3 (left). The power penalty at a bit error rate (BER) of 10^{-10} is only 0.5 dB after transmission over a 17-km SMF with the VSB filtering. It is also observed the difference of receiver sensitivity among all the WDM channels at a BER of 10^{-10} is less than 0.5 dB. As a comparison, the BER curve is measured when only the longest channel is present, as shown in Fig. 2.3 (right). The receiver sensitivity at a BER of 10^{-10} is degraded by 2 dB in the WDM case as compared to the single-channel situation, which comes from the nonlinear crosstalk among different channels in the FWM process and the reduced OSNR in the WDM case.

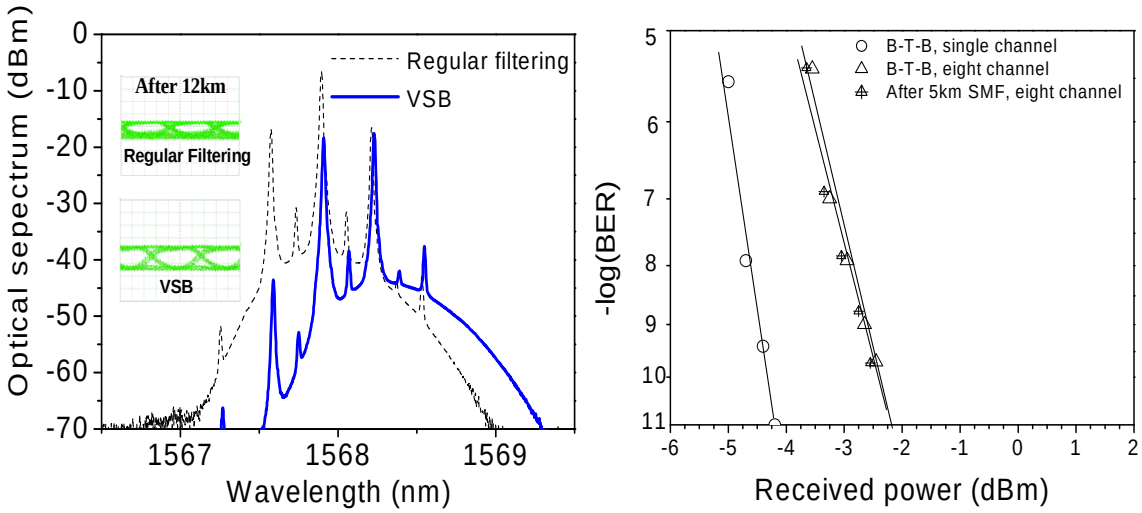

Figure 2.3: Experimental results for optical millimeter-wave signal generation based on FWM in HNL-DSF: VSB filtering (left), BER curvers (right).

The advantage for FWM-based all-optical up-conversion is that the FWM is transparent to the signal bit rate and modulation formats, which make it easy to realize up-conversion for different WDM signals. In addition, because of the ultra-fast nonlinear response of the fiber, it is possible to realize THz response for all-optical mixing or up-conversion. Meanwhile, the HNL-DSF has higher Raman gain compared to standard DSF [73], which can be utilized to assist the FWM process.

2.2.2 XPM in HNL-DSF: NOLM or straight line

XPM is another important nonlinear effect with many applications on optical signal processing [74]. XPM refers to the nonlinear phase change of an optical field induced by another channel signals. Basically, there are two structures to take advantage of XPM effect of the HNL-DSF. They are nonlinear optical loop mirror (NOLM) [75] and straight line [76] in HNL-DSF. The optical millimeter-wave generation and up-conversion using XPM in HNL-DSF is also possible for more wavelength channels without any interference and saturation effect limitation. The conceptual diagrams using OCS as the control signal are shown in Fig. 2.4 (a) and (b). Regarding the NOLM architecture, the symmetry between the counter-propagation paths of the probe signal is broken because of the XPM-induced phase shift by the control signal. So the NOLM is changed into the optical mixer between the probe and control signal. For the straight-line structure, while propagating in the HNL-DSF, the intensity of the control signal modulates the electric field of the probe data signal via the XPM effect. Therefore, the RF sinusoidal clock is imposed onto the probe signal as the sidebands. In the experiment, we use the same HNL-DSF depicted in Table 1.

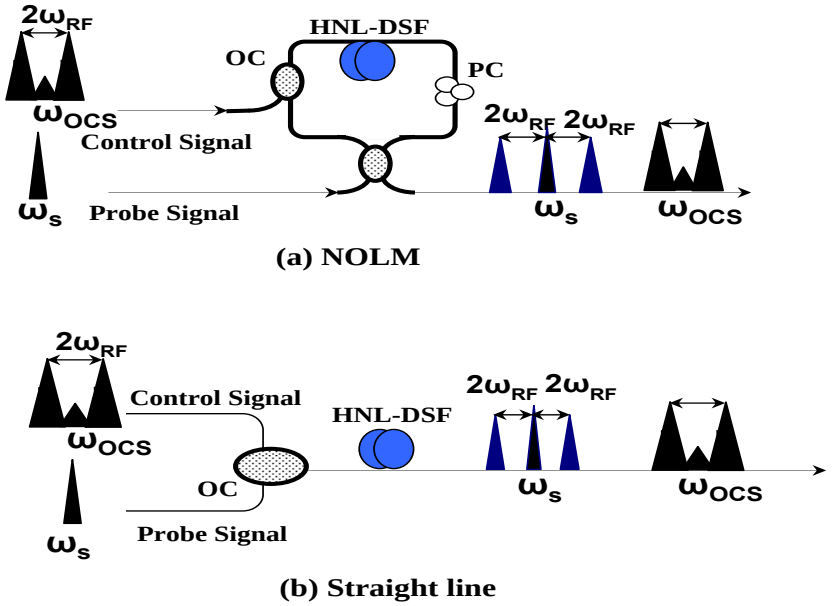

Figure 2.4: Concept of using XPM-based all-optical up-conversion.

NOLM has been commonly used in demultiplexing, switching, and wavelength conversion (WC), especially after overcoming the polarization problem. The experiment setup of XPM-based up-conversion in the NOLM is shown in Fig. 2.5. The NOLM is made up of two 50:50 optical couplers, one polarization controller (PC), and HNL-DSF [77]. The control signal is generated by using the OCS modulation scheme. A PC in the loop is used to obtain best performance of the converted pulses; the unwanted nonlinear phase shift of the counter propagating wave can also be compensated by adjusting the state of the PC in the NOLM.

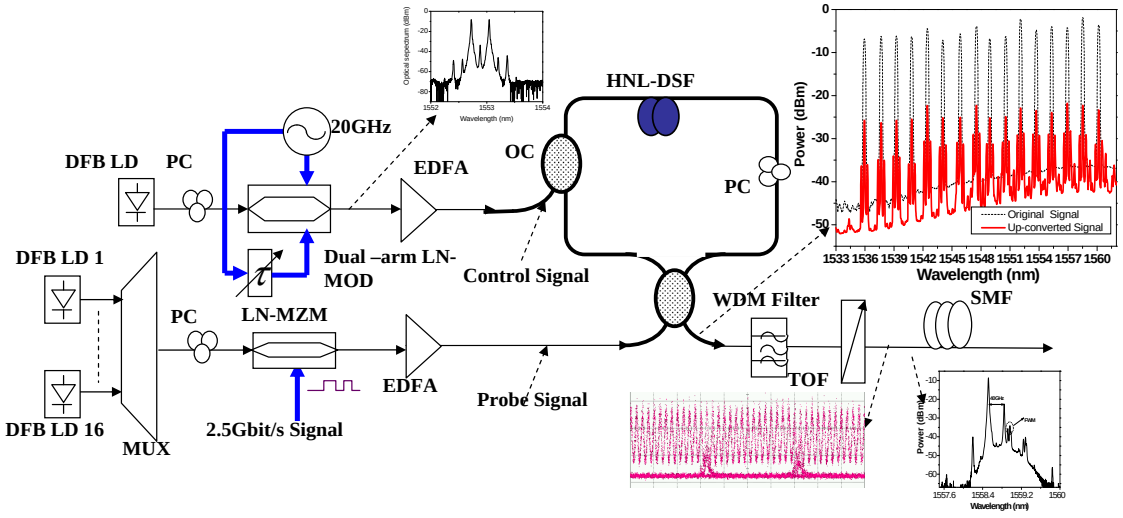

Figure 2.5: Experimental setup of XPM-based all-optical up-conversion in NOLM.

OCS-generated 40-GHz LO signal at wavelength 1563.86 nm is used as the control signal. The carrier suppression ratio is larger than 25 dB, and the duty cycle of the LO is 0.6. A DFB laser array is employed to generate 16 probe signals from 1535.94 nm to 1560.16 nm with adjacent 200-GHz spacing. The control and the probe signals are amplified via EDFAs before they are coupled into the NOLM. The up-converted signals are separated from the LO signal using a WDM filter. Then, an EDFA is used to boost optical power before a TOF is employed to suppress amplified spontaneous emission (ASE) noise and simultaneously realize single-wavelength VSB filtering. As an illustration, the measured eye diagram after up-conversion at wavelength of 1535.94 nm is inserted in Fig. 2.5 when the LO power is 17 dBm. The original 16x2.5-Gb/s signal and the up-converted signal are also shown in Fig.

2.5. All 16x2.5-Gb/s signals have the -22-dBm receiver sensitivity; the maximum difference among them is less than 0.5 dB.

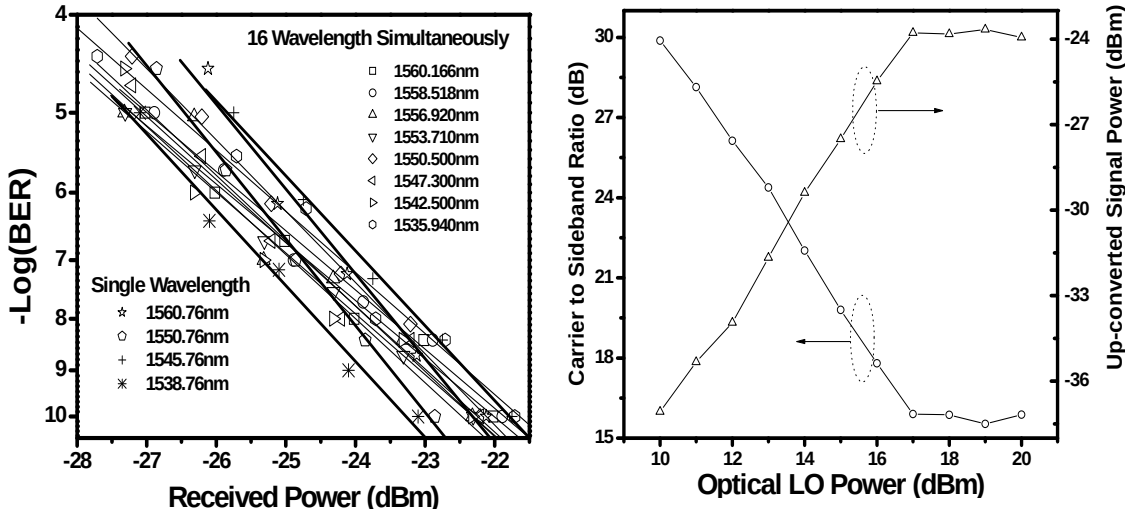

Figure 2.6: Experimental results: BER curves in two situations: 16 WDM signal (thin line) and single wavelength (thick line); Optical power and CSR of the up-conversion signal as a function of input power of LO signal.

The BER curves are measured when the optical LO power is 17 dBm. Eight wavelengths from the shortest at 1535.94 nm to the longest channel at 1560.16 nm are selected for the measurement, which is shown in Fig. 2.6 (left). There is no big difference among them, even some of them are totally overlapped. To further investigate the multi-channel interference in the NOLM, the DFB laser array source is replaced with a tunable laser source whose range could reach the whole C-band while keeping the probe power (15 dBm) the same as the total power of 16 wavelength channels. Four wavelengths are measured respectively, which is also shown in Fig. 2.6 (left) as thick lines. The maximum difference of receive sensitivity at a BER of 10^{-10} is within 1.5 dB.

Figure 2.6 (right) shows the sideband optical power and CSR of the mixed optical signal as a function of the input power of the LO signal. When the LO power is between 20 and 17 dBm, NOLM has the optimum conversion efficiency and gets the maximum CSR at around 15.5 dB. Larger control signal power results in extra nonlinear effects such as FWM, stimulated Brillouin scattering (SBS), and stimulated Raman scattering (SRS). Below 17 dBm, both the CSR and the power of the sideband signal have a significant

reduction because of the weak XPM effect, which leads significant degradation of OSNR for the up-converted signal. So, the optimum optical LO power is 17 dBm in this setup.

Since the NOLM suffers from stability problems resulting from the sensitive polarization state in the loop, XPM-based up-conversion in straight-line HNL-DSF is simpler and more robust. In this experiment, the setup based on straight-line XPM is shown in Fig. 2.7. The 16 continuous wave (CW) channels are multiplexed via arrayed waveguide grating (AWG) and simultaneously modulated by an M-Z modulator driven by a 2.5-Gb/s pseudo-random bit sequence (PRBS) electrical signal with a word length of $2^{31} - 1$. The optical spectrum of WDM signals is shown in Fig. 2.7 inset (i). Then, the generated 16x2.5-Gb/s signals are transmitted over 10-km SMF for signal decorrelation and then coupled into the HNL-DSF. The optical spectrum of up-converted signals is also inserted in Fig. 2.7 inset (ii). The HNL-DSF output is processed via O/E- and down -conversion, which are the same modules as the FWM-based setup in Fig. 2.2.

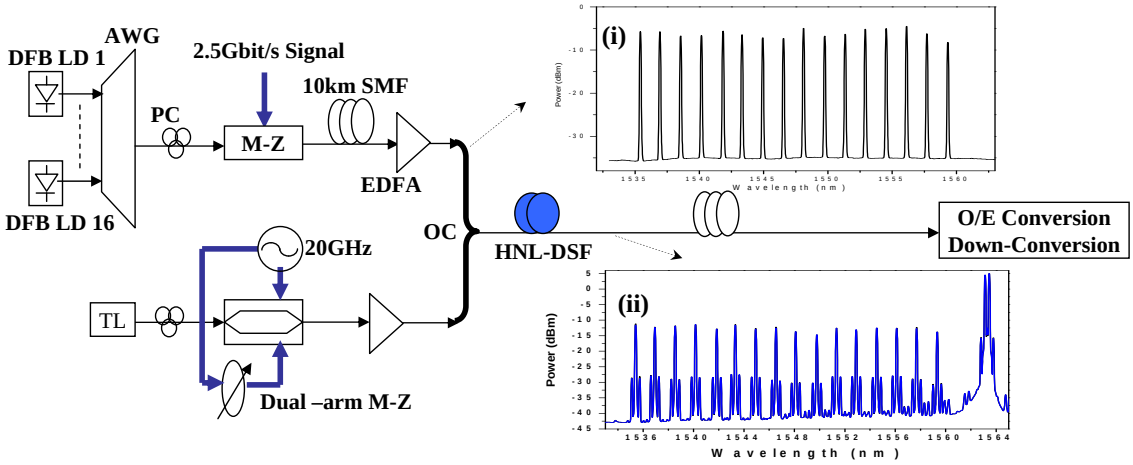

Figure 2.7: Experimental setup of XPM-based all-optical up-conversion in straight-line HNL-DSF.

It is noted that the optical CSR influences system performance because the millimeter-wave signals are generated by the interaction between the optical powers in the carrier and sideband [78]. CSR refers to carrier-to-sideband ratio, the ratio of the optical power in the optical carrier to that of the first-order sideband within a defined resolution bandwidth (here set as 0.01 nm). While maintaining the CSR at 13 dB, the measured receiver sensitivities

at a BER of 10^{-10} of all 16 up-converted channels are around -24 dBm, and the difference among them is less than 0.8 dB, as shown in Fig. 2.8 (left). So, there is no major crosstalk among multiple channels. The optical and electrical eye diagrams are also shown in Fig. 2.8 insets (i) and (ii). The BER curves at different control power while preserving the CSR at 13 dB are shown in Fig. 2.8 (right). It is observed that 18.7 dBm is the optimal value for high receiver sensitivity and there is around 0.8-dB power penalty compared to 13.7 dBm. In this experiment, the VSB method is also used to enhance the receiver sensitivity and simultaneously reduce the occupied bandwidth.

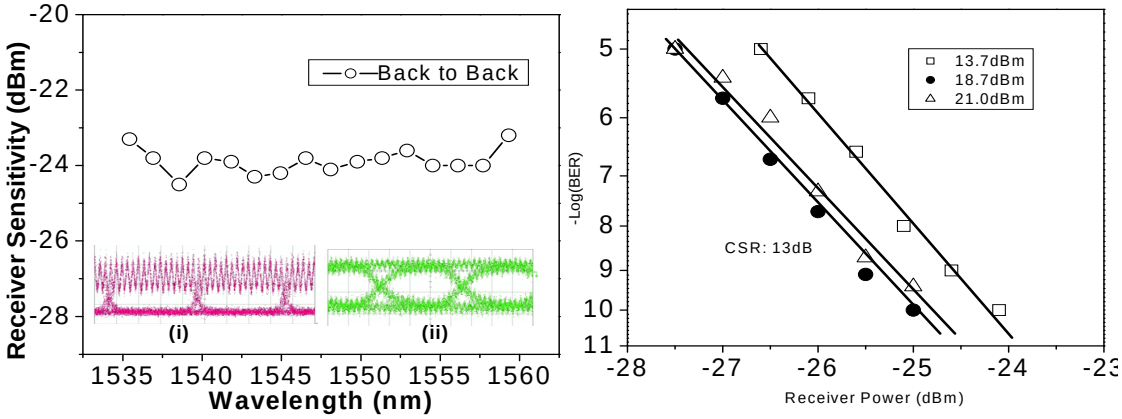

Figure 2.8: Experimental results based on XPM in straight-line HNL-DSF: receiver sensitivities (left), BER curvers (right).

This scheme exhibits very good conversion performance at high data rate and can provide more wavelength channels in the whole optical fiber transmission band without any interference and saturation effect limitation.

2.2.3 XAM in EAM

The principle of up-conversion based on EAM is similar to its wavelength conversion mechanism at high bit rate [79] [80]; the main difference from wavelength conversion is that the modulated data signal will be used to replace the CW source [81] [82]. The experimental setup is shown in Fig. 2.9 (a). An EAM (CyOptics: EAM 40) with 3-dB bandwidth of 32 GHz, fiber-to-fiber insertion loss of 8 dB, and polarization sensitivity lower than 1 dB is used to realize the signal up-conversion.

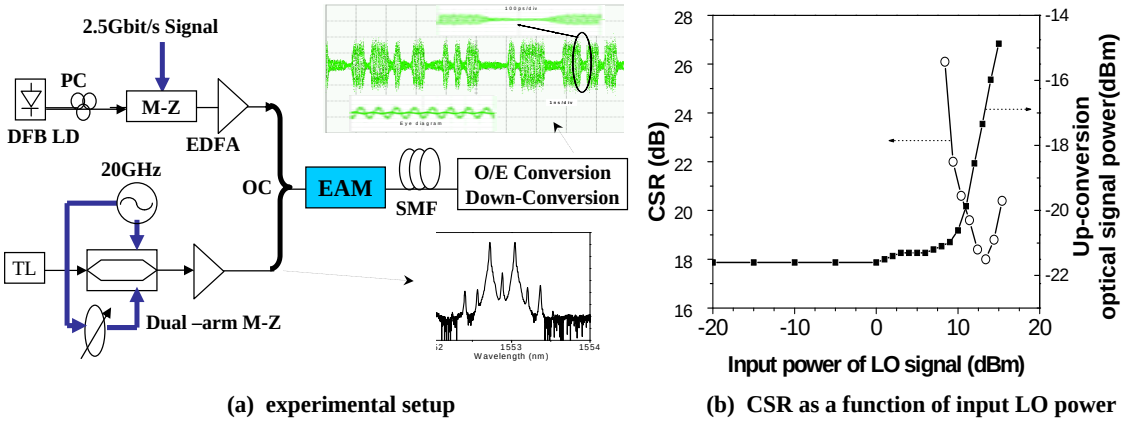

(a) experimental setup (b) CSR as a function of input LO power

Figure 2.9: Experimental setup of XAM-based all-optical up-conversion (a) and results (b).

Optical LO signals are generated using the OCS modulation scheme with a carrier suppression ratio of larger than 25 dB. The electrical signal and waveform are also inserted as an inset in Fig. 2.9 (a). When the DC bias on the EAM is -3 V and the 2.5-Gb/s data signal is -4 dBm, the optical power and the CSR of the mixed optical signal after the EAM as a function of the input power of LO signal are shown in Fig. 2.9 (b). The measured static transfer curve slope of the EAM at -3V bias is 3.5 dB/V. Because of the absorption effect of the EAM, the data signal is almost absorbed when the LO signal is smaller than 10 dBm. Once the LO signal is larger than 10 dBm, it is mixed with the data signal because of XAM in the EAM. As the power of the LO signal is 12.5 dBm, CSR is the smallest. Figure 2.9 (b) also shows that CSR will be reduced with the LO signal enhancement when the LO signal is larger than 12.5 dBm. The reason is that the LO signal will saturate the EAM; CSR could be further reduced as long as we increase the DC bias on the EAM. But larger DC bias will reduce the power and OSNR of the up-conversion signals. Therefore, the maximum bias in the experiment is -3 V.

The optical spectrum and eye diagram of the up-converted signal are shown in Fig. 2.10 when the DC bias on the EAM, the LO power and data signal power are -3 V, 12.2 dBm, and -4 dBm, respectively. The CSR of the mixed signals is 19 dB and the mixed signals will occupy 80 GHz bandwidth to keep the three frequency tones, separated by 40 GHz when the LO power is 12.2 dBm.

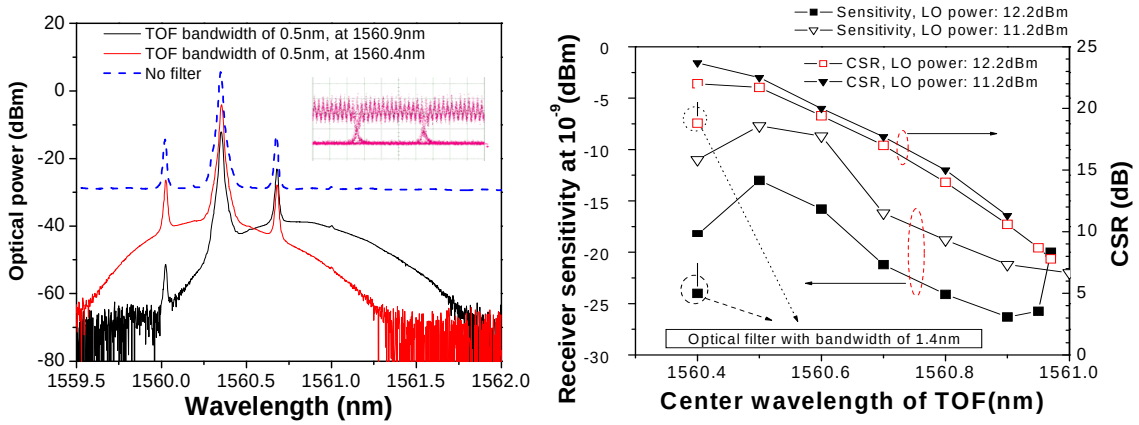

(a) Optical spectra **(b) Receiver sensitivities and CSR**

Figure 2.10: Experimental results of the XAM-based up-conversion scheme.

A high CSR will lead to weak receiver sensitivity, while a wide bandwidth will reduce spectral efficiency of the WDM system. In this experiment, the VSB filtering method is used to enhance the receiver sensitivity and simultaneously reduce the occupied bandwidth. The receiver sensitivity at a BER of 10^{-9} and the CSR of the mixed signals at different center wavelength of TOF are shown in Fig. 12. As the center wavelength of the TOF is 1560.4 nm, the same wavelength as the data signal, the dual-sideband signals can almost be maintained; therefore the receiver sensitivity is a little higher than in other cases. When the center wavelength is tuned longer than 1560.5 nm, the CSR will be reduced because the optical carrier is suppressed, which leads to the improved receiver sensitivity.

This scheme has some advantages, such as low power consumption, compact size, polarization insensitivity, easy integration with other devices, and higher speed operation because of EAM inherent characteristics.

2.3 Based on external intensity modulation

2.3.1 Comparison of DSB, SSB, and OCS schemes for up-conversion

External intensity modulation [83] [84] is another simple way to realize direct transport of the radio signals over optical fiber at the RF transmission carrier. People have demonstrated the millimeter-wave generation and transmission using external modulators based on DSB and SSB [85] [86]. SSB modulation is superior to DSB scheme on extending the delivery

distance for the optical millimeter-wave signals because of its high tolerance of chromatic dispersion in the optical fiber. However, the receiver sensitivity of SSB modulation is relatively low because of the high DC component at the central wavelength [87]. To further simplify the configuration and increase the spectral efficiency and receiver sensitivity, we develop the third scheme for optical millimeter-wave signal generation based on the OCS modulation method [88].

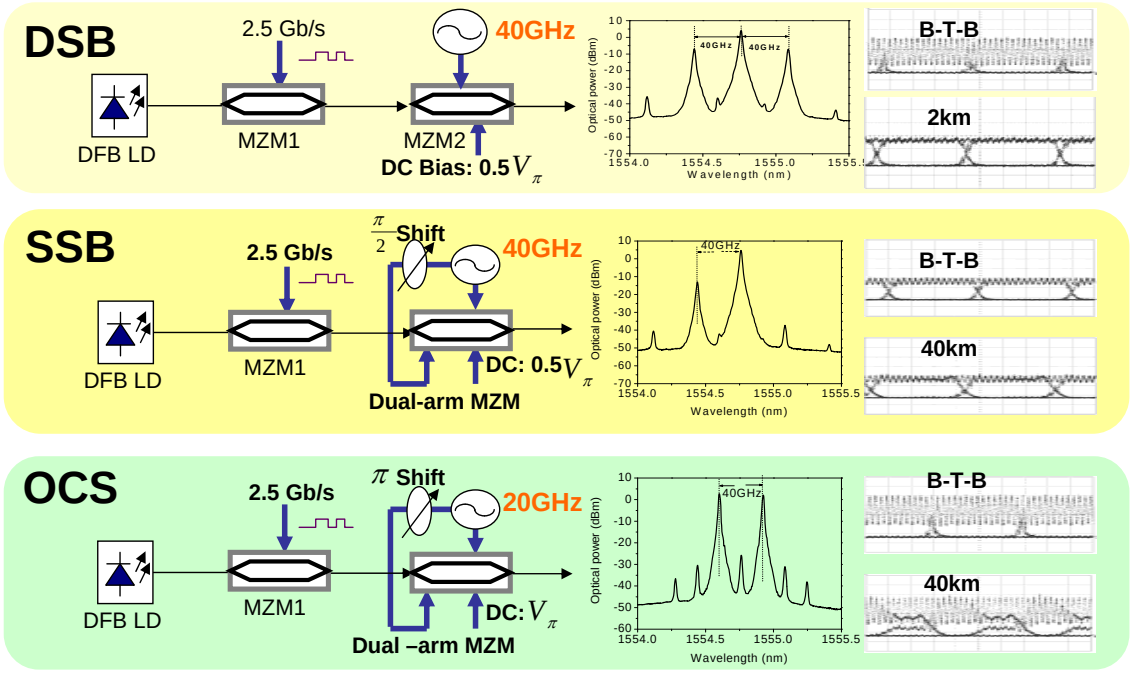

Figure 2.11: All-optical up-conversion using DSB, SSB, and OCS.

Figure 2.11 shows optical millimeter-wave generation based on DSB, SSB, and OCS modulation schemes, respectively. The corresponding optical spectra and eye diagrams after mixing with the 40-GHz RF signal are also inserted. The baseband data signal is generated by a Mach-Zehnder modulator (MZM) driven by a 2.5-Gb/s PRBS electrical signal with a word length of $2^{31} - 1$. For the DSB modulation scheme, the MZM2 is biased at $0.5V_\pi$ and the frequency of the driven RF signal is 40 GHz. The generated millimeter-wave signal will occupy over 80-GHz bandwidth because it has two sidebands. Since the two sidebands have different velocities in SMF, the RF power at 40 GHz will disappear after transmitting over a certain length of SMF. As an example, the eye diagram after transmission over 2 km

is inserted in Fig. 2.11. It is seen that RF power at 40 GHz is almost faded, which leads to a large power penalty. The measured BER curves in Fig. 2.12 (1) show that the power penalty is 17 dB at a BER of 10^{-10} after 2-km fiber transmission. These results indicate that the DSB modulation-based scheme is not suitable for a wide-area access network.

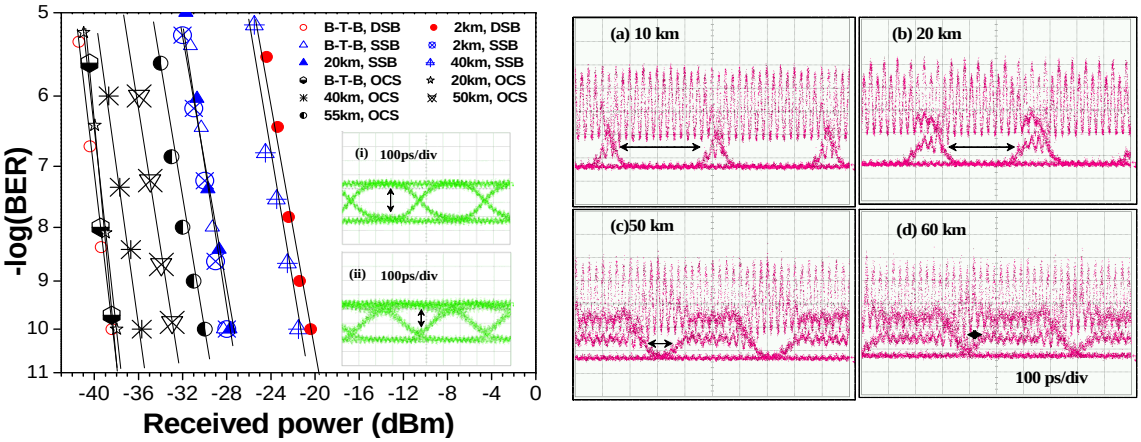

(1) BER curves of DSB, SSB, and OCS

(2) Optical eye diagrams of OCS-based millimeter-wave

Figure 2.12: Experimental results of optical millimeter-wave generation using external intensity modulator.

A dual-arm MZM is employed to achieve SSB modulation. Two electrical RF signals to drive the dual-arm MZM have a phase shift of $\pi/2$, and the DC bias is at $0.5V_{\pi}$. The generated optical millimeter-wave signal only occupy 40-GHz bandwidth, but the optical CSR is generally larger than 15 dB, which means it is full of DC components at the peak of center wavelength. Hence, it results in a low receiver sensitivity. Figure 2.12 (1) shows that the receiver sensitivity of back-to-back (B-t-B) for SSB modulation is around 10 dB lower than that of DSB modulation. Although there is no power penalty after 20-km transmission, it is more than 5 dB after 40-km transmission because of the fiber dispersion and large CSR. When the phase of the two electrical RF signals to drive the dual-arm MZM is set to π difference and the DC bias is at the minimal intensity-output point or V_{π}, the OCS modulation is realized. In this scheme, only a 20-GHz RF signal is needed and the bandwidth for the MZM is also only 20 GHz. Moreover, the generated optical spectrum just occupies 40-GHz bandwidth. At a BER of 10^{-10}, the receiver sensitivity of the B-t-B millimeter-wave signal is -39.7 dBm, which is similar to that of the millimeter signal

generation based on DSB modulation. There is no power penalty after 20-km transmission, and the power penalty is less than 2 dB after 40-km transmission. The electrical eye diagrams after 10-km and 50-km transmission are shown as insets (i) and (ii) in Fig. 2.12 (1).

Since the optical millimeter-wave has two peaks after the OCS modulation, it will suffer from dispersion in fiber when transmitted over SMF. The pulse width of the 2.5-Gb/s signal carried by the optical millimeter-wave is approximately 400 ps. The two peaks with a wavelength spacing of 0.32 nm will have a walk-off time of 400 ps caused by fiber dispersion after transmission over 74-km SMF with a group velocity dispersion (GVD) of 17 ps/nm/km, which means the eye will be fully closed after this distance. While considering the limited rise and fall times of the optical receiver and electrical amplifier, the maximum delivery distance will be shorter. Figure 2.12 (2) clearly shows the evolution of the optical eye diagrams at different transmission distances. The un-flat amplitudes of the optical carriers at 40 GHz as shown in Fig. 2.12 (b) are caused by chromatic dispersion. The reports in [89] [90] show that fiber dispersion causes the amplitude fluctuation of the carrier but the RF power at 40 GHz does not disappear when the carrier is a pure dual-mode lightwave. Fig. 2.12 (d) shows that the eye is almost closed after the optical millimeter-wave is transmitted over 60-km SMF.

2.3.2 Integration with 32-channel WDM-PON using the OCS scheme

Using the OCS modulation scheme, 32x2.5-Gb/s DWDM signals after 40-km transmission are simultaneously up-converted to integrate with a WDM-PON network [91]. The experimental setup for DWDM signal transmission, up-conversion, and post-transmission is shown in Fig. 2.13. A 32 DFB-laser array is used to realize 32 wavelength signals from 1536.1 nm to 1560.9 nm with adjacent 100-GHz spacing. An AWG is used to combine the 32 CW lightwaves before modulation by a modulator. The optical spectrum of the WDM source is shown in Fig. 2.13 inset (i). The generated 32x2.5-Gb/s signals are transmitted over 40 km for emulating a metro optical network before they are up-converted using a dual-arm MZM based on the OCS technique. The optical spectrum of the up-converted signals is shown in

Fig. 2.13 inset (ii).

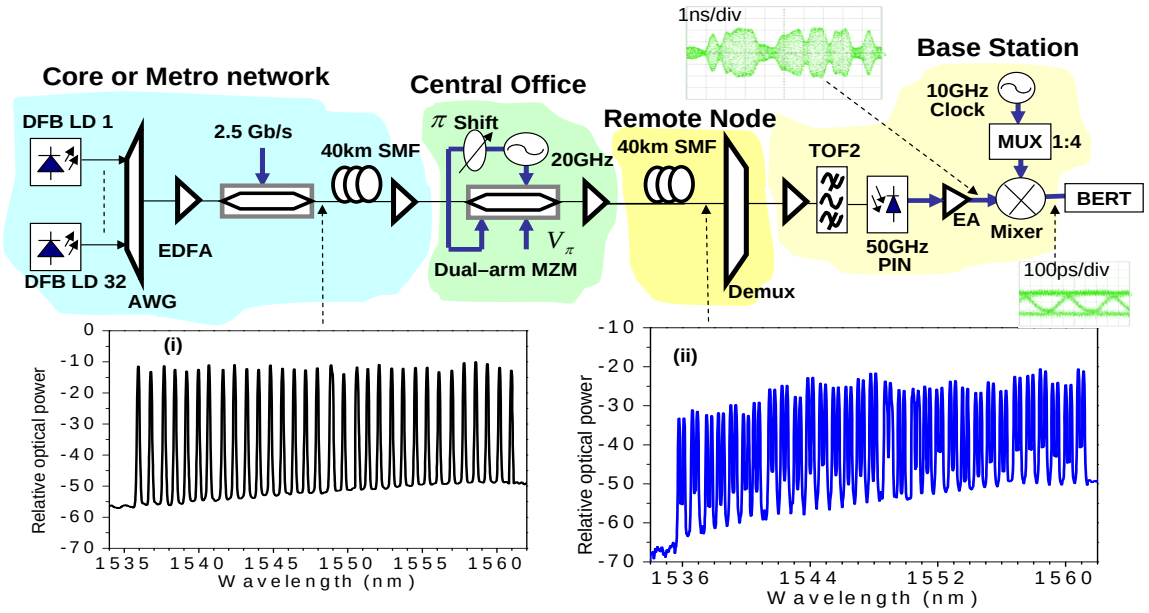

Figure 2.13: Experimental setup of OCS-based up-conversion of 32 WDM channels.

The up-converted millimeter-waves are amplified by an EDFA to get a power of 20 dBm before transmission over variable length SMF. At the receiver, the desired channel is selected by using the same O/E and down-conversion components as in the aforementioned setup.

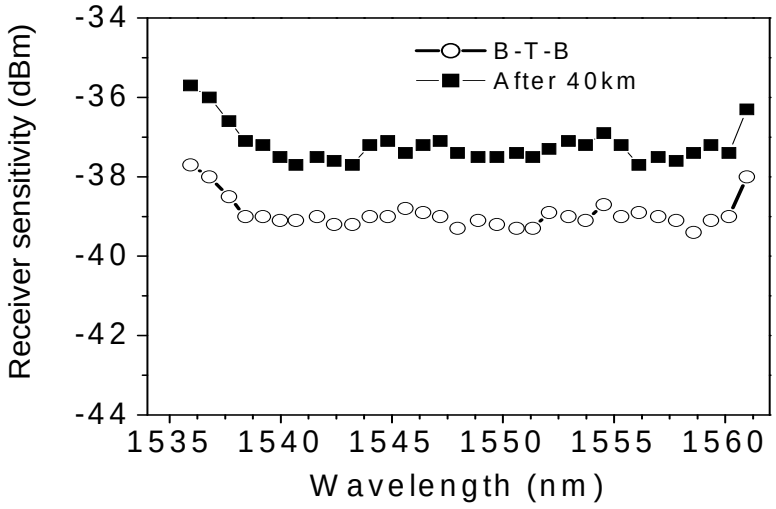

Figure 2.14: Receiver sensitivities of OCS-based up-conversion of 32 WDM channels.

The sensitivities for all channels after 40-km transmission at a BER of 10^{-10} are shown

in Fig. 2.14. The preamplifier at short wavelength (<1540 nm) or long wavelength (>1560.5 nm) has a smaller gain; therefore, the receiver sensitivities at these wavelengths are a little lower. The power penalty for all channels is roughly 2 dB after 40-km SMF delivery. It is also observed that the penalty is the same as in the multi-channel situation when one channel is kept on with 10-dBm input power. The up-conversion signals based on the OCS modulation scheme have shown the best performance in terms of highest receiver sensitivity, highest spectral efficiency, and smallest power penalty over long-distance delivery compared with the DSB and SSB modulation schemes.

2.4 Based on phase modulation and optical filtering

In addition to the intensity modulation, external phase modulation [92] [93] is also utilized to produce downstream optical millimeter-wave signals in optical-wireless networks.

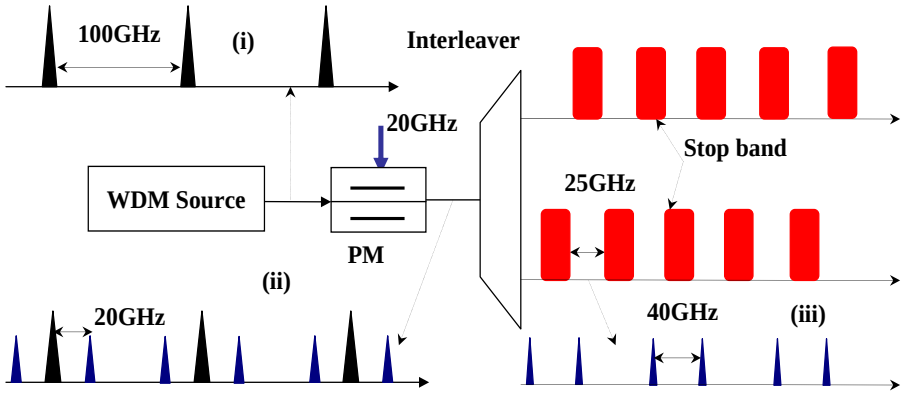

Figure 2.15: Schematic of using PM and interleaver for millimeter-wave generation.

Figure 2.15 shows the principle of using a phase modulator (PM) and subsequent optical filtering for optical millimeter-wave signal generation. As a schematic illustration, the case of WDM signals with 100-GHz channel spacing as inset (i) is considered. When the WDM sources are modulated by a PM driven by a 20-GHz sinusoidal RF clock, the signal field of one channel at the output of the PM can be written as a few sidebands

$$E_{output1} = A_s \sum_{n=-\infty}^{+\infty} J_n(m_d) \cos((\omega_s + n\omega_{RF})t + n\pi/2), \tag{2.3}$$

where A_s is the amplitude of the original optical carrier, $J_n(m_d)$ is the $n^(th)$ Bessel function of the first kind, $m_d = \pi V_{RF}/V_\pi$ is the modulation depth of PM, V_{RF} is the driving voltage

of the RF signals, and $n\omega_{RF}$ is the generated sideband. The number of sidebands that can be generated depends on the amplitude of the driven RF signal on the PM. Here, we assume that only the first-order sideband is generated through optimizing the modulation depth m_d. The peak of the first sideband is 20 GHz away from the original optical carrier, as shown in inset (ii). The interleaver, with one input and two out-ports of 25-GHz bandwidth, is used to suppress the optical carrier. When the central wavelengths of the WDM light sources can match up well to the interleaver, the optical carrier of each channel will be suppressed. The output signal of the interleaver is expressed as

$$E_{output1} = A_s\{\sum_{n=-\infty}^{+\infty} J_n(m_d)\cos((\omega_s + n\omega_{RF})t + n\pi/2) - \alpha J_0(m_d)\cos(\omega_c t)\}, \qquad (2.4)$$

where α is the attenuation coefficient of the interleave filter at the peak of center frequency. The optical spectrum from output 1 of the interleaver is shown in Fig. 2.15 inset (iii). In this way, optical millimeter-wave WDM signals are generated.

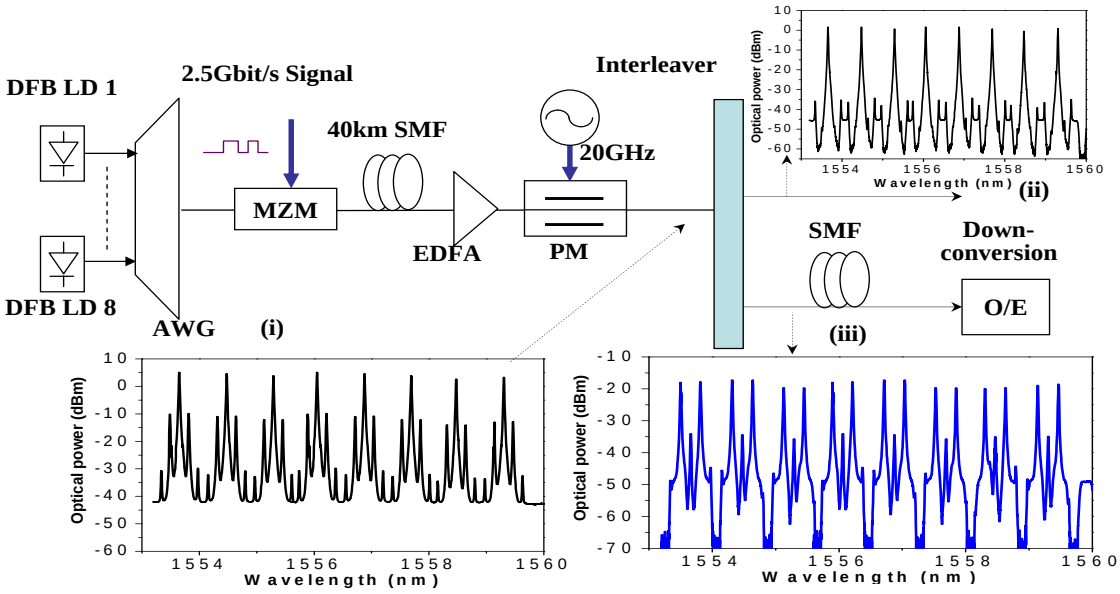

Figure 2.16: Experimental setup of up-conversion based on PM and optical filtering.

The experiment setup for WDM optical millimeter-wave generation and transmission is shown in Fig. 2.16. A laser array with eight DFB LDs is used to achieve WDM signals from 1553.7 to 1559.3 nm with 100-GHz spacing. The generated 8x2.5-Gb/s signals are transmitted over 40-km SMF for decorrelation. The decorrelated WDM signals are modulated

by a PM driven by a 20-GHz sinusoidal clock with peak-to-peak amplitude of 3 V. The optical spectrum after the phase modulator is inserted in Fig. 2.16 inset (i). The half-wave voltage of the phase modulator is 11 V. Since the driving voltage is much smaller than the half-wave voltage of the PM, the second-order sideband of each channel is 25 dB lower than the first-order sideband. Therefore, the second-order sidebands have little effect on the transmission of the optical millimeter-wave signal in the SMF. An optical interleaver with two output ports and 25-GHz bandwidth is used to suppress the optical carriers and convert the modulated WDM lightwaves to WDM optical millimeter-waves. After the optical interleaver, the carrier suppression ratio of all channels is larger than 15 dB, as shown in inset (iii), and the repetition frequency of the optical millimeter-wave is 40 GHz. The total power of the optical millimeter-wave signals is 1 dBm. The remaining optical carrier from the other port of the interleaver is shown in Fig. 2.16 inset (ii). At the receiver, one channel is selected using a TOF, the identical O/E and down-conversion components as in the HNL-DSF setup.

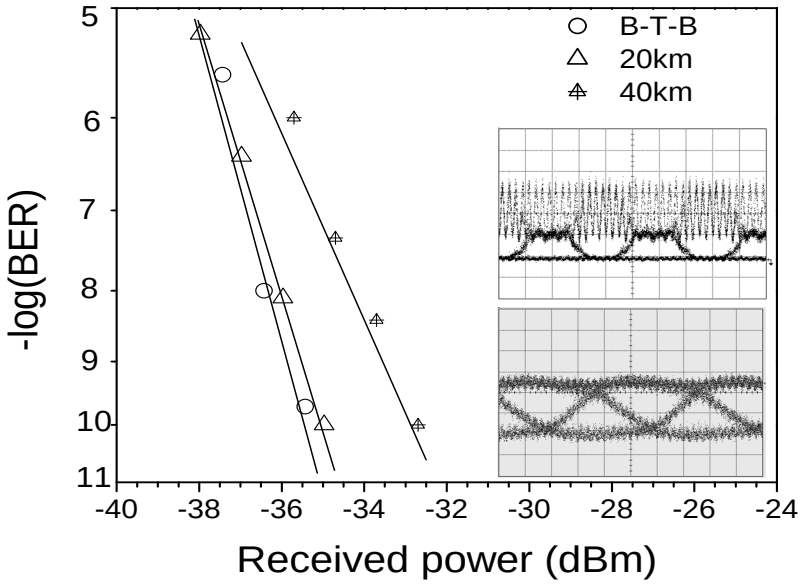

Figure 2.17: Experimental results of channel 4 at 1556.1 nm.

Figure 2.17 shows the BER curves and eye diagrams of channel 4 at 1556.1 nm after transmission over 40-km SMF. For a BER of 10^{-10}, the receiver sensitivity for the B-t-B

signal is -36.1 dBm. The penalty after 20-km transmission is 0.3 dB. At 40-km distance, the power penalty is 2 dB. It is also observed that there is little difference between the single-wavelength situation and the simultaneous multi-channel case. By optimizing the amplitude of the RF signal to drive the PM for suppressing the high-order sidebands of the optical millimeter-wave, the signals can be transmitted over longer distances. This scheme also exhibits better performance on system stability because of the removal of any DC-bias controller compared with the external intensity modulation methods.

2.5 Based on SCM and optical filtering

Optical subcarrier multiplexing (SCM) is a scheme where the baseband data is first modulated on an RF subcarrier and transmitted by a single wavelength. A significant advantage of SCM is that microwave devices are more mature than optical devices, and the stability of a microwave oscillator and the frequency selectivity of a microwave filter are much better than their optical counterparts [94]. In addition, the advanced modulation formats can be applied easily. A popular application of SCM technology in fiber optic systems is analog CATV distribution [95]. Because of the simple and low-cost implementation, SCM can also be proposed to generate optical millimeter-wave signals for optical access networks. The experimental setup of generating optical millimeter-wave signals using SCM and optical filtering is shown in Fig. 2.18.

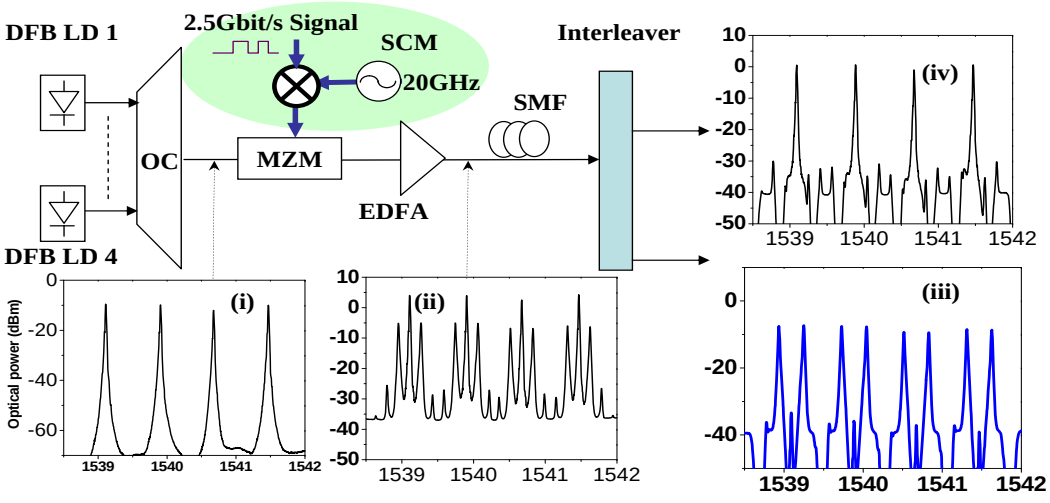

Figure 2.18: Experimental setup of up-conversion based on SCM and optical filtering.

Four CW lightwaves are generated by DFB LDs at 1539.1, 1539.9, 1540.7 and 1541.5 nm with 0.8-nm channel spacing before they are multiplexed by a 4:1 optical coupler (OC). The downstream signals at 2.5 Gb/s are mixed with a 20-GHz LO signal by a 20-GHz electronic mixer. After amplification, the mixed electrical signals are used to drive an external intensity MZM to generate SCM signals. The optical SCM signals are then transmitted to the BS after passing 20-km SMF. At the BS, an optical interleaver with two output ports and 25-GHz channel spacing is employed to separate the optical carrier and subcarrier signals. The optical spectra at different positions are inserted in Fig. 2.18. Inset (i) and inset (ii) are the optical spectra before and after SCM. It is seen that optical carrier to sideband ratio is 9 dB in inset (ii). After separation by the interleaver, the optical spectra from the two ports are shown in insets (iii) and (iv). It is seen that the carriers in inset (iii) are suppressed over 30 dB.

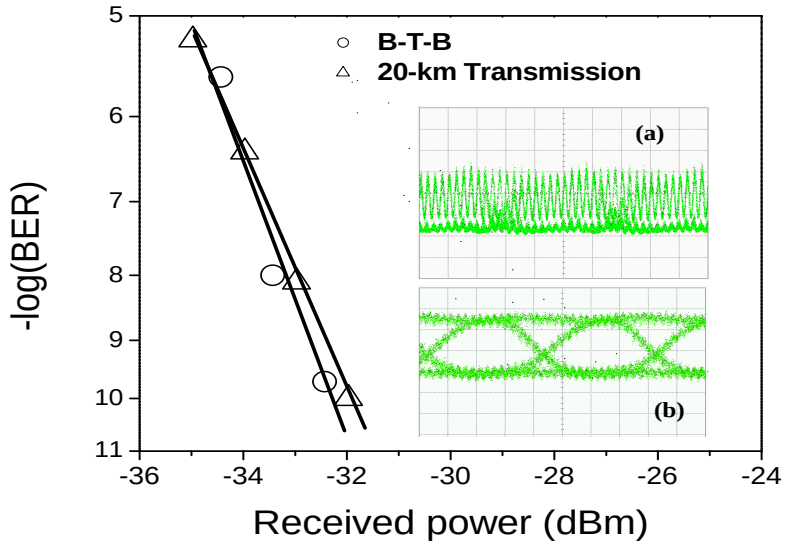

Figure 2.19: Experimental results of optical millimeter-wave generation based on SCM and optical filtering.

The measured BER curves are shown in Fig. 2.19. A preamplifier is employed. The power penalty is 0.4 dB at a BER of 10^{-9}. The optical eye diagrams of millimeter-wave signals after transmission and down-conversion are shown in Fig. 2. 19 insets (a) and (b). The clear and open signal eyes are obtained.

2.6 Chapter summary

Optical techniques are considered cost-efficient ways to the generation, amplification, modulation, and transmission of optical millimeter-wave signals for optical-wireless access networks [96]. In this chapter, six new schemes for optically generating millimeter-wave signals are presented. Table 2.2 summarizes the advantages and disadvantages of several up-conversion technologies. The experimental results suggest that the up-conversion method based on external modulation (intensity and phase modulation) schemes show practical advantages in terms of the low cost, simplicity of system configuration, and performance over long-distance transmission. These results imply that these developed schemes will be the desirable candidates for downlink connection in full-duplex optical-wireless networks.

Table 2.2: Comparison of millimeter-wave generation technologies

Schemes		Advantages	Disadvantages
HNL-DSF	FWM	Transparent to data rates and formats; support WDM signals; THz mixing bandwidth	High input power requirement; un-flatten amplitude response for WDM signals.
HNL-DSF	XPM	Supporting WDM signals; THz mixing bandwidth;	Polarization sensitive; need to optimize the input power and CSR to get high conversion efficiency.
SOA/SOA-MZI	XGM	High conversion efficiency; polarization immunity;	Limited XGM bandwidth in SOA; high input power requirement; crosstalk among multiple channels.
SOA/SOA-MZI	XPM	Low input power requirement with good linearity; polarization immunity;	Limited XGM bandwidth in SOA; complicated conversion structure; nonlinear crosstalk among multiple channels.
Direct modulation		The simplest one;	Limited modulation bandwidth of lasers.
EAM	XGM	Polarization immunity, compact size, low power consumption;	Need to optimize the CSR, diffcult in supporting multiple channels.
Intensity modulation	OCS	Easy to integrate with WDM-PON; high receiver sensitivity; low spectral occupancy and low bandwidth requirement for RF signals;	Need a control electrical circuit to optimize the DC bias and phase shift.
Intensity modulation	SCM	Simple and stable scheme; high receiver sensitivity; one modulator for simultaneous modulation and up-conversion;	Need an optical notch filter with matching channel spacing for WDM situations; electrical power matching between LO and baseband signals
Phase modulation		Simple and stable scheme; high receiver sensitivity;	Need an optical notch filter with matching channel spacing for WDM situations, high driving voltage.
Optical heterodyning		Full modulation depth; dispersion-tolerant transmission;	Strict requirement for the light source in terms of bandwidth and phase match.

CHAPTER III

ARCHITECTURE DESIGN FOR BIDIRECTIONAL CONNECTIONS

Generation and distribution of optical millimeter-wave signals from a CO to a BS is the firs step for optical-wireless access networks. To have a reliable access infrastructure, more considerations should be given to the whole architecture design for both downlink and uplink connections. Simplified design of the BS and full-duplex operation through two separated fibers or a single fiber span are discussed in this chapter. Three different optical-wireless systems for full-duplex transmission are presented based on a centralized light source in the CO in sections 3.2, 3.3, and 3.4. The bidirectional transmission of 60-GHz millimeter-wave signals over a single span of SMF is demonstrated in section 3.5. Finally, all these designed systems for bidirectional connections are summarized in section 3.6.

3.1 Introduction

As discussed in the previous chapters, future optical-wireless access systems will operate in the millimeter-wave frequency range to support higher data rates and overcome spectral congestion at lower microwave frequencies [97]. The negative side for a signal in the millimeter-wave band is the limited radio propagation distance because of high attenuation caused by atmospheric absorption [98]. Consequently, the broadband optical-wireless access network architecture incorporating millimeter-wave radio transmission requires a microcell or picocell, which brings forth the needs for a large number of remote antenna BSs within a small geographical area [99]. In this situation, it is necessary to minimize the cost of the BS and shift the system complexity and expensive devices to the CO. Hence, the overall architecture design and the scheme of RF signal generation and transmission for the uplink and downlink play key roles in the successful deployment in the real networks.

Regarding the downlink connection, several approaches for up-converting and transmitting millimeter-wave signals are investigated in Chapter 2. As far as the uplink connection is

concerned, some methods have been recently proposed. However, most of them only demonstrate uplink connections over short transmission distances at lower microwave frequencies [100] [101] [102]. Full-duplex operation using high RF carriers still raises difficulties that have to be addressed. The network architecture consisting of a single light source at the CO and the reuse of the downlink wavelength at the BS is an attractive solution for low-cost implementation, as it requires no additional light source and wavelength management at the BS. In this Chapter, three different architecture for full-duplex connections based on wavelength reuse are presented. We also show the first demonstration of a 60-GHz ROF system simultaneously transmitting 2.5-Gb/s data for both directions over a single span of 25-km SMF-28. OCS-based spectral-broadening technology is used in this scheme to relieve backreflecting impairments.

3.2 DPSK format for downstream and remodulated OOK for upstream

The schematic diagram of symmetric full-duplex optical-wireless system based on different modulation format is shown in Fig. 3.1.

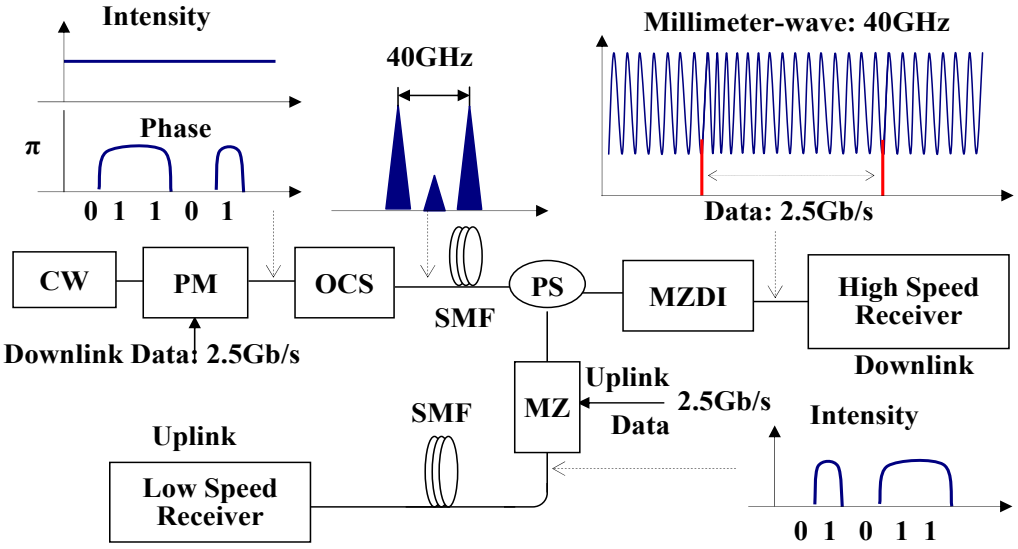

Figure 3.1: Schematic diagram for delivering bidirectional services in the ROF system.

The phase modulator is used to generate differential phase-shift keyed (DPSK) signals [103], where a bit "1" is coded by a π phase shift of the optical phase, whereas a bit "0" leaves it unaffected. An OCS scheme is employed to simultaneously generate an optical 40-GHz

millimeter-wave and up-convert a 2.5 Gb/s baseband data signal for the downstream. At the BS, a power splitter (PS) is used to divide the incoming signal into two parts. The first one (downstream signal) is demodulated by a Mach-Zehnder delay interferometer (MZDI) and later detected by a high-speed photodetector. The second one (upstream signal), considered a CW, is modulated with the symmetric ON-OFF keying (OOK) upstream signal and sent back to the CO where a low-cost, low-frequency receiver is used for uplink detection [104].

The experimental setup for the bidirectional ROF system is depicted in Fig.3. 2. At the CO, a CW lightwave is generated by a tunable laser (TL) at 1553.1 nm and modulated by a PM driven by a 2.5-Gb/s PRBS $2^{31}-1$ electrical signal with amplitude V_π. The resulting DSPK signal is passed to a dual-arm MZM biased at V_π and driven by two complementary 20-GHz clocks. It simultaneously generates the optical millimeter-wave and up-converts the 2.5-Gb/s DPSK data into this optical millimeter-wave signal. The optical millimeter-wave signal is then amplified by an EDFA to 13 dBm before its transmission over various lengths of SMF-28. At the BS, a 50:50 optical PS is used to divide the incoming signal power for the downlink detection and uplink connection [105].

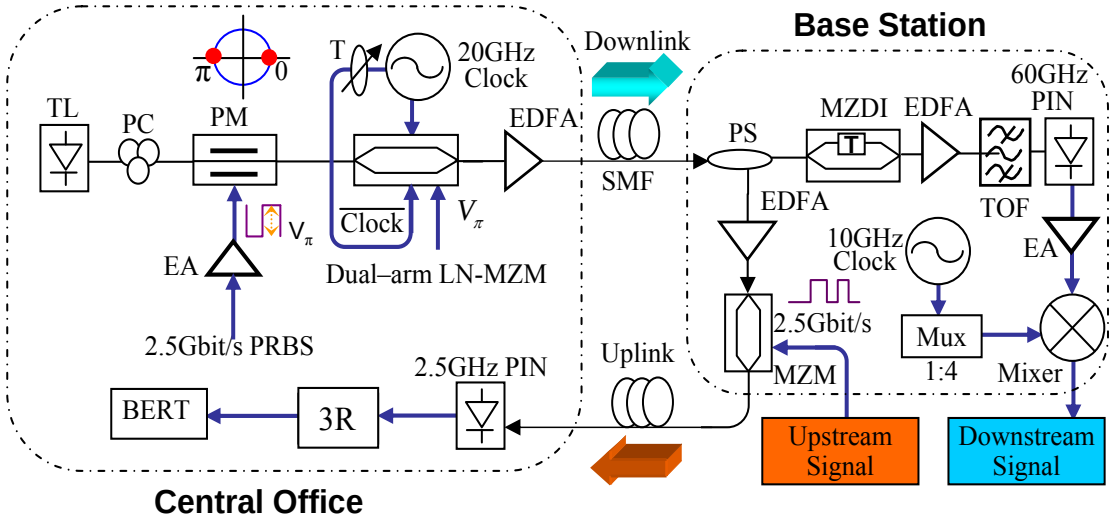

Figure 3.2: Experimental setup of delivering bidirectional services based on different modulation formats.

Because photodetection is phase insensitive, a phase-to-intensity conversion is needed at the receiver. So, an MZDI is inserted in the downlink path to demodulate the DPSK signal

and retrieve the data. In this experiment, the fiber-based MZDI is made from two thermally insulated optical couplers. The length difference between the two arms needed to perform a 1-bit delay is 7.98 cm. Before detection, the signal is preamplified by a regular EDFA with a 30-dB small-signal gain and filtered by a 0.5-nm bandwidth TOF for ASE noise reduction. The direct detection is made by a 60-GHz bandwidth PIN photodiode. A 10-GHz clock is used in combination with a frequency multiplier to produce the 40-GHz electrical signal later mixed to down-convert the electrical millimeter-wave signal to its baseband form. For the uplink, the signal is amplified by an EDFA before its remodulation by a symmetric 2.5-Gb/s PRBS $2^{31} - 1$ electrical OOK signal.

In real network implementations, the diplexer connected with the antenna would act as a circulator to handle the up- and downstream signals at the BS. The baseband upstream signals would be obtained after down-conversion of the end user's information coming from the diplexer in the BS. In this experiment, the same fiber length is used for both up- and downstream signals. The uplink signal is detected by a low-frequency response receiver that also filters out the residual part of the high-frequency millimeter-wave signal.

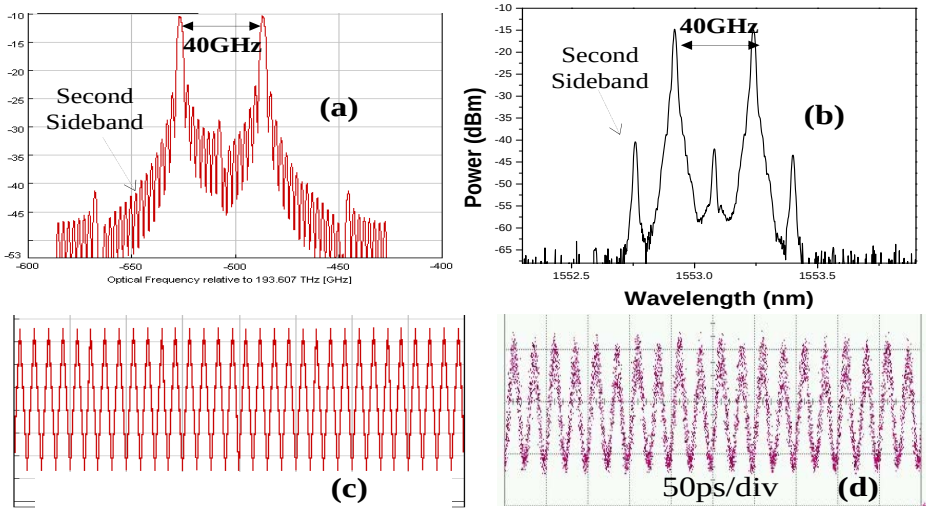

Figure 3.3: Optical spectrum (BW: 0.01 nm) and eye diagram after OCS modulation. (a), (c) for simulation results; (b), (d) for experimental results.

Figure 3.3 shows the optical spectrum and eye diagram directly obtained after the OCS modulation. It can be seen that the carrier suppression ratio is around 25 dB, and the

frequency of the generated optical LO signal is 40 GHz. Despite an overall good agreement between the simulation and experimental results, we can however notice a difference in the spectra in terms of the even-order sidebands power level. The higher measured power level is due to the imperfect control of the delay to obtain the MZM complementary driving signals performing the OCS modulation. The exact phase-shift set of the simulation provides a better suppression of the even-order (0 and second) sidebands, which results in a higher dispersion tolerance.

Because the OCS modulation creates a spectrum with two peaks separated by 40 GHz, the millimeter-wave signal will suffer from chromatic dispersion impairments experienced throughout its propagation in the SMF-28. Figure 3.4 shows the optical eye diagrams in the B-t-B configuration and after the 40-km propagation in the SMF. The power fluctuations of the 40-GHz modulation arise from the chromatic dispersion. As far as the 2.5-Gb/s signal is concerned, the difference between the experimental and simulation results are caused by the setup imperfections. In particular, the MZDI, considered perfect in the simulations, does not produce an exact and stable 1-bit delay, impacting the overall performance.

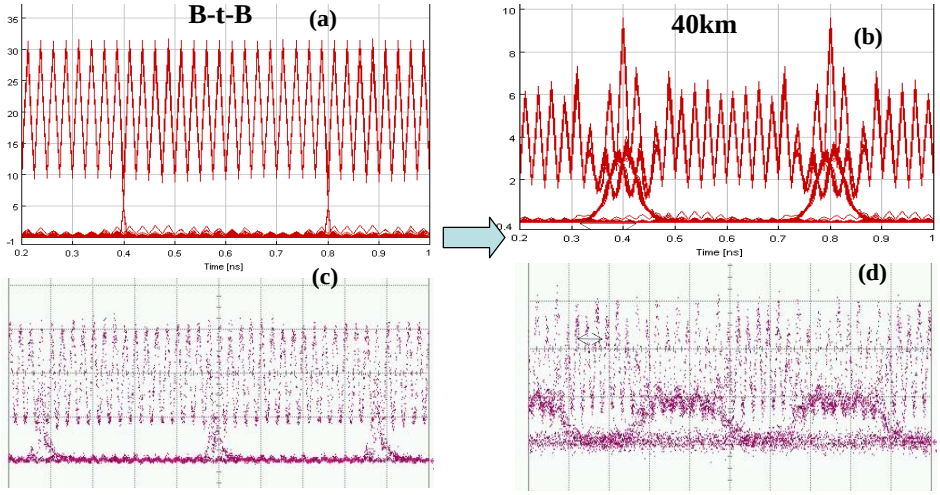

Figure 3.4: Optical eye diagrams at B-t-B and 40km transmission for (a), (b) simulation results; (c), (d) for experimental results (50 ps/div).

Figure 3.5 shows the BER curves measured for both directions as a function of the received optical power for various propagation distances. For the downlink, the optical

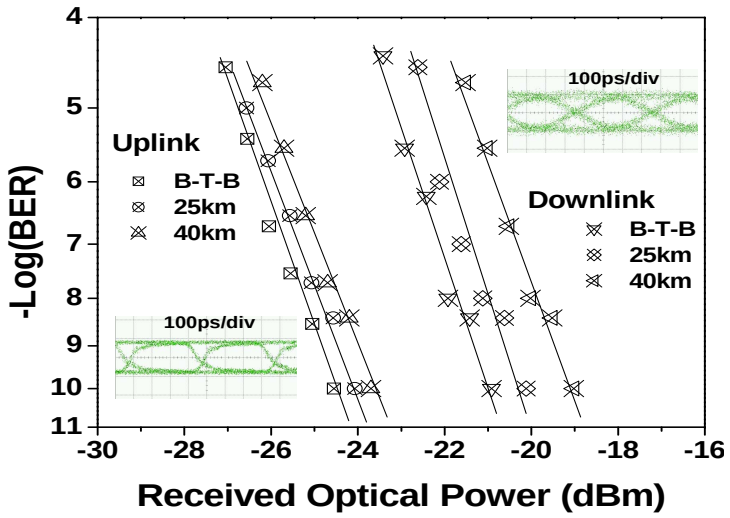

Figure 3.5: Experimental BER curves for both directions.

power is measured at the output of MZDI. After transmission over 25- and 40- km SMF, the power penalties at the given BER of 10^{-10} are 1.1 and 1.9 dB, respectively. For the uplink, since the signal at the RF carrier is filtered out by the low-speed receiver, it exhibits a better performance than the downlink. After 40-km downlink transmission, the power penalty for the remodulated optical carrier is less than 0.9 dB over the same uplink transmission distance. The eye diagrams of the B-t-B configuration for both directions are also inserted in Fig. 3.5.

In this scheme, the need for additional light source at the BS is avoided by reusing the same optical carrier via OOK modulation. The experimental results agree well with the simulation results and show that this scheme is a feasible solution for future ROF-based optical-wireless access networks.

3.3 Optical carrier suppression for downstream and reuse for upstream

The second one is based on optical carrier suppression for downstream and reuse for upstream [106], as shown in Fig. 3.6. The OCS scheme is employed to generate optical millimeter-wave and up-convert baseband data signals simultaneously for the downstream.

The original carrier is split prior to the OCS operation and then coupled with the optical millimeter-wave signal before they are transmitted to the BS. At the BS, a sharp

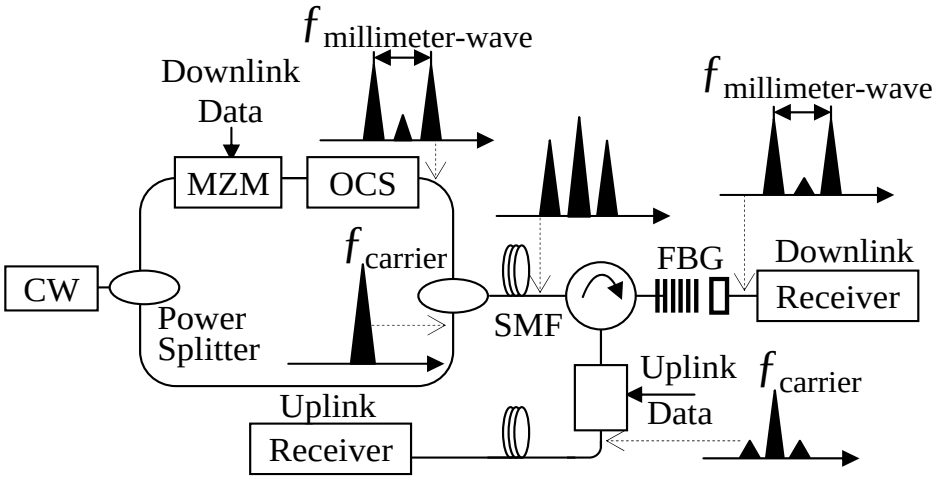

Figure 3.6: Schematic diagram of a full-duplex ROF system based on optical carrier suppression and reuse.

notch band-pass fiber Bragg grating (FBG) is used to reflect the carrier while passing the optical millimeter-wave signal to the downlink receiver. The reflected carrier acts as the continuous wave and it is remodulated with the symmetric upstream signal, and then is transmitted back to the CO, where a low-cost, low-frequency receiver detects the upstream signal [107].

The experiment setup for the OCS-based full-duplex ROF system is shown in Fig. 3.7. At the CO, a CW lightwave is generated by a TL at 1549.1 nm and split into two parts via a 50:50 optical power splitter. The first part is modulated via an MZM driven by a 2.5-Gb/s PRBS electrical signal with a word length of $2^{31} - 1$. A dual-arm MZM biased at V_π and driven by two complementary 20-GHz clocks is followed to generate optical millimeter-wave and simultaneously up-convert the 2.5-Gb/s data via the OCS. The carrier suppression ratio is around 25 dB, the repetitive frequency is 40 GHz. The optical spectrum and eye diagram after OCS are measured at points A, B and insets (i), (ii) in Fig. 3.7, respectively. Then, the generated optical millimeter-wave is amplified by an EDFA to get a power of 6 dBm for transmission. The second part is sent directly for amplification by an EDFA to obtain a power of 9 dBm and is then combined with the first part via optical coupler before they are transmitted over the SMF-28.

At the BS, an FBG is used to take on two roles: one is to reflect the optical carrier to

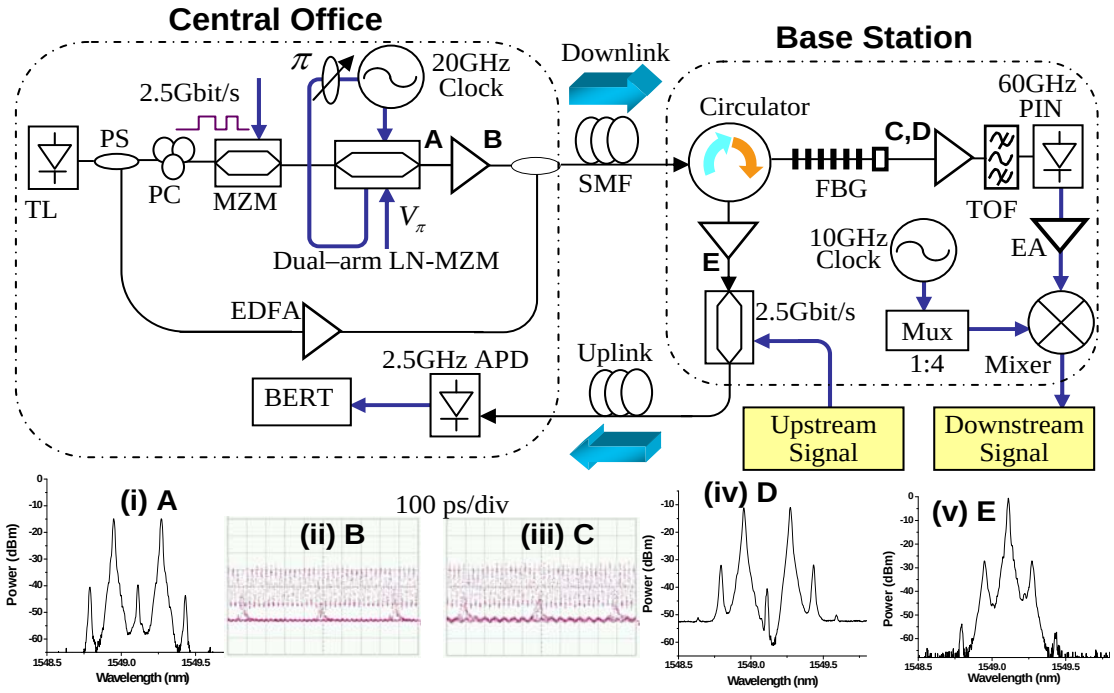

Figure 3.7: Experimental setup for full-duplex ROF system based on optical carrier suppression and reuse.

provide a CW light source for uplink connection; the other is to pass the two sidebands generated by the OCS simultaneously. As a consequence, the FBG filtering increases the carrier suppression ratio up to 30 dB as a result of sharp notch characteristics. The transmission spectrum of the FBG is shown in Fig. 3.8. This filter has a 3-dB reflection bandwidth of 0.2 nm and reflection ratio larger than 50 dB at the reflection peak wavelength. This filter performs two functions simultaneously: one is to filter the carrier to generate optical millimeter-wave for the downlink; the other is to reflect this carrier acting as the CW for the uplink. The eye diagrams and the spectrum of the passing part and reflected part are measured at points C, D, E and shown in insets (iii), (iv), and (v) in Fig. 3.7.

For the downlink, the optical millimeter-wave signal is preamplified by a regular EDFA with a small-signal gain of 30 dB, then, filtered by a tunable optical filter with the bandwidth of 0.5 nm to suppress ASE noise before O/E conversion via a PIN photodetector with a 3-dB bandwidth of 60 GHz.

The converted electrical signal is amplified by an electrical amplifier with a bandwidth

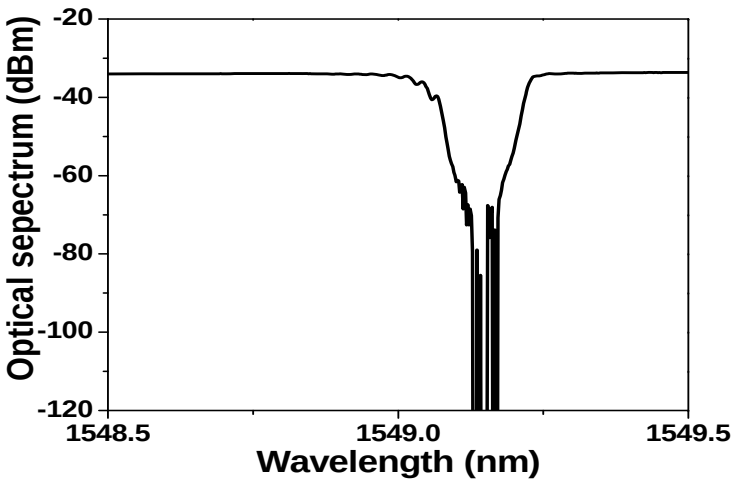

Figure 3.8: Transmission spectrum of the FBG filter.

of 10 GHz centered at 40 GHz. An electrical LO signal at 40 GHz is generated by using a frequency multiplier from 10 to 40 GHz. We use the electrical LO signal and a mixer to down-convert the electrical millimeter-wave signal to the baseband signal. The down-converted 2.5-Gb/s signal is detected by a BER tester. Eye diagrams are recorded by a high-speed oscilloscope and shown in Fig. 3.9 at different transmission distances. It is clearly seen that the eye still remains open despite transmission over 40-km SMF, but the crossing point of the eye increases quickly, which arises from the dispersion-induced pulse expansion.

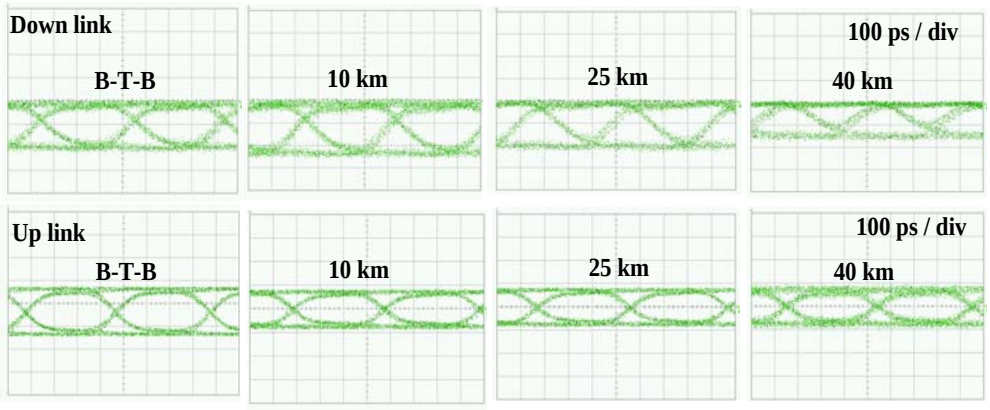

Figure 3.9: Electrical eye diagrams after different length transmission for the downlink and uplink.

On the other hand, for the uplink, the reflected signal is amplified by an EDFA to compensate the insertion loss of the filter before it is modulated by a symmetric 2.5-Gb/s PRBS electrical signal with a word length of $2^{31}-1$. After transmission over the same length SMF-28 as the downlink channel, a low-frequency response receiver is employed to detect 2.5-Gb/s data signal and filter out the residual part of the high-frequency millimeter-wave signal. Compared with the downlink millimeter-wave signals, the uplink signals might be transmitted a longer distance because most of the components of high frequency are already removed by the FBG filter before they are sent back to the CO.

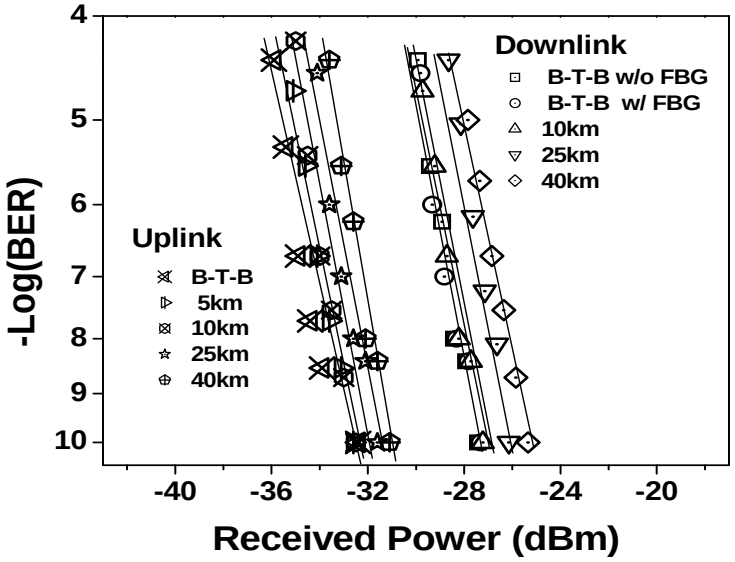

Figure 3.10: BER curves for both directions in the OCS-based ROF system.

3.4 A PM with optical filter for downstream and SOA for upstream

The third one is based on a PM with a subsequent filter for downstream and directly modulated SOA for upstream [108]. In Chapter 2, we demonstrate that optical millimeter-wave can be generated by an optical phase modulator in tandem with an optical filter. This scheme shows excellent performance in terms of the system configuration simplicity, stability, and high performance after long transmission distance, making it a desirable candidate for the downlink transmission. As far as the uplink connection is concerned, the network architecture consisting of a single light source at the CO and the reuse of the downlink wavelength at the BS is an attractive solution for low-cost implementation.

However, the optical amplifier and external modulator are still required to compensate the power loss and modulate upstream signals at the BS. Here we present the experimental demonstration of one single SOA as both the amplifier and the modulator for the upstream signal. The schematic diagram of this full-duplex optical-wireless system is shown in Fig. 3.11 [109].

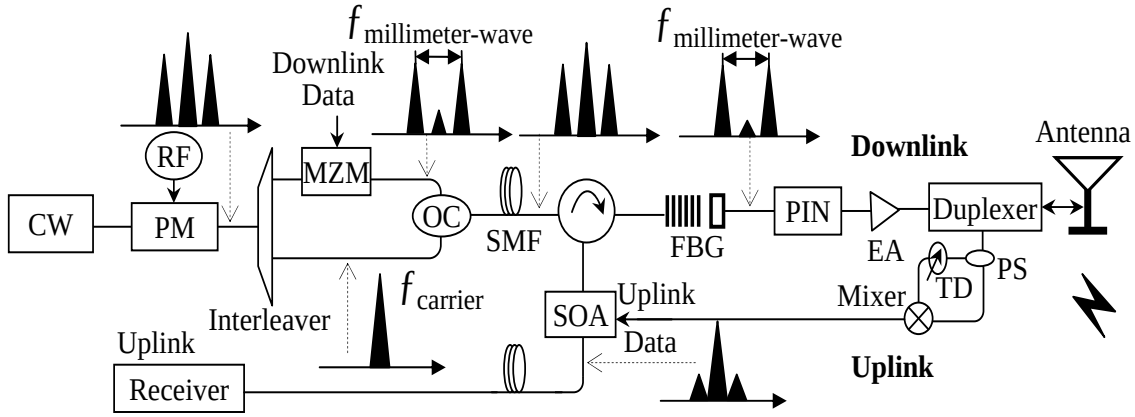

Figure 3.11: Architecture of a full-duplex optical-wireless system based on PM and SOA.

An optical PM is driven by a small RF signal (1/4 half-wave voltage of the PM) to create first-order sidebands while suppressing the second-order components for increasing dispersion tolerance. An optical interleaver is employed to separate the optical carrier from the first-order sidebands to generate an optical millimeter-wave carrier. After modulation by downlink data, the up-converted optical signal is combined with the original optical carrier and transmitted over the SMF. At the BS, an FBG is used to reflect the optical carrier while passing the optical millimeter-wave signal to O/E conversion at the downstream receiver side. Then, the boosted electrical millimeter-wave signal is broadcasted by an antenna through a diplexer acting as a circulator to handle the up- and downstream signals at the BS. Meanwhile, the upstream signals are down-converted through a mixer and a tunable delay (TD) line. The reflected optical carrier is considered the continuous wave and is directly modulated by the basedband upstream signals in the SOA and sent back to the CO, where a low-cost and low-frequency response receiver is used for the detection. In this scheme, the SOA performs the function of both amplification and modulation, which

eliminates the requirements of an extra optical amplifier and external modulator at the BS.

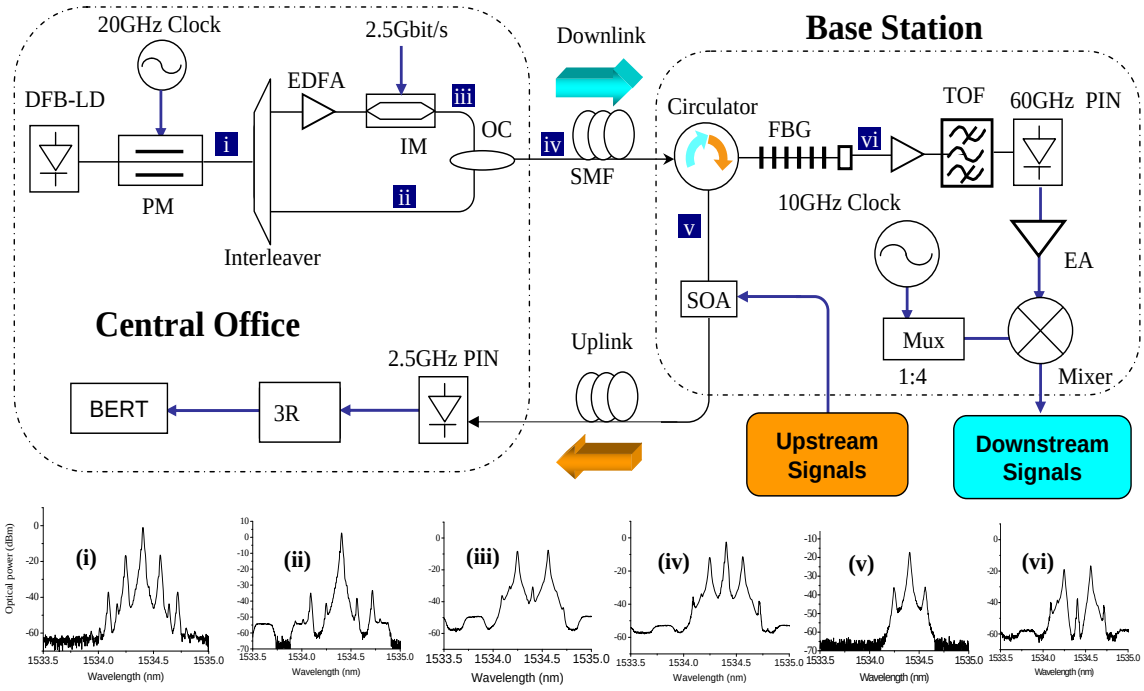

Figure 3.12: Experimental setup for the full-duplex optical-wireless system by using wavelength reuse and directly modulated SOA. The optical spectra measured at point a, b, c, d, e, f are all inserted as insets.

Figure 3.12 depicts the experiment setup for the full-duplex optical-wireless system using wavelength reuse and directly modulated SOA. At the CO, A CW lightwave is generated by a DFB-LD at 1534.4 nm and modulated by a LiNbO3 PM driven by a 20-GHz RF sinusoidal wave with amplitude 6 V (half-wave voltage of the PM is 11 V). The optical spectrum (measured at point i) after modulation is shown in Fig. 3.12 inset (i). Since the driving voltage is much smaller than the half-wave voltage of the PM, the second-order components are 21 dB lower than the first-order sidebands, which greatly increases the fiber dispersion tolerance of the optical millimeter-wave signal. A 50/25-GHz optical interleaver with 35-dB channel isolation is used to separate the remaining optical carrier from the first-order sidebands. The generated optical millimeter-wave is then amplified and modulated by an intensity modulator (IM) driven by a 2.5-Gb/s PRBS $2^{31} - 1$ electrical downstream signals. The separated optical carrier is directly sent to combine with up-converted baseband signals via optical coupler before its transmission over 40-km SMF-28 with 8-dBm input

power. The optical spectra of the separated optical carrier, optical millimeter-wave signal, and combined signals are shown in Fig. 3.12 inset (ii), inset (iii), and inset (iv), respectively.

At the BS, an FBG is used to reflect the optical carrier and simultaneously transmit the optical millimeter-wave signals. The FBG filter has a 3-dB reflection bandwidth of 0.24 nm and reflection ratio larger than 50 dB at the reflection peak wavelength. The spectra of reflected carrier and transmitted optical millimeter-wave signals are shown in Fig. 3.12 inset (v) and inset (vi). Before downstream detection, the signal is preamplified by a regular EDFA with a 30-dB small-signal gain and filtered by a 0.5-nm bandwidth tunable optical filter for ASE noise reduction. The direct detection is made by a 60-GHz bandwidth PIN photodiode. The converted electrical millimeter-wave signal is then amplified by an electrical amplifier with a bandwidth of 10 GHz centered at 40 GHz. A 10-GHz clock is used in combination with a frequency multiplexer to produce a 40-GHz electrical LO signal later mixed to down-convert the electrical signal to its baseband form.

For the uplink, the reflected optical carrier is directly modulated in an SOA driven by a 250-Mb/s (PRBS $2^7 - 1$) electrical signal with amplitude 3.1 V and 165-mA bias. The gain is 10 dB in the 34-nm spectral width, and the polarization sensitivity is smaller than 0.5 dB. In this experiment, the same fiber length is used for both up- and downstreams. The uplink signal is detected by a low-frequency response receiver, which also filters out the residual part of the high-frequency millimeter-wave signal resulting from imperfect filtering by the FBG.

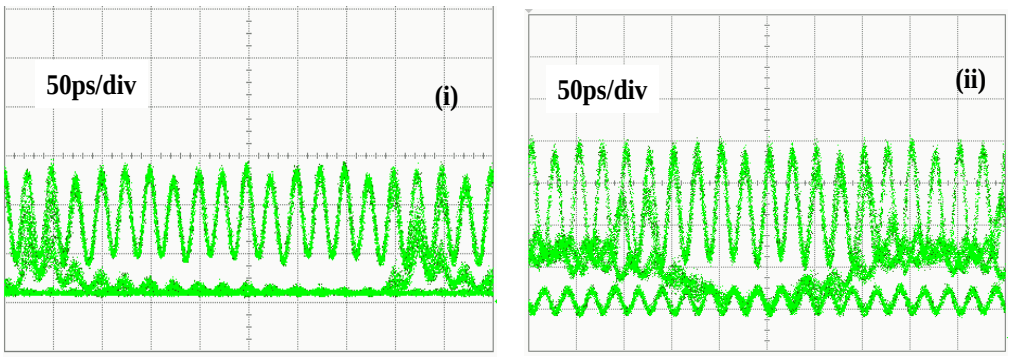

Figure 3.13: Measured optical eye diagrams for downstream signals at (i) B-t-B and (ii) after 40-km transmission.

Figure 3.13 shows the optical eye diagrams in the B-t-B configuration and after the 40-km propagation in the SMF. The power fluctuations of the 40-GHz modulation arise from the chromatic dispersion in the fiber. Figure 3.14 shows the BER curves measured for both up- and downlinks as a function of the received optical power. For the downlink, the power penalty at the given BER of 10^{-9} is 2.0 dB after 40-km transmission. For the uplink, the power penalty for the remodulated optical carrier is around 0.5 dB over the same transmission distance. The eye diagrams of the B-t-B configuration for both directions are also inserted in Fig. 3.14.

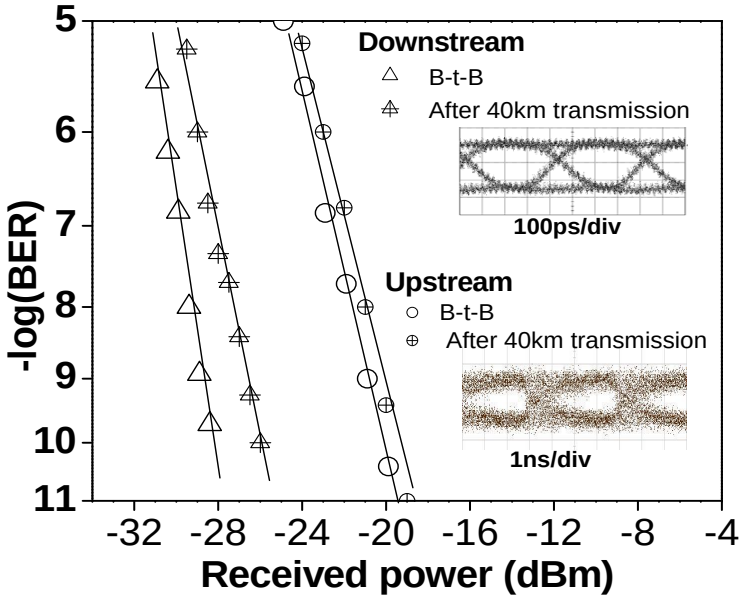

Figure 3.14: BER curves for both directions in the ROF system using the PM and SOA.

In this scheme, the PM and subsequent interleaver demonstrate unique advantages in terms of the system simplicity and transmission performance. For the uplink, the need for additional light source, optical amplifier and external modulator in the BS are avoided by the use of the directly modulated SOA as the colorless amplified modulator. The experimental results exhibit that this scheme is a highly practical solution for future optical-wireless access networks.

3.5 60-GHz signals over a single span of optical fiber

The previous three advanced schemes are all based on wavelength reuse for both downlink and uplink connections using two separated optic fiber spools. In this section, we present the experimental demonstration of a 60-GHz ROF system simultaneously transmitting a 2.5-Gb/s data for both directions over a single spool of 25-km SMF-28. For the downlink connection, OCS technology is used to optically up-convert the baseband signals to the 60-GHz carrier. To mitigate the signal degradation caused by backreflection in the same fiber, the spectral-broadening scheme has been shown to be effective in this respect [110]. In this work, low-frequency OCS and subcarrier multiplexing techniques are used to spectrally broaden the upstream signal for the reduction of the spectral overlap of the signal and the backreflected light.

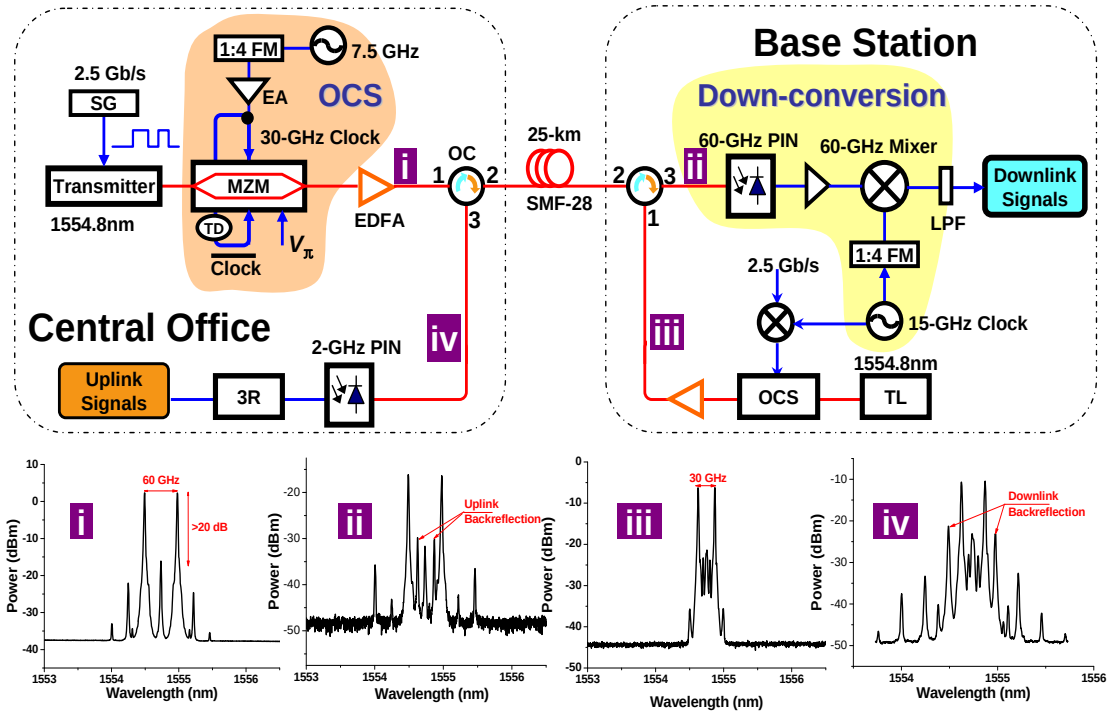

Figure 3.15: Experimental setup of 60-GHz bidirectional transmission over a single spool of SMF.

The experimental setup for the 60-GHz bidirectional ROF system is shown in Fig. 3.15. At the CO, a CW lightwave is generated in a transmitter at 1554.8 nm and is modulated by a 2.5-Gb/s PRBS electrical signal with a word length of $2^{31}-1$. A dual-arm MZM biased at V_π

and driven by two complementary 30-GHz clocks is followed to generate optical millimeter-wave and simultaneously up-convert the 2.5-Gb/s data via the OCS. The 30-GHz clock is generated using a 1:4 frequency multiplier (FM) and a 7.5-GHz microwave synthesizer. The carrier suppression ratio is around 20 dB, the repetitive frequency of the generated optical LO signal is 60 GHz, and the duty cycle of the LO is 0.6. The optical signal is then amplified by an EDFA to 8 dBm before transmission over the optical circulators and a 25-km SMF link. The optical spectrum of modulated signals after amplification is shown in Fig. 3.15 inset (i). The optical eye diagrams of the generated optical millimeter-wave signal is shown in Fig. 3.16 insets (i) and (iii).

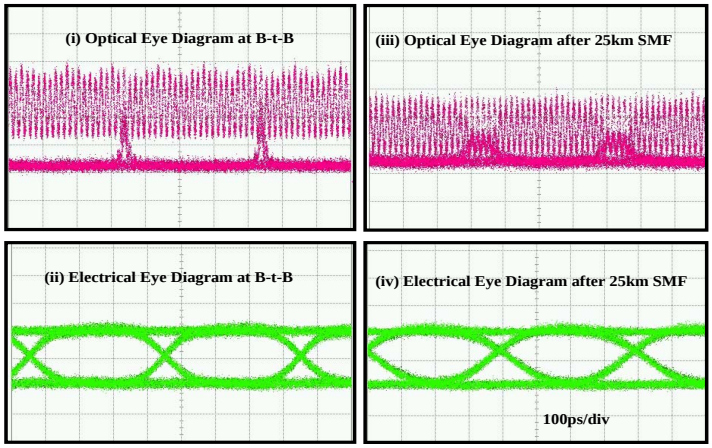

Figure 3.16: Eye diagrams of the downlink connection.

Regarding the downlink connection in the BS, direct detection is made by a 60-GHz bandwidth PIN photodiode to realize O/E conversion. The converted electrical millimeter-wave signal is then amplified to 3.55 Vpp by an electrical amplifier with 5-GHz bandwidth centered at 60 GHz. A 15-GHz clock is used in combination with an FM to produce a 60-GHz electrical LO signal later mixed to down-convert the electrical signal to its baseband form. For the uplink direction, the 15-GHz clock from the same source as the down-conversion is used to mix with the 2.5-Gb/s signal to generate a SCM signal for the low-frequency OCS realization. The modulated uplink signals are spectrally broadened to be 30-GHz allocation. After amplification, the upstream signals pass through the optical circulators and the same fiber spool to the CO. The insertion loss and directivity of each optical circulator is 1 dB,

and larger than 50 dB, respectively. A 2-GHz bandwidth receiver is employed to detect the 2.5-Gb/s data signal and simultaneously filter out the residual part of the high-frequency signal. The insets (ii) and (iv) in Fig. 3.15 show the optical spectra at the receiver side for bidirectional signals. The backreflected noise arises from the 25-km SMF and optical components with comparable power level of suppressed optical carrier.

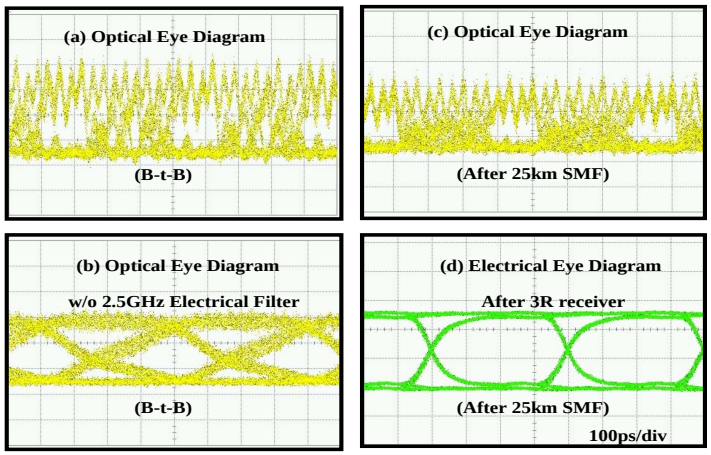

Figure 3.17: Eye diagrams of the uplink connection.

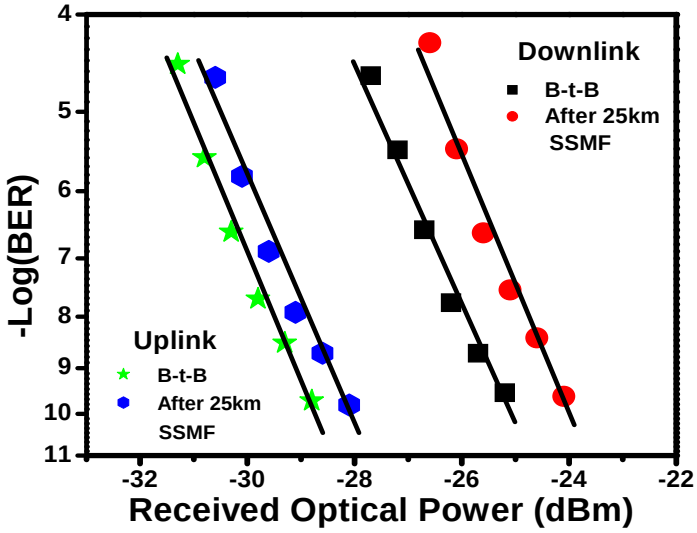

Figure 3.18: BER curves of both directions with 2.5-Gb/s signals in 60-GHz ROF systems.

Figure 3.16 and 3.17 shows the optical and electrical eye diagrams at B-t-B and 25-km SMF-28 transmission for both down- and uplinks. It is seen that the power of 60-GHz carrier is faded resulting from the chromatic dispersion. The measured BER curves in Fig.

3.18 show that the power penalty after 25-km transmission is less than 1.1 dB for downlink connection while 0.6 dB for uplink at a BER of 10^{-10}. The penalty mainly arises from the chromatic dispersion of the fiber, ASE noise of the EDFAs, and backreflection along the optical link. The receiver sensitivity is relatively high because of the use of optical preamplifier. The results show transport feasibility of super-broadband wireless signals at 60-GHz band over a single fiber in future cost-efficient optical-wireless access networks.

3.6 Chapter summary

In this chapter, four full-duplex optical-wireless systems have been presented. Table 3.1 summarizes the advantages and disadvantages of the four designs of the full-duplex system. Three schemes use the sole centralized light source for both directions based on the wavelength reuse method. The experimental results suggest that the system using one colorless SOA as both the amplifier and the modulator for the upstream signal is a practical solution for future optical-wireless access networks in terms of low cost and easy maintenance.

Table 3.1: Comparison of full-duplex operation schemes

Schemes	Advantages	Disadvantages
Modulation format	High tolerance for nonlinear effect and coherent crosstalk, and high-spectral efficiency.	Need athermal design of MZDI for temperature sensitivity.
OCS and reuse	High receiver sensitivity and simple configuration.	Need a control electrical circuit to optimize the DC bias.
PM and SOA	Eliminate the need for amplifiers and external modulators at the BS using a colorless SOA.	Need reflective SOA (RSOA) to increase the direct modulation bandwidth ($<$ 3 Gb/s).
Single span of fiber	High power budget, no need for a sharp optical filter.	Backscattering influence, extra laser source in the BS.

CHAPTER IV

OPTICAL-WIRELESS CONVERGENCE FOR ACCESS NETWORKS

To exploit the benefits of both wired and wireless systems, carriers and service provides are seeking a converged access network architecture that simultaneously delivers wired and wireless services in a unified platform. The convergence of optical and wireless technologies can offer such services to the end users. In this chapter, three different technologies are presented for simultaneous delivery of baseband and wireless signals in a single platform. These include the technology based on cascaded modulation in section 4.2, the technology using a single dual-arm intensity modulator in section 4.3, and the technology based on photonic frequency tripling in section 4.4. Finally, all these technologies for dual-service generation and transmission in a single system are summarized in section 4.5.

4.1 Introduction

Today's wired networks, based on passive optical network (PON) access technologies, have the capability of providing huge bandwidth to end users using optical fiber, but are not flexible enough to allow convenient roaming connections. On the other hand, wireless-based access solutions offer portability and flexibility to users, but do not possess abundant bandwidth to meet the ultimate demand for multi-channel video services with HD quality. To exploit the benefits of both wired and wireless technologies, carriers and service provides are actively seeking a convergent network architecture to deliver multiple services to serve both fixed and mobile users [111]. This can be accomplished by using hybrid optical-wireless networks, which not only can transmit wireless signals at the BS over fiber, but also simultaneously provide the wired and wireless services to the end users [112] [113]. In this Chapter, three different methods for simultaneously providing wired and wireless services are presented. The real air transmission is implemented in the cascaded modulation scheme. Moreover, we design and experimentally demonstrate an efficient photonic frequency tripling technology for a 60-GHz ROF system to simultaneously realize millimeter-wave, microwave,

and baseband signal generation (multi-band generation). The technique utilizes vestigial sideband (VSB) filtering in combination with the OCS to generate novel alternate subcarrier modulations for high tolerance of fiber chromatic dispersion.

4.2 Dual signals generation based on two cascaded modulation schemes

The generation methods of optical millimeter-wave signals have been presented in the previous chapter. These include the technologies based on optical nonlinear effect, external intensity modulation, and external phase modulation. In such developed systems, a part of baseband signal also exists in the whole electrical spectrum in addition to the millimeter-wave carrier after all-optical up-conversion. To illustrate this point, the process of all-optical up-conversion schemes are simulated based on the FWM in the HNL-DSF and the OCS modulation.

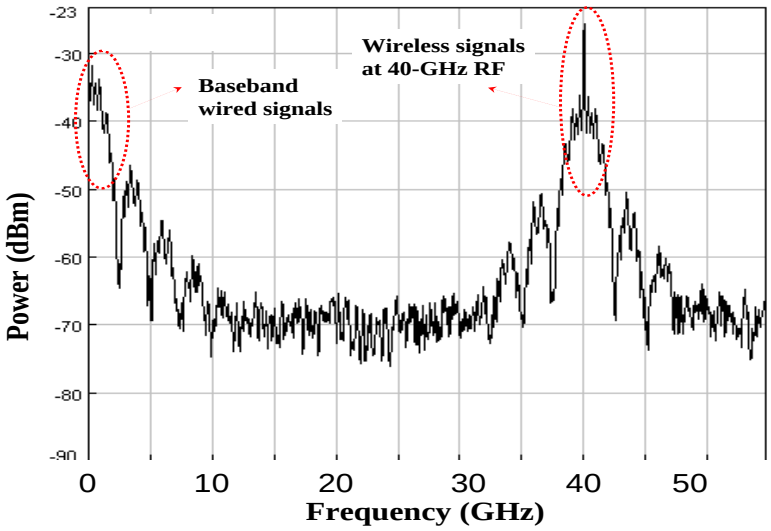

Figure 4.1: Electrical spectrum after all-optical up-conversion scheme based on the FWM in HNL-DSF.

Figure 4.1 shows the electrical spectra after all-optical up-conversion based on the FWM effect in the HNL-DSF. The LO frequency for the up-conversion scheme is 40 GHz and the baseband signal is a 2.5-Gb/s nonreturn-to-zero (NRZ) signal. It is clearly seen that there are two components in the electrical spectrum after all-optical up-conversion, one part occupies the baseband, the other occupies high-frequency band at 40 GHz. Figure 4.2 shows that the OCS-based optical millimeter-wave generation has the same signal spectrum

allocation as the FWM-based scheme. So, we propose a new architecture to use the baseband signals for broadband optical wired access and RF signal for wireless connection.

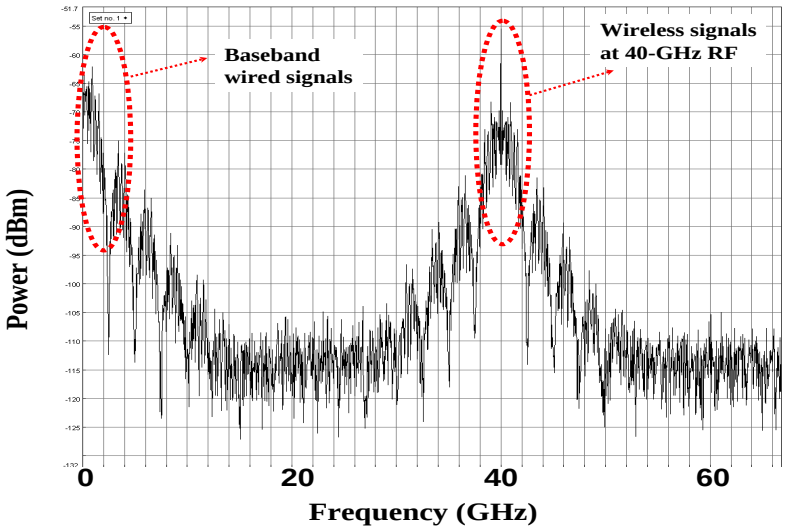

Figure 4.2: Electrical spectrum after all-optical up-conversion scheme based on the OCS modulation.

Figure 4.3 illustrates the architecture for concurrently providing super-broadband wireless and wired services. The content providers or upstream networks send the data to the CO, where the multi-channel millimeter-wave carriers are generated using our developed all-optical up-conversion methods. These up-conversion techniques offer many advantages that allow data to be transmitted over wired and wireless medium in a single platform. First, the generation of the millimeter-wave carrier and the up-conversion of the original data channel are performed simultaneously in the optical domain. Second, as a result of this process, two identical data signals are generated concurrently: one at the electrical baseband and another at the RF-carrier frequency. The up-converted signals are then multiplexed before they are transmitted over fiber to the BS where an AWG in a WDM-PON system is used to route the signals to the customer premise. At the customer premise, the signal is divided by an optical PS into two. The first part is detected by a high-speed receiver and then electrically amplified using a narrow-band RF amplifier before it is broadcasted by an antenna as a wireless signal. The other part is sent directly to a wall-mounted optical port through a fiber access, and a user can utilize a simple, low-cost receiver to detect the

baseband data signal by filtering out the high-frequency millimeter-wave signal.

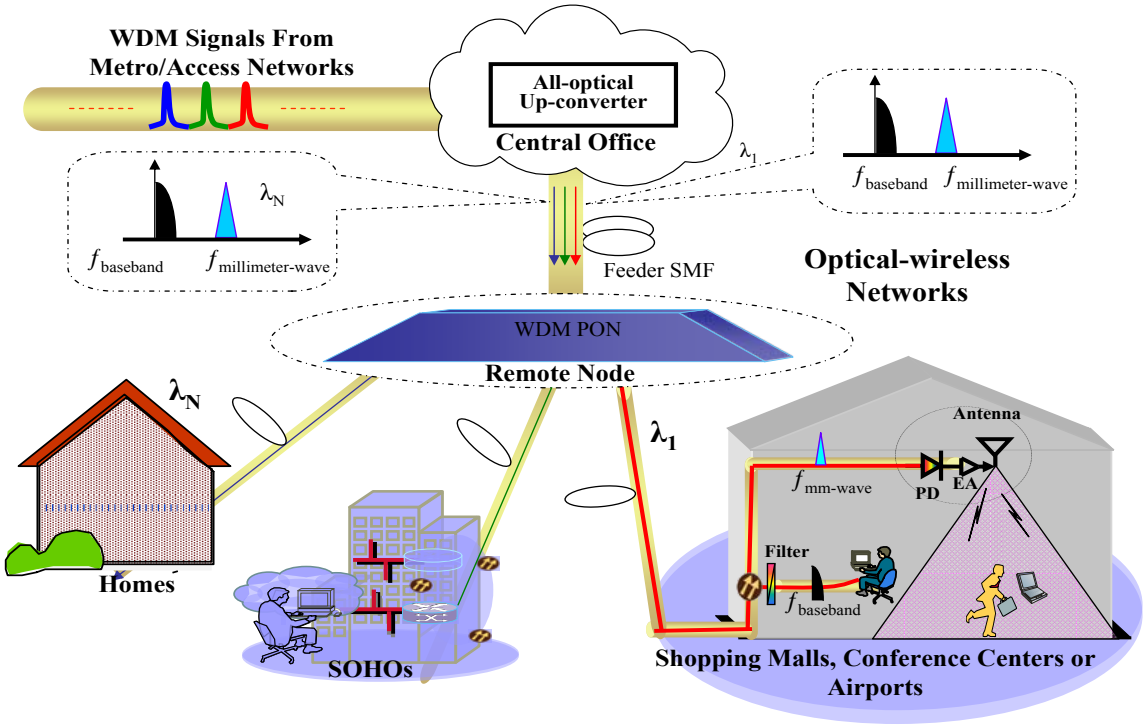

Figure 4.3: A novel network architecture for simultaneously providing wired and wireless services in an optical-wireless network.

This newly hybrid system can allow wired and wireless transmission of the same content such as high-definition video, data and voice up to 100 times faster than current networks. The same services will be provided to customers who either plug into the wired connection in a wall or access the same information through a wireless system. The customer premise can be conference centers, airports, hotels, shopping malls and ultimately homes and small offices.

4.2.1 Dual signals generation using OCS-based up-conversion

The OCS-based experimental platform is shown in Fig. 4.4. A DFB laser array is turned on and modulated by a LiNbO3 MZM driven by a 2.5-Gb/s electrical signal with a PRBS word length of $2^{31} - 1$. The modulated signals are transmitted over a 40-km SMF-28 for decorrelation before they are up-converted using the OCS technique. Up-conversion using the OCS is realized using a dual-arm MZM biased at V_π and driven by two complementary 17.5-GHz clocks. This results in a carrier suppression ratio of larger than 25 dB, and the

separation frequency of the two optical sidebands of 35 GHz (Ka-band). The up-converted millimeter-wave signals are then amplified by an EDFA to obtain 12-dBm power before transmission over a 25-km SMF-28 to the BS.

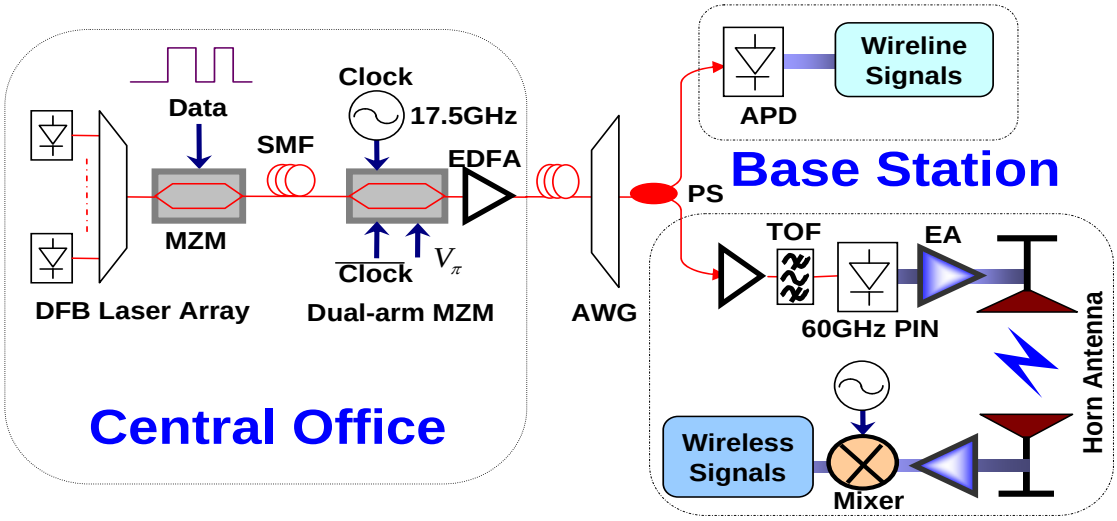

Figure 4.4: Experimental setup for simultaneously delivering wired and wireless services in the OCS-based platform.

At the BS, one optical millimeter-wave channel is selected via an optical filter and then divided into two branches. One part, used for the wired link, is passed through a low-speed avalanche photodiode (APD) that has 2-GHz bandwidth. Because the response bandwidth is limited at 2 GHz, the high-frequency RF components are filtered out. To produce the wireless signal, the second branch is preamplified by an EDFA with a small-signal gain of 30 dB. It is then filtered by a TOF before it is detected by a PIN PD with a 3-dB bandwidth of 60 GHz. The converted electrical signal is boosted by an RF electrical amplifier with a bandwidth of 10 GHz centered at 40 GHz before it is broadcasted through a double ridge guide antenna with 19.2-dBi gain. After wireless propagation, the signal is received by another identical millimeter-wave horn antenna. A 35-GHz electrical LO signal is generated using a 1:4 frequency multiplier, and it is used to down-convert the electrical millimeter-wave signal to its baseband form. The receiver sensitivities and eye diagrams for 2.5 Gb/s at different air distances are shown in Fig. 4.5. The power penalty after transmission over 25-km SMF is less than 1.5 dB.

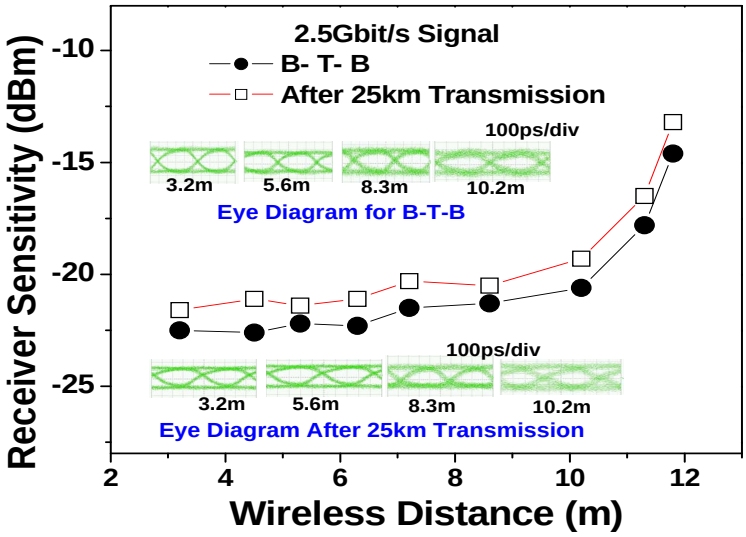

Figure 4.5: Receiver sensitivity for 2.5-Gb/s signal at different wireless distance.

The receiver sensitivity degrades quickly when the wireless signals are transmitted beyond approximately 10 m because the power is dispersed over air space. The signal degradation through multiple reflections from the wall is also a key factor that limits the maximum transmission distance for the 2.5-Gb/s wireless signal in our testbed environment (an office building hallway). We then set the data rate to 1.25 Gb/s, the BER curves and eye diagrams are measured and shown in Fig. 4.6 after 25-km fiber transmission. It is observed that the receiver sensitivity is increased by about 1.5 dB compared to the 2.5-Gb/s case.

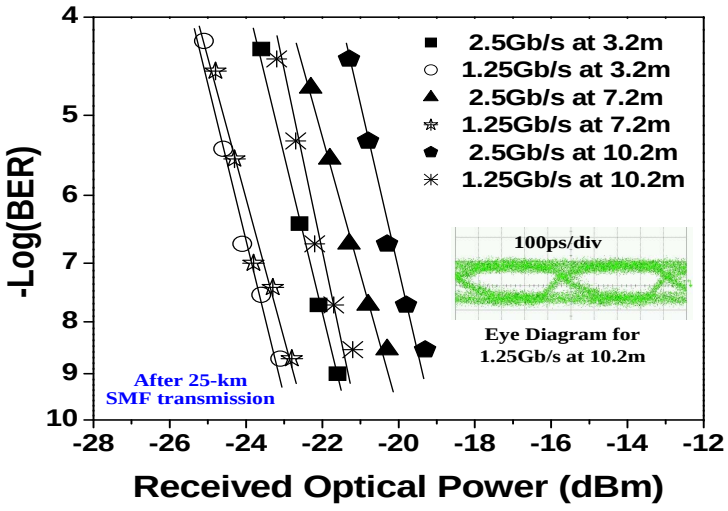

Figure 4.6: BER curves for 2.5 and 1.25 Gb/s signals.

4.2.2 Dual signals generation using PM and an optical filter

Figure 4.7 shows the experimental setup for the wired and wireless optical-wireless system using an optical PM and an FBG. At the CO, a tunable CW laser at 1549.1 nm is modulated by a LiNbO3 PM driven by a 15-GHz RF sinusoidal wave with amplitude of 6 V (the half-wave voltage of the PM is 11 V).

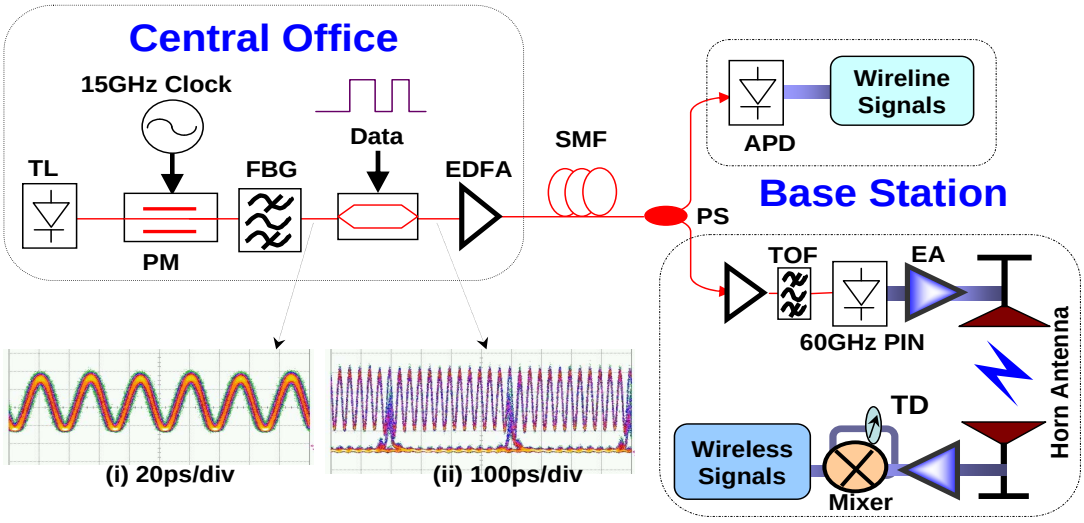

Figure 4.7: Experimental setup for 30-GHz millimeter-wave generation and wireless transmission based on an optical PM and an FBG.

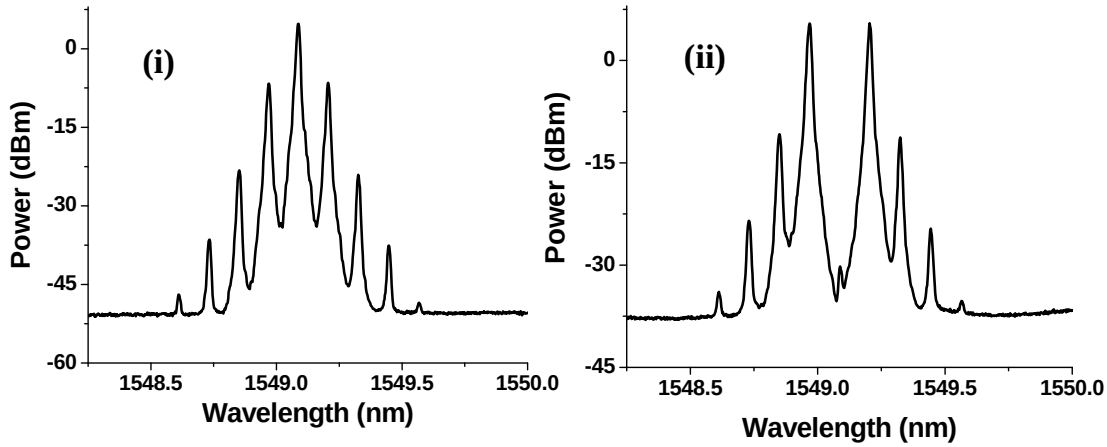

Figure 4.8: Optical spectra after PM (i) and FBG (ii) (resolution: 0.01 nm).

The optical spectrum after phase modulation is shown in Fig. 4.8 (i). It is seen that the power ratio between first- and second-order sidebands is larger than 15 dB. Then an FBG

is used to suppress the optical carrier and realize the frequency modulation to intensity modulation (FM-IM) conversion, which is shown as inset (ii) in Fig. 4.8. This FBG has a 3-dB reflection bandwidth of 0.2 nm and a reflection ratio larger than 50 dB at the reflection peak wavelength. It is seen that the suppression ratio for the carrier is larger than 35 dB. Next, the generated optical millimeter-wave is modulated by an MZM driven by an electrical PRBS signal. The corresponding optical spectrum and eye diagram are shown in Fig. 4.7 insets (i) and (ii). The optical millimeter-wave is then amplified by an EDFA to 13 dBm before transmission over SMF-28.

At the BS, the optical millimeter-wave is divided into two parts. The wired part is sent to a low-speed APD that has a 3-dB bandwidth of 2 GHz. In the case of the wireless part, the signal is preamplified by an EDFA and filtered by a TOF to suppress ASE noise, then detected by a PIN PD with a 3-dB bandwidth of 60-GHz. The converted electrical signal is boosted by an EA before it is broadcasted through a double ridge guide antenna. After wireless transmission, the signal is received by another identical millimeter-wave antenna and down-converted through a mixer and tunable delay line. Here we use the incoming signal as an LO signal.

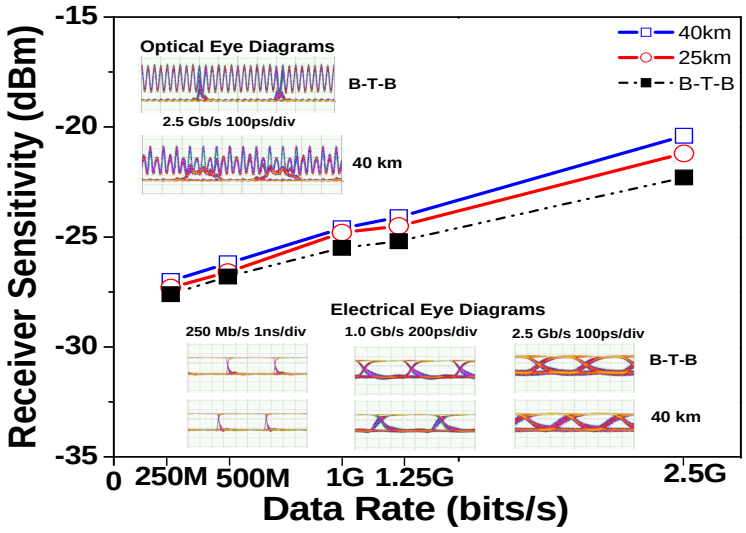

Figure 4.9: Receiver sensitivity at various data rates and transmission distances.

The receiver sensitivities and eye diagrams at different data rates and transmission distances are shown in Fig. 4.9. The 4-m wireless transmission distance is set to emulate

coverage of a picocell room. The power fluctuations after 40-km SMF propagation in the optical eye diagrams arise from the chromatic dispersion. The power penalties of four data rates are less than 2 dB after 40-km transmission. We observe that the 250-Mb/s data signal has a 5-dB improvement in receiver sensitivity through the same SMF and air transmission distance compared to the 2.5-Gb/s signal. The eye diagrams and BER curves after 25-km fiber transmission for wired and wireless data at 1 and 2.5 Gb/s are shown in Fig. 4.10. It is observed that 3.5-dB improvement of receiver sensitivity at a BER of 10^{-10} can be obtained when the data rate is decreased from 2.5 Gb/s to 1.0 Gb/s.

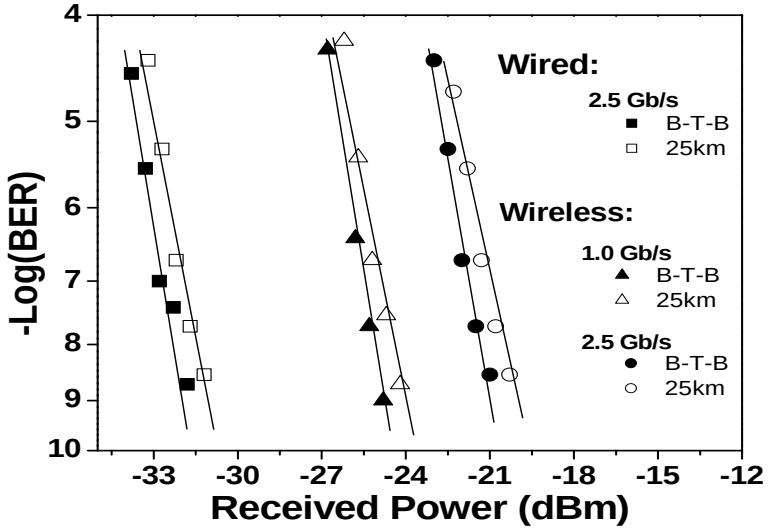

Figure 4.10: BER curves for both wired and wireless signals.

The wireless link power budget is also analyzed [114] for a 35-GHz (8.57 mm) system over a 10.2-m wireless link based on the Friis transmission equation, which is given as follows

$$P_R = P_T + G_T + G_R - 20\log(4\pi R/\lambda). \tag{4.1}$$

The parameters are shown in Fig. 4.11. In our platform, the transmitted power P_T is 15 dBm, and the antenna gain G_T is 19.2 dBi. At the position A_1, it is assumed that the emitted power is P_T if there is no loss from the passive antenna. The equation (4.1) gives the received power P_R as -30.1 dBm. The noise is dominated by the LNA noise figure (5 dB) based on Friis' formula (the mixer phase noise and return loss are not considered here). Therefore, the signal to noise ratio (SNR) in this situation is 37.9 dB. The real SNR

should be smaller than this if we include the multi-path distortion and phase noise from other components.

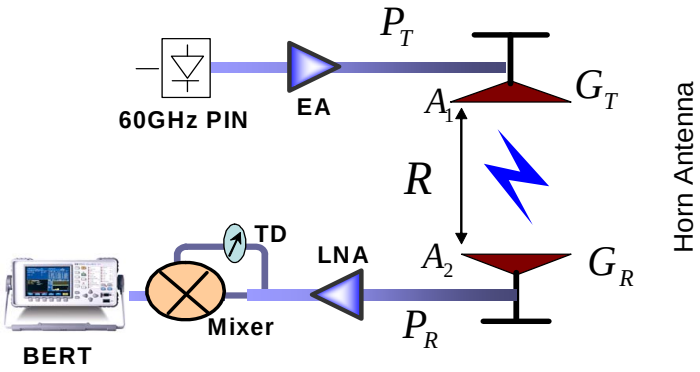

Figure 4.11: Estimation of wireless link power budget.

4.3 Dual signals generation based on a single intensity modulator

We have demonstrated that the wired and wireless services can be provided by the cascaded platform in Section 4.2. However, these systems require two modulators to perform baseband signals modulation and up-conversion separately, which increases the cost and complexity of the ROF system. Recently, the simultaneous multi-band modulation and transmission have been demonstrated. The techniques in [115] and [116] use an EAM to simultaneously generate baseband, microwave-band, and 60-GHz-band signals. However, the signal performance is limited by the EAM nonlinearity, residual chirp, and the crosstalk among three signals. Additionally, this method requires lossy splitters and high-frequency LO signals. The work in [117] and [118] employs an MZM to realize hybrid integration of ROF and FTTH systems. However, the techniques either need multiple laser sources and costly AWG or an integrated modulator consisting of three single-electrode MZMs. In [119], another system using a single dual-arm MZM and remote LO delivery has been proposed. But, it needs electrical up-conversion at the BS and only provides wireless signals.

In this section, we experimentally demonstrate a novel ROF scheme to simultaneously provide independent wired and wireless services using a single dual-arm intensity modulator [120]. The schematic using a single modulator for the generation of wired and wireless services is shown in Fig. 4.12.

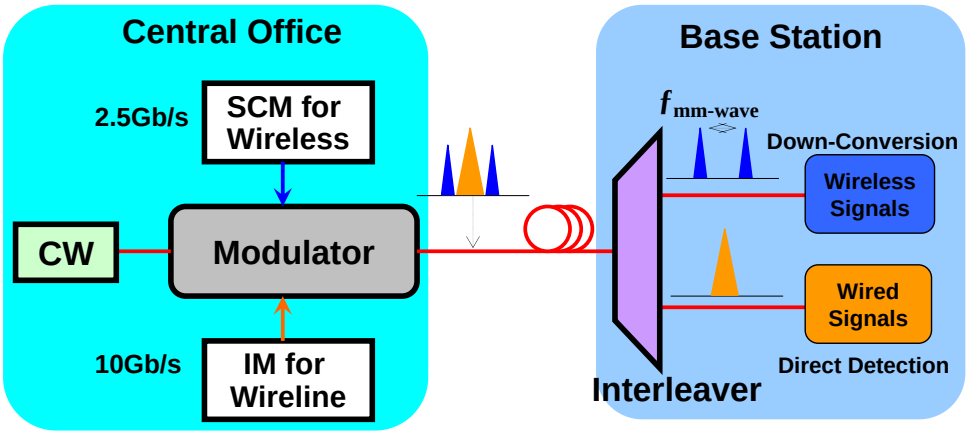

Figure 4.12: Schematic diagram of a simultaneous generation of wired and wireless services using a single modulator.

In the CO, a 2.5-Gb/s wireless signal and an RF signal at half of the LO frequency are mixed by using SCM. The mixed signal and the 10-Gb/s wired baseband signal are applied simultaneously to drive a dual-arm MZM biased at the optimal modulation condition. As a result, 2.5-Gb/s wireless signals are carried on two subcarriers separated by a frequency of LO in the optical domain while 10-Gb/s wired signals are imposed on the optical carrier. At the BS, an interleaver is used to separate the incoming signals into two branches: the SCM signals are detected by a high-speed receiver and broadcasted by an antenna for wireless access. Another one is sent directly to a low-cost receiver to detect the wired signal.

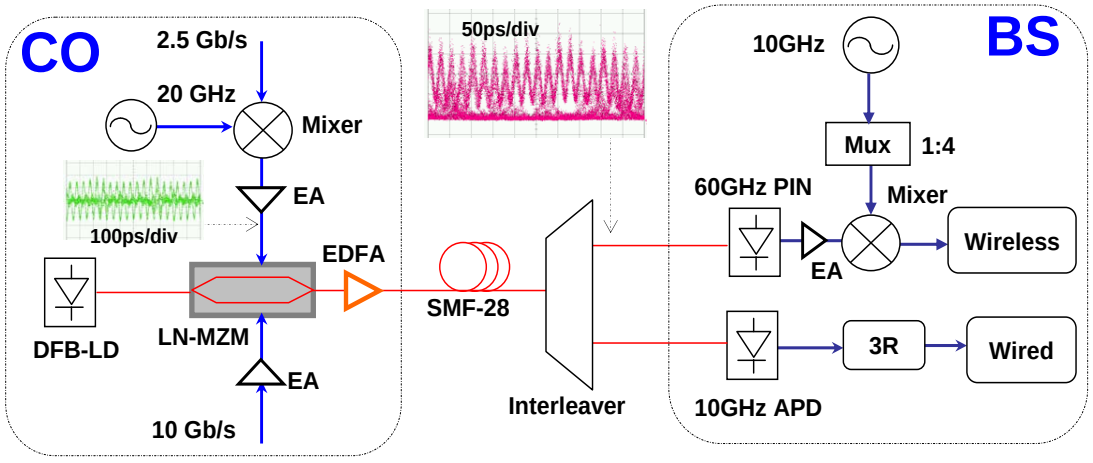

Figure 4.13: Experimental setup for simultaneous generation and delivery of dual services using simple configuration.

Figure 4.13 depicts the experimental setup for the simultaneous generation of wired and wireless services using a single modulator. At the CO, a CW is generated by a DFB-LD at 1548.8 nm and modulated by a LiNbO3 dual-electrode MZM. One electrode is driven by 10-Gb/s data signals with a PRBS word length of $2^{31} - 1$. A 2.5-Gb/s signal with the same pattern format is mixed with a 20-GHz sinusoidal wave to realize SCM for the wireless signals and then used to drive the other electrode of MZM. The driving amplitude of mixed signals is 6.34 V, and the IM is biased at 1.34 V. The electrical waveform of the mixed signals is shown in Fig. 4.13 inset (i). The optical spectra of the original carrier and modulated signals are shown in Fig. 4.14. It is clearly seen that the subcarriers are generated and separated by 40 GHz (0.32 nm) for optical millimeter-wave carrier while the original carrier is modulated by the wired 10-Gb/s NRZ signals.

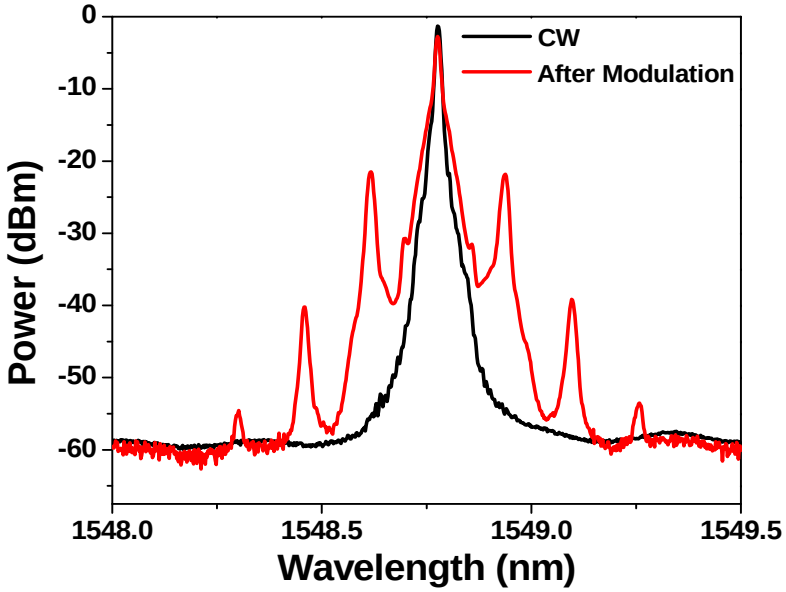

Figure 4.14: Optical spectra of the original CW and modulated signals (resolution: 0.01nm).

Then, the generated optical millimeter-wave and baseband wired signals are amplified before their transmission over a 20-km SMF-28 with 11-dBm input power. At the BS, a 50/25 GHz optical interleaver with 35-dB channel isolation and two outputs is used to separate the optical carrier and the sub-carriers. Figure 4. 15 shows the simulation and experimental results of optical spectra after the modulation and separation. In Fig. 4.15 (a)

and (a'), the high-order (second and third) sidebands of modulated signals in the simulation come from the better linearity of the MZM in the simulation model [121]. We use an optical bandpass filter in the simulation to act as the optical interleaver. It can be observed that the overall good agreement between the simulation and experimental results in Fig. 4.15 (b) and (c). The carrier is suppressed larger than 15 dB. The optical eye diagrams of the millimeter-wave signals are also shown in Fig. 4.15 (d) and (d'). In the experiment, the received optical power of wired and wireless signals is -5 dBm and -16 dBm, respectively.

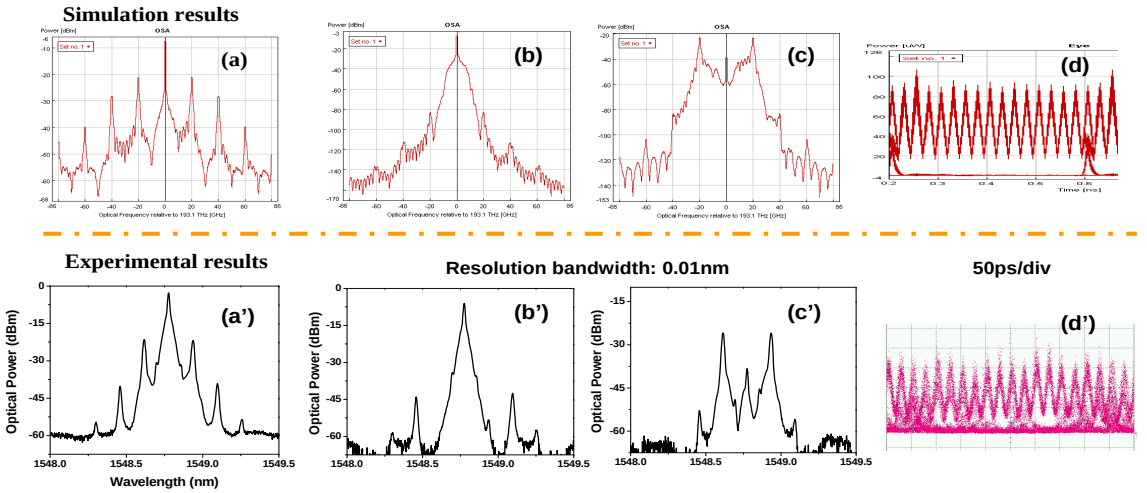

Figure 4.15: Simulation and experimental results for optical spectrum (a)-(c), (a')-(c') and optical eye diagrams (d), (d').

For the wireless part, direct detection is made by a 60-GHz bandwidth PIN photodiode. The converted electrical millimeter-wave signal is then amplified by an electrical amplifier with 10-GHz bandwidth centered at 40 GHz. A 10-GHz clock is used in combination with a frequency multiplier to produce 40-GHz electrical LO signal later mixed to down-convert the electrical signal to its baseband form. On the other hand, the wired signals are detected by a 10-Gb/s receiver with 3R function, which further filters out the residual part of the high-frequency components because of imperfect separation by the optical interleaver.

Figure 4.16 shows the BER curves for wireless and wired signals. The electrical eye diagrams at B-t-B and after 20-km propagation are also inserted in Fig. 4.16. Regarding the wireless data, it is observed that the power penalty at the given BER of 10^{-9} is 1.4 dB after 20-km transmission.

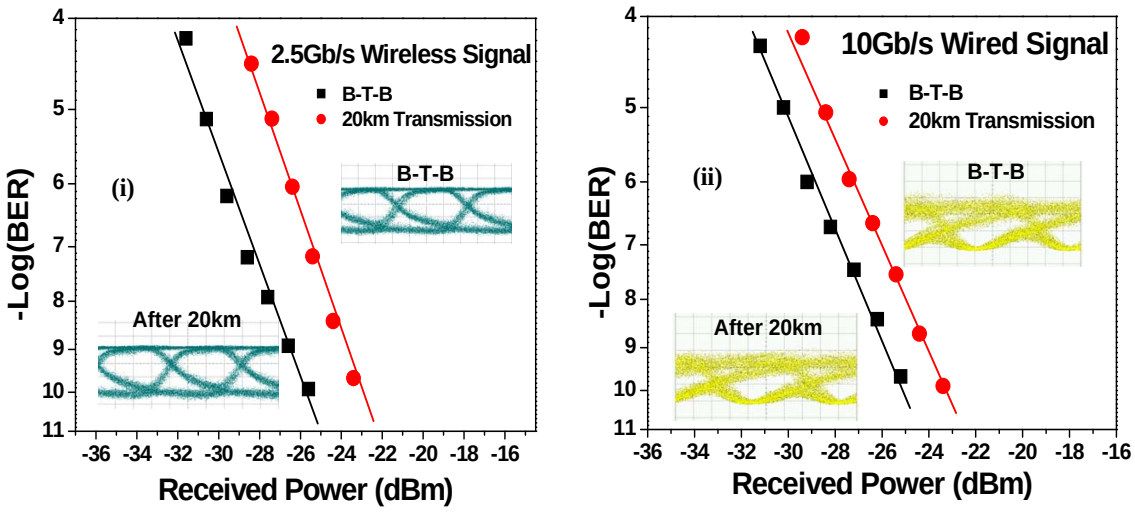

Figure 4.16: BER curves for wireless (i) and wired signals (ii).

The penalty arises from the chromatic dispersion for the two subcarriers. The power penalty for the 10-Gb/s wired signal is around 1.2 dB over the same fiber. Because the 20-GHz frequency separation of the optical carrier and its subcarrier is not matched with even and odd channel spacing of 50/25-GHz interleaver, part of frequency components of modulated wired signals are filtered out. Both the filtering impact and crosstalk between two signals result in the deformed eye diagrams.

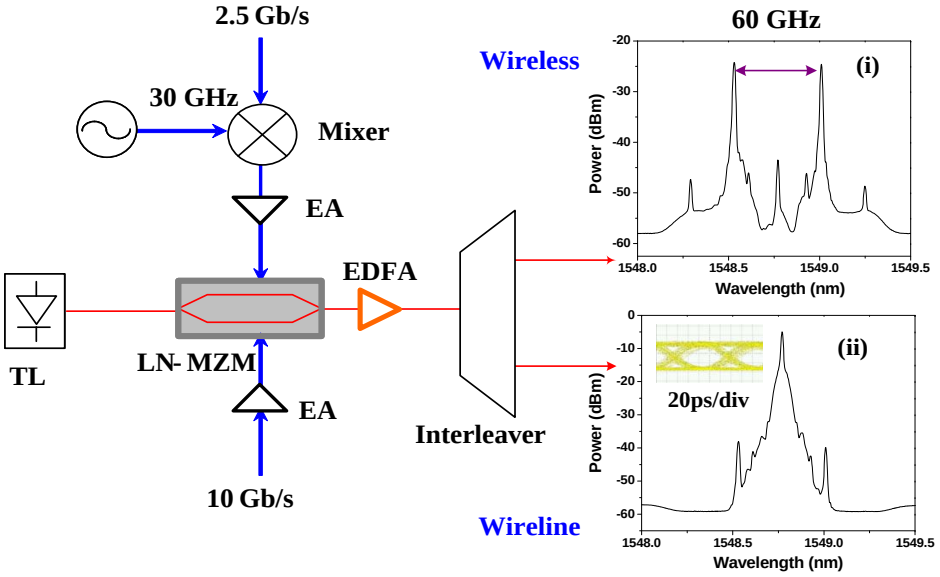

Figure 4.17: Generation of 60-GHz wireless carrier, resolution: 0.01nm).

We also investigate the 60-GHz optical-wireless carrier generated by a single modulator. As shown in Fig. 4.17, a tunable laser is used to generate CW lightwave at 1548.7 nm to match up the passband of optical interleaver. The dual electrode IM is biased at 2.54 V and driven by 10-Gb/s data at one electrode while a 2.5-Gb/s signal mixed with 30-GHz clock at the other electrode. By adjusting the driving amplitude of wired signals and the bias on the modulator, the crosstalk between the wireless and wired signals can be reduced. A 100/50-GHz optical interleaver with 35-dB channel isolation is used to separate the optical carrier and the subcarriers before optical amplification by an EDFA. The optical spectra of the separated optical carrier and 60-GHz millimeter-wave signals are inserted in Fig. 4.17 insets (i) and (ii). The carrier is suppressed larger than 15 dB and the spacing between two subcarriers is 60 GHz (0.48 nm).

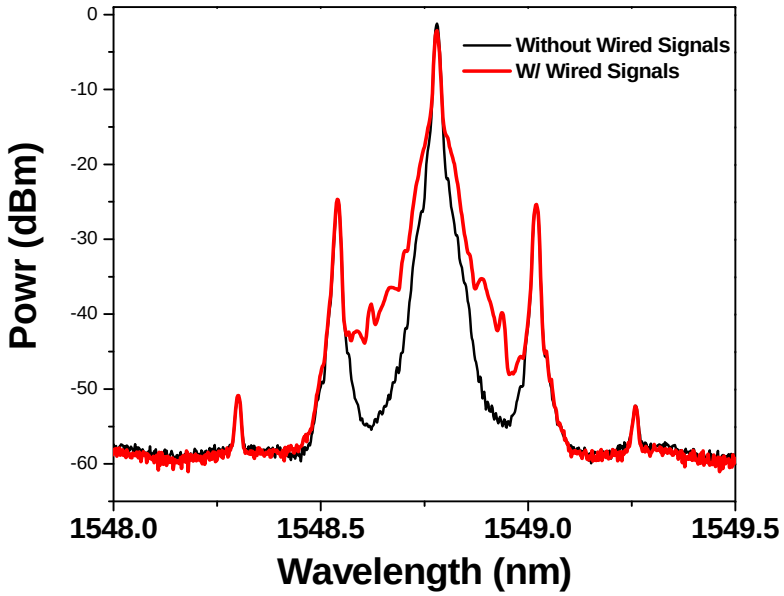

Figure 4.18: Optical spectra of the original CW and modulated 60-GHz signals (resolution: 0.01nm).

Compared to the 40-GHz setup, 50-GHz passband of the interleaver is more suitable to separate the carrier and subcarriers. Additionally, the crosstalk from wireless signals is reduced due to the wider subcarrier spacing. So, the clearer eye diagram is obtained, and it is shown in inset (b) in Fig. 4.17.

4.4 Multi-band signal generation and transmission based on photonic frequency tripling technology

As discussed in the previous chapters, ROF systems operating at 60-GHz have gained much attention owing to the 7-GHz bandwidth available over the unlicensed millimeter-wave band. In such fiber-fed wireless access systems, the long-distance transmission of multi-band signals with low-frequency component requirement is vital to achieving the successful deployment of ROF systems in real networks. At millimeter-wave frequencies especially for 60-GHz band, the transmission distance of ROF links is severely limited by power fading arising from chromatic dispersion in the fiber link. To overcome the dispersion fading effect, several techniques have been reported [122] [123] [124]. These show that two-tone-based optical SSB or polarization-dependent modulation schemes are more suitable for optical millimeter-wave signal distribution. The basic idea to increase the dispersion tolerance in the optical heterodyne mixing systems is to place the data in a single spectral sideband. However, these schemes require a high-frequency LO signal, optimized bias control, or complex control of the state of polarization (SOP) with low receiver sensitivity.

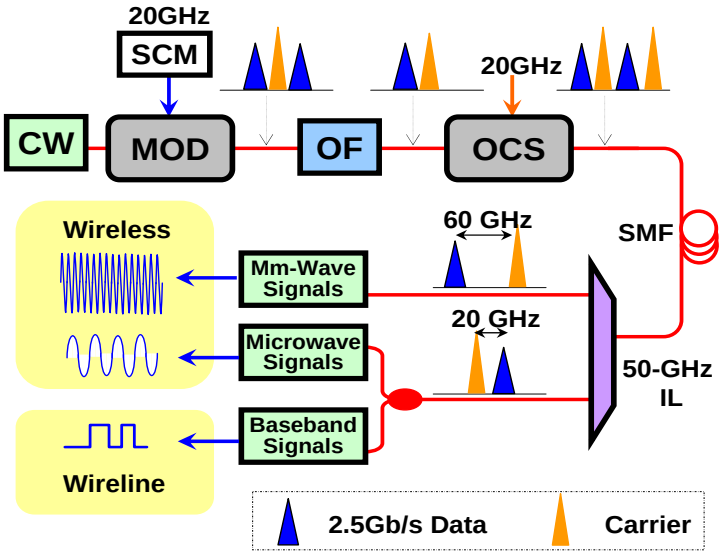

Figure 4.19: Schematic diagram of photonic frequency tripling scheme. OF: optical filter.

Meanwhile, simultaneous multi-band modulation has been demonstrated for flexible configuration in hybrid fiber-fed wireless systems. However, most work only focuses on the

generation of dual- or multi-band signals while little effort is made to extend the fiber transmission distance. Moreover, no work has been undertaken for multi-band generation using a dispersion-tolerant scheme within the 60-GHz millimeter-wave band with low-frequency components.

In this Section, we propose and experimentally demonstrate a novel photonic frequency tripling technology for a 60-GHz ROF system to realize millimeter-wave, microwave, and baseband signal generation and dispersion-tolerant transmission. As shown in Fig. 4.19, wireless baseband signals initially modulate an RF signal at 20 GHz (one third of the LO frequency). The resulting signal is then subcarrier multiplexed onto the optical carrier using an intensity modulator, thus forming dual sidebands. An optical filter with a sharp passband window is used for the VSB filtering. The filtered signals are then injected into a dual-arm MZM to perform the OCS using the same RF clock. After the OCS, the optical carrier and the remaining sideband have been suppressed, leaving four longitudinal subcarriers, equally-spaced by 20 GHz, two of which carry the signal. At the BS, a 50/100-GHz optical interleaver is used to separate the different frequency bands that are needed for wired and wireless connections.

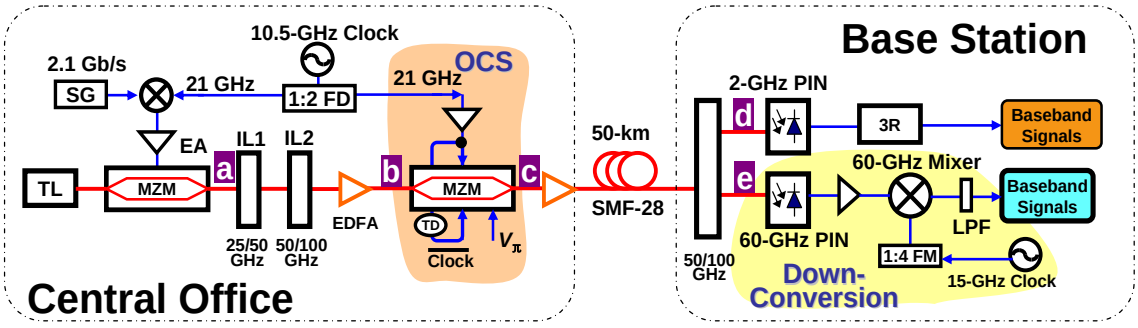

Figure 4.20: Experimental setup of photonic frequency tripling technology for 60-GHz millimeter-wave band.

Figure 4.20 depicts the experimental setup of the simultaneous multi-band generation and transmission based on photonic frequency tripling technology in the millimeter-wave ROF system. At the CO, a CW optical carrier is generated by a tunable laser at 1552.6 nm and is modulated by a LiNbO3 MZM. The 21-GHz sinusoidal wave is generated using

a frequency doubler (FD). This is then mixed with a 2.1-Gb/s data having a PRBS word length of $2^{31}-1$ to drive the modulator. The driving amplitude (Vp-p) of the mixed signals is 7.1 V, and the IM is biased for carrier suppression to obtain the CSR ratio needed to optimized the beating efficiency in the optical detector.

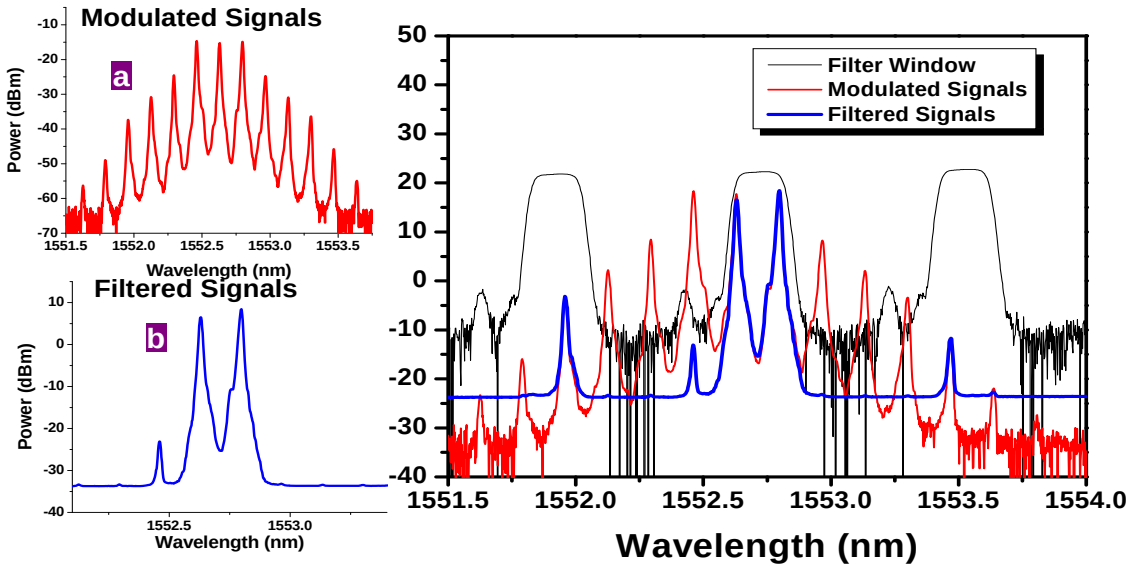

Figure 4.21: Optical spectra for the modulated and filtered signals (resolution: 0.01nm).

The optical spectrum after modulation is shown in Fig. 4.21 inset (a). The VSB filtering is achieved by cascading a 25/50- and a 50/100-GHz optical interleaver with 100-GHz periodicity and 3-dB passband width of 21 GHz. The transmission window of the two cascaded interleavers and the filtered signals are also shown in Fig. 4.21. It is clearly seen that the multiple sidebands are removed while keeping the original carrier and the modulated first upper-order sideband. The suppression ratio is larger than 30 dB. The filtered spectrum consists of the original optical carrier and one modulated subcarrier.

An EDFA is used to compensate around 11-dB insertion loss from intensity modulator and the cascaded interleavers. A dual-arm MZM biased at V_π and driven by two complementary 21-GHz clocks follows to suppress the two injected carriers while generating four subcarriers with alternate modulation as shown in Fig. 4.21. The spacing between two neighboring subcarriers is 21 GHz. Before transmission over 50-km of SMF-28, an EDFA is used to amplify the modulated signals to have 12-dBm input power to compensate the

fiber loss.

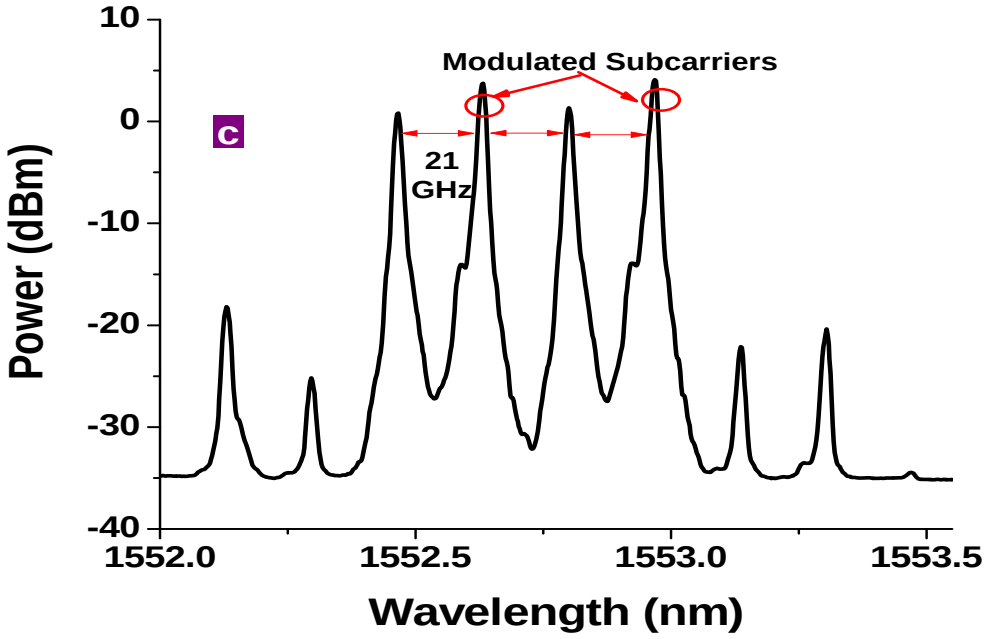

Figure 4.22: Optical spectra of separated signals (resolution: 0.01nm).

The other 50/100-GHz optical deinterleaver shown in Fig. 4.20 is then used to separate the four subcarriers. The optical spectra of the 63-GHz millimeter-wave and the 21-GHz microwave signals are shown in Fig. 4.23 (d) and (e), respectively.

Direct heterodyne detection of the 63-GHz wireless signal is achieved by a 60-GHz bandwidth PIN photodiode. The converted electrical millimeter-wave signal is then amplified by an electrical amplifier with a 5-GHz bandwidth centered at 60 GHz. A 15.75-GHz clock with 4.48 Vp-p is used in combination with a 1:4 frequency multiplier to produce a 63-GHz electrical LO signal later mixed to down-convert the electrical signal to its baseband form. The 21-GHz microwave signals are directly detected by a 2-GHz receiver with 3R function for wireline baseband signal.

Figure 4.24 shows error-free optical eye diagrams of the 63-GHz millimeter-wave and the 21-GHz microwave signals. The electrical eye diagram of the down-converted baseband signals at 2.1-Gb/s is also shown in Fig. 4.24. The slight distortion of the eye diagram for the 21-GHz signals is due to the imperfect edge response of optical separation from the 50-GHz interleaver.

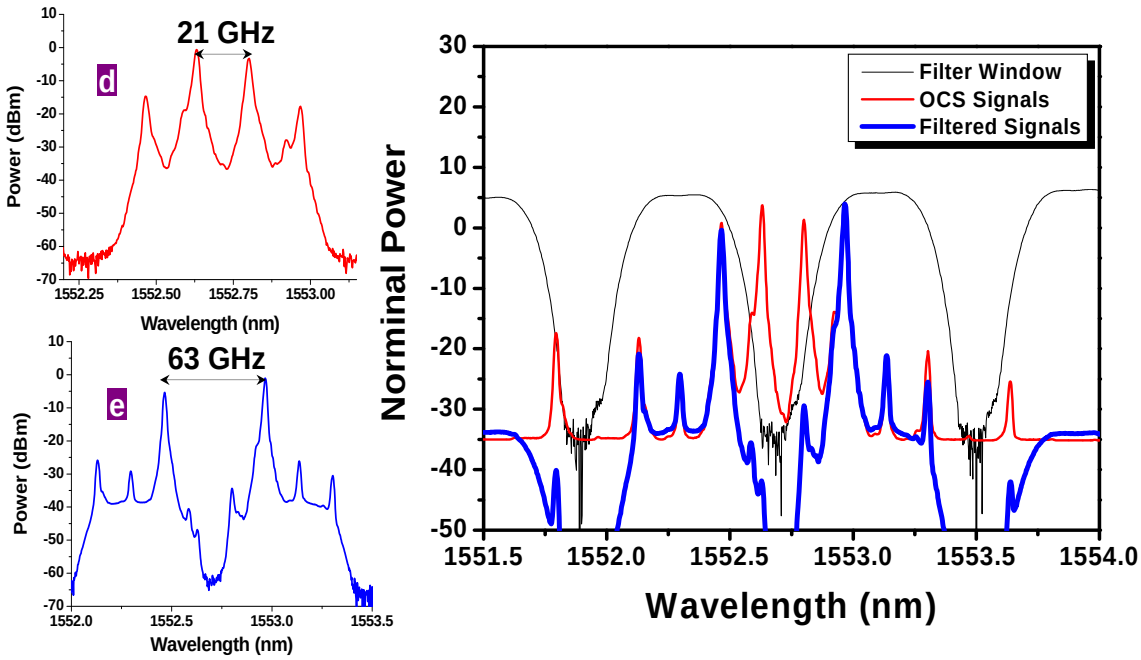

Figure 4.23: Optical spectra of separated signals (resolution: 0.01nm).

The BER as a function of the received optical power at B-t-B and after transmission over 50-km SMF-28 is shown in Fig. 4.25. A power penalty of less than 0.5 dB is observed for the baseband signals from the 21-GHz microwave carrier at a BER of 10^{-9}. The sensitivity at this BER is approximately -29 dBm because of the use of 3R signal regeneration. Regarding the frequency tripled millimeter-wave signals, the power penalty at the given BER of 10^{-9} is less than 1.0 dB after 50-km transmission. The penalty mainly arises from the amplified spontaneous emission (ASE) noise from two EDFAs. This is expected to reduce further with better optical power balance and the use of an additional optical filter. The insets in Fig. 4.25 show the electrical eye diagrams after 50-km SMF-28 transmission. No eye penalty from the chromatic dispersion is observed for both situations.

This technology has unique advantages in terms of low-bandwidth requirements for both optical and electrical components to realize dispersion-tolerant transmission for 60-GHz ROF systems. Moreover, the scheme can be scalable to WDM situations with 100-GHz channel spacing. The results show that it is a suitable solution for future ROF access networks.

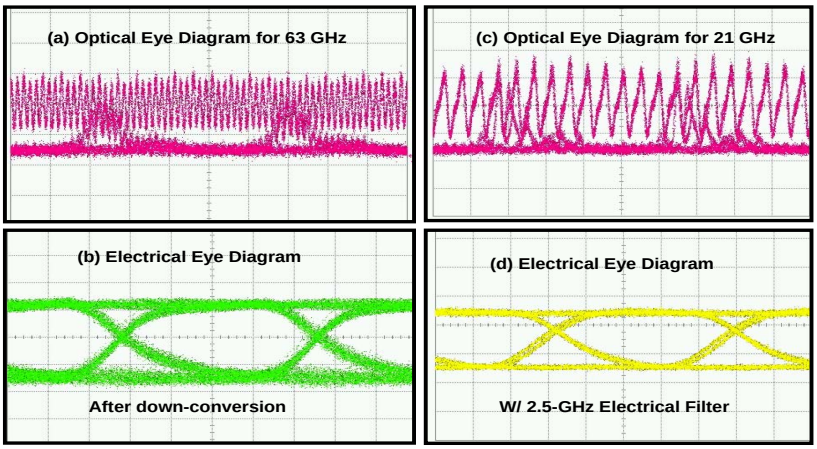

Figure 4.24: Optical and electrical eye diagrams of 63-GHz, 21-GHz, and baseband signals (100ps/div).

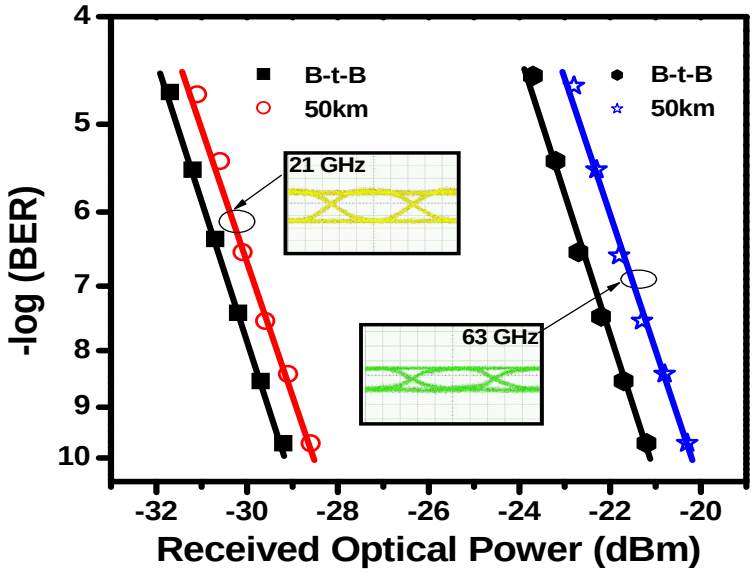

Figure 4.25: BER curves and error-free electrical eye diagrams of 2.1-Gb/s signals after 50-km transmission (100ps/div).

4.5 Chapter summary

In this chapter, we design and demonstrate three novel techniques for simultaneously delivering wired and wireless services over an optical fiber and an air link in a single transport platform. Our efficient techniques for generating dual- or multi-band signals do not require expensive high-frequency electrical components. Moreover, baseband and millimeter-wave signals can be easily separated and distributed at the users' premises.

Table 4.1 summarizes the advantages and disadvantages of the three designs for simultaneous generation of wired and wireless signals. The experimental results suggest that the system using a single intensity modulator is the simplest way to realize simultaneous independent dual signals generation, while the technology based on the photonic frequency tripling technology has unique advantages in terms of low-bandwidth requirement for both optical and electrical components to realize dispersion-tolerant transmission for 60-GHz ROF systems.

Table 4.1: Comparison of three dual signals generation schemes

Schemes	Advantages	Disadvantages
Cascaded modulation	No crosstalk between wired and wireless signals because of separated modulation; high receiver sensitivity	the need for two cascaded modulators; Limited transmission distance by chromatic dispersion.
Single intensity modulator	The simplest system configuration; independent signals generation for wired and wireless services	Limited transmission distance by chromatic dispersion; crosstalk between baseband and wireless signals; the need for sharp and matched optical filter.
Photonic frequency tripling	Reduction of the bandwidth requirement for electronic devices; high dispersion tolerance, longer transmission distance; simultaneous baseband, microwave, and millimeter-wave generation	Complicated structure; generation of identical signals; the need for sharp and matched optical filter for multi-band separation

CHAPTER V

DWDM MILLIMETER-WAVE SIGNALS OVER ROADM-BASED WIDE-AREA ACCESS NETWORKS

Dense wavelength division multiplexing (DWDM) technology is an efficient way to increase the capacity of the fiber distribution networks in millimeter-wave fiber radio systems. Reconfigurable optical add/drop multiplexers (ROADMs) have become a standard part of long-haul DWDM networks. Now, with the cost savings, ROADMs are expected to be deployed in metro and wide-area access networks to realize flexible optical routing in DWDM optical feeder networks. In this chapter, the transport feasibility in metro and wide-area access networks with multiple ROADMs is explored for 40-GHz and 60-GHz optical millimeter-wave signals in sections 5.2 and 5.3. The use of wavelength selective switch (WSS)-based ROADM aims at dynamically allocating wireless capacity to meet instantaneous traffic load on demand.

5.1 Introduction

The need for more bandwidth flexibility, operational efficiencies, and technology advances in DWDM networks [125] bring the optical add/drop multiplexers (OADMs), to add or drop off wavelengths at a node point [126]. But carriers can never know when or where the next need of bandwidth will come from, thus driving urgency for quick provisioning and re-provisioning of the large amounts of bandwidth coursing over the wavelengths of a DWDM network. So, in the past three years, we have seen the next logical step, which is the remotely reconfigurable optical add/drop multiplexer, or ROADM. ROADMs are used to give add/drop flexibility to nodes in a ring and to efficiently interconnect rings or construct a mesh [127]. Currently, ROADMs are evolving from their original functions to the third generation, as shown in Fig. 5.1, optical wavelength selective switch (WSS)-based intelligent nodes. WSSs are more versatile and smaller, consume less power, and are less expensive than 2nd generation ROADMs. The WSS is an N-degree ROADM, which allows reconfiguration

beyond typical 2-degree (usually east-west) configurations. This means that wavelengths can be routed from any node to any other node across multiple rings and networks [128].

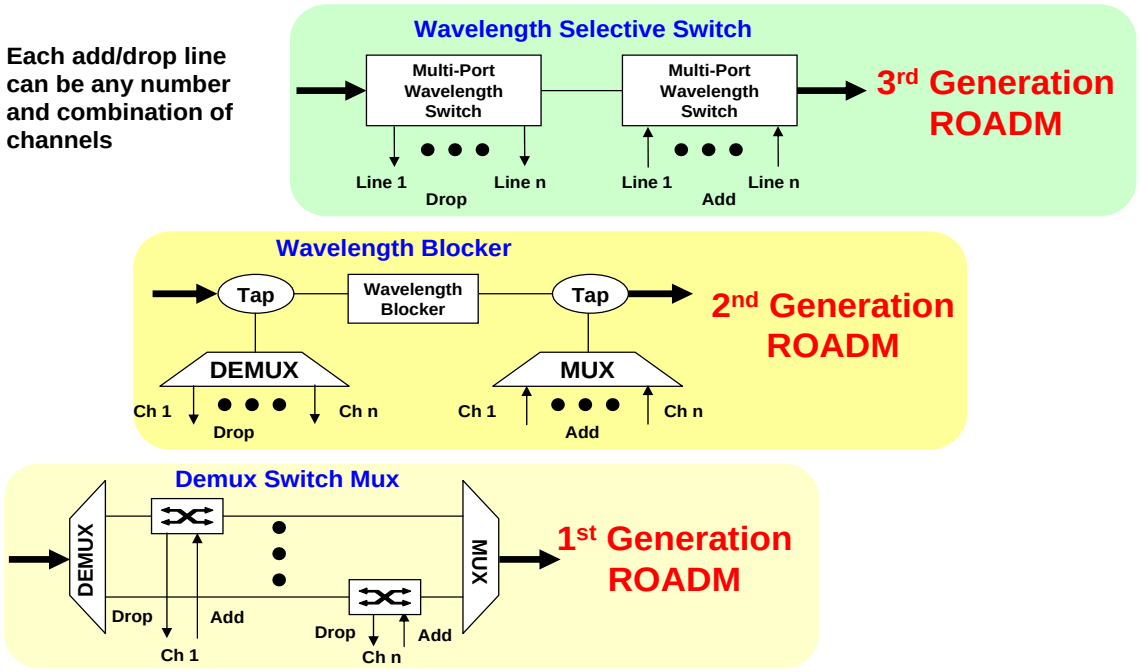

Figure 5.1: ROADM technology evolution.

Currently, the WSS-based ROADMs have become a standard part of long-haul networks and they have become a major update objective for existing networks because they can easily and remotely switch any incoming wavelength to any output port at an individual wavelength granularity [129]. It is expected that the use of low-cost ROADMs on the edge of the network is the next logic step, as shown in Fig. 5.2.

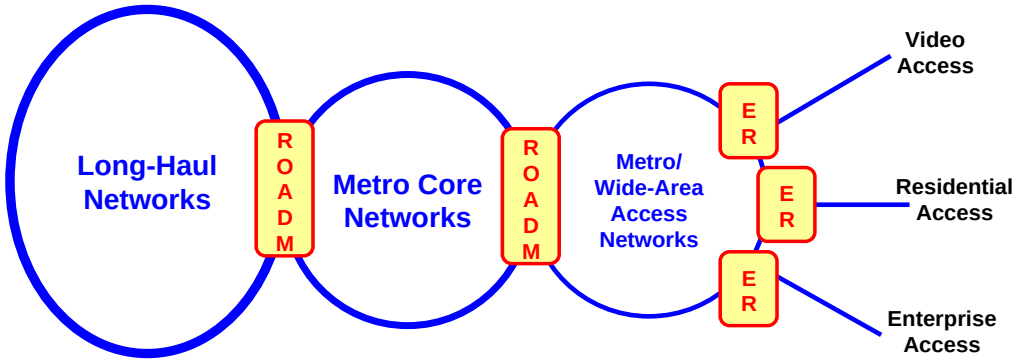

Figure 5.2: ROADM network evolution.

WSS-based ROADM with a low-cost configuration are expected to be compatible with DWDM-ROF networks to support flexible optical routing in optical-wireless networks. Using the flexibility offered by ROADMs, the number of BSs sharing a wavelength channel can be adapted, and thus the available capacity per BS can be tuned to match its traffic demands. For example, when a hot spot with high traffic load emerges, the respective BS can provide extra millimeter-wave carrier as soon as another wavelength channel is directed to this hot spot via remote software control in ROADMs.

In such ROADM-based systems, however, one important topic needs to be considered: multiple cascades of ROADMs along with fundamental filtering impact introduce a considerable implementation constraint on high-bandwidth optical-wireless signals. As shown in Fig. 5.3, this distortion will lead to the intersymbol interference (ISI) in which one symbol interferes with subsequent symbols. Some assessment and analysis have been conducted for different modulation formats such as duobinary-NRZ, carrier suppression return-to-zero (CS-RZ), and DPSK with re-circulating loop in metro or long haul optical links [130]. However, there are very few papers related to millimeter-wave ROF systems in the wide-area access environment. In the following sections, the millimeter-wave signals over the ROADM-based system are presented.

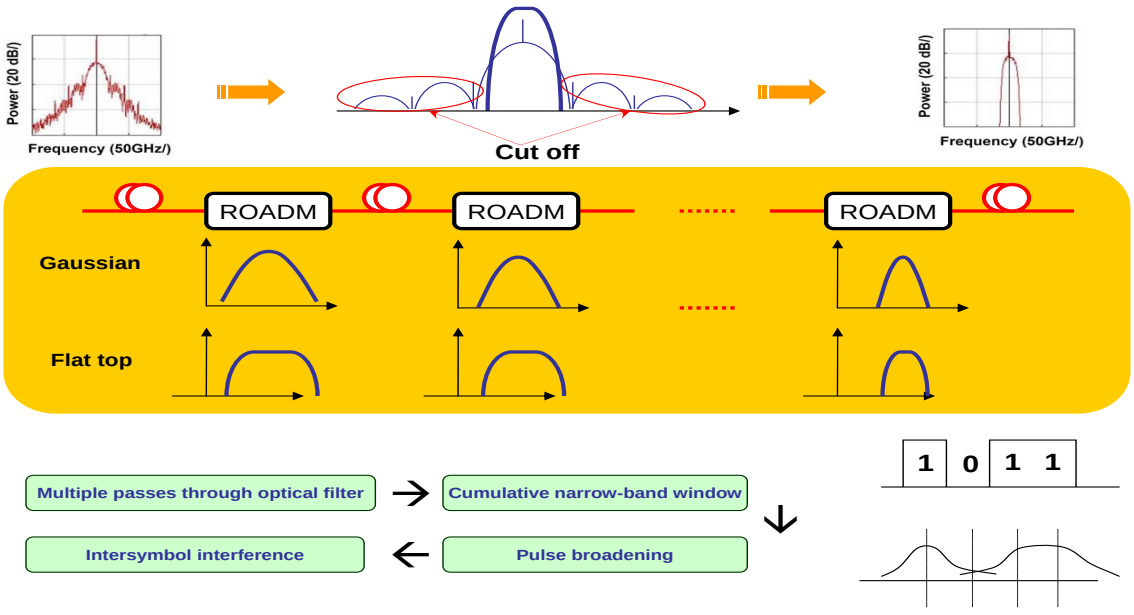

Figure 5.3: Impact of repeated optical filtering.

5.2 40-GHz millimeter-wave signals over 12 straight-line WSSs

Figure 5.4 illustrates the architecture for providing high-bandwidth wireless services over agile ROADM nodes in the wide-area access networks [131].

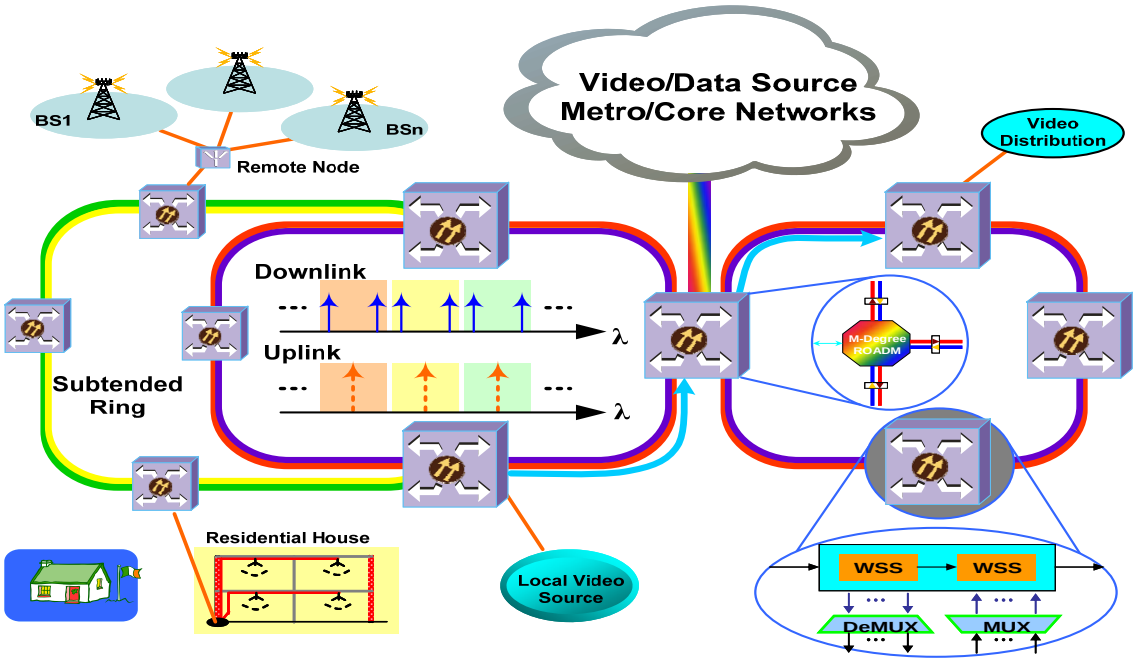

Figure 5.4: Proposed architecture for dynamically allocating radio capacity.

The content provider or upstream network operator send the multiplexed data to the wide-area fiber backbone network in the CO. The connected multi-degree ROADM nodes can switch the services to any neighboring ring nodes. The super-broadband wireless signals and an RF signal at half of the LO frequency are mixed by using SCM to drive the intensity modulator for generation of optical millimeter-wave signals. As a result, wireless signals are carried on two subcarriers separated by a frequency of LO in the optical domain. At the BS, an interleaver is used to separate subcarriers for downlink connection and original carrier acting as CW for upstream remodulation to realize full-duplex operation. The services could be the high-bandwidth data or real-time high-definition video over fiber for outdoor or indoor wireless access. The major advantages of the ROADM-based network are the flexibility for service configuration and extension of the topology such as the subtended ring. For example, each node can be the video source center and distribute the services

to any nodes in the topology by software control. Additionally, the centralization of all required light sources in the CO allows for a simple and low-cost BS configuration.

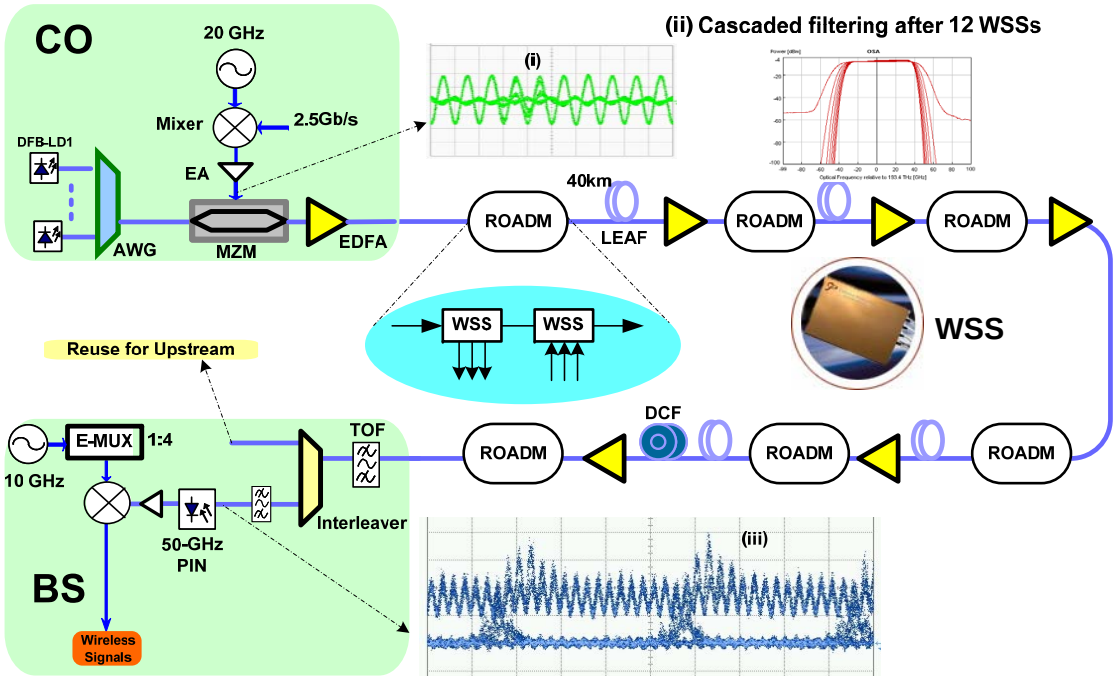

Figure 5.5: Experimental setup for 8x2.5-Gb/s WDM-ROF signals in the optical link with 12 cascaded WSSs.

Figure 5.5 depicts the experimental setup for DWDM-ROF signals over an optical link with 12 cascaded WSSs. At the CO, one laser array is used to generate 8 wavelength signals from 1551.68 nm to 1563.06 nm with adjacent 100-GHz spacing. We employ an AWG to multiplex the eight lightwaves before they are modulated by a LiNbO3 MZM. 2.5-Gb/s electrical signals with a PRBS word length of $2^{31} - 1$ are mixed with a 20-GHz sinusoidal wave to realize SCM for the wireless signals. The eye diagram of mixed electrical signals is shown in Fig. 5.5 inset (i). The modulated optical signals are amplified via an EDFA with 11-dBm output power. Then, the WDM signals pass through the linear 12 cascaded WSSs optical links (2 WSSs in one ROADM as shown in Fig. 5.5). Transmission is performed through 6 ROADM nodes and four 40-km LEAF with the dispersion coefficient of 4.5 ps/nm/km. The output power of each EDFA in the transmission link is around 8 dBm. The insertion loss of each WSS is around 4.5 dB for all the wavelengths. The cumulative

filtering shape of WSSs is shown in Fig. 5.5 inset (ii). After transmission over 160-km LEAF, the dispersion compensation fiber (DCF) with total dispersion of 694 ps and 10-dB loss is used to compensate fiber chromatic dispersion. The residual dispersion in the link ranges from 20 ps/nm to 30 ps/nm across the channels.

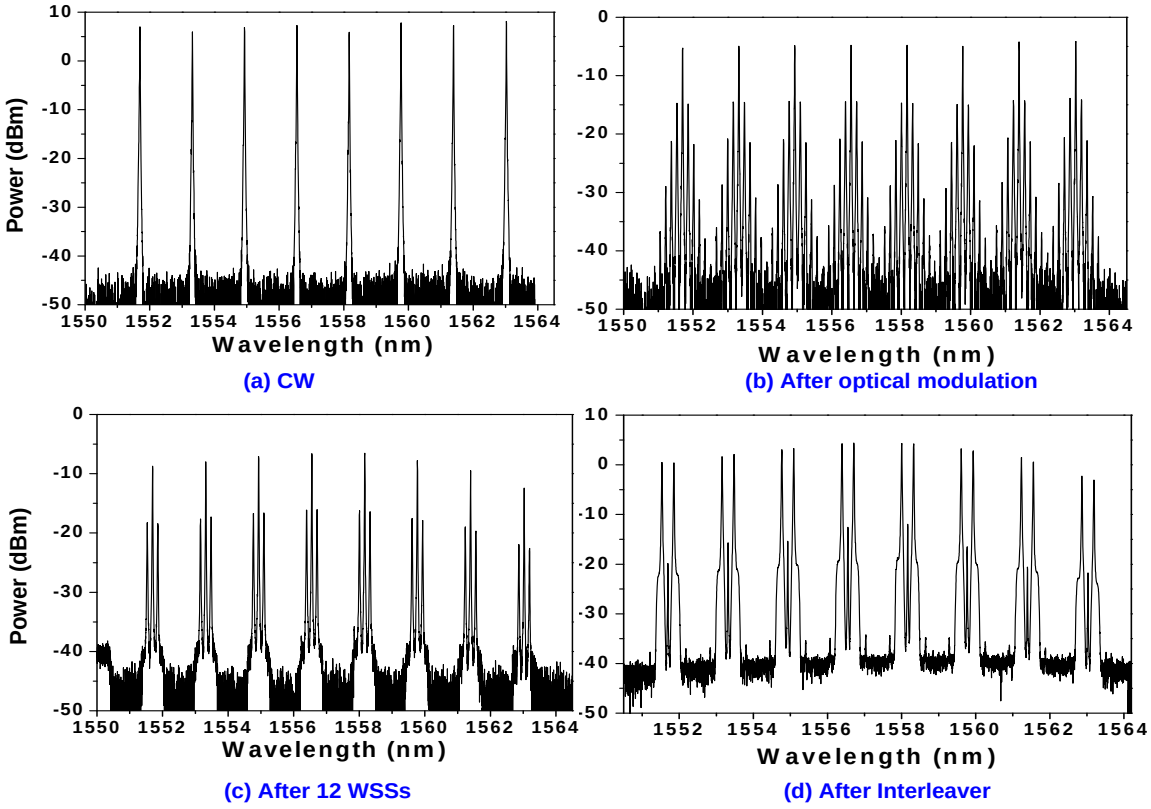

Figure 5.6: Optical spectra evolution., (resolution: 0.01nm).

At the BS, a 50/25 GHz optical interleaver with 35-dB channel isolation and two outputs is used to separate the optical carrier and the subcarriers. The uplink transmission is similar to our previous work. Compared with the optical millimeter-wave signals without cascaded WSSs, high-order sidebands are filtered out while keeping first-order sidebands intact after passing through 12 WSSs. The unflat spectrum arises from the smaller gain accumulation at long wavelengths in multiple EDFAs. It is noted that the carrier is suppressed larger than 20 dB. Regarding the downlink connection, direct detection is made by a 50-GHz bandwidth PIN photodiode after a tunable optical filter with a bandwidth of 0.5 nm. The eye diagram of optical millimeter-wave is shown in Fig. 5.5 inset (iii). Then, the converted electrical

millimeter-wave signal is then amplified by an electrical amplifier with 10-GHz bandwidth centered at 40 GHz. A 10-GHz clock is used in combination with a frequency multiplexer to produce 40-GHz electrical LO signal later mixed to down-convert the electrical signal to its baseband form. The optical spectra evolution of all the channels along the optical links are shown in Fig. 5.6. The power fluctuation arises from the cumulative gains of multiple EDFAs after transmission. The suppression ratio is larger than 20 dB for all channels.

Figure 5.7 shows the receiver sensitivity measured for B-t-B, after 12 WSSs without and with 160-km LEAF transmission as a function of the received optical power. The electrical eye diagrams for all eight wavelengths after 160-km LEAF propagation are also inserted in Fig. 5.7. The power penalty for all channels is roughly less than 0.5 dB and 1.5 dB after 12 cascaded WSSs without and with 160-km LEAF transmission, respectively. The results show the transport feasibility of super-broadband wireless signals over optical millimeter-wave for advanced DWDM metro networks using the low-cost WSS-based multiple ROADMs for increasing agility and flexibility.

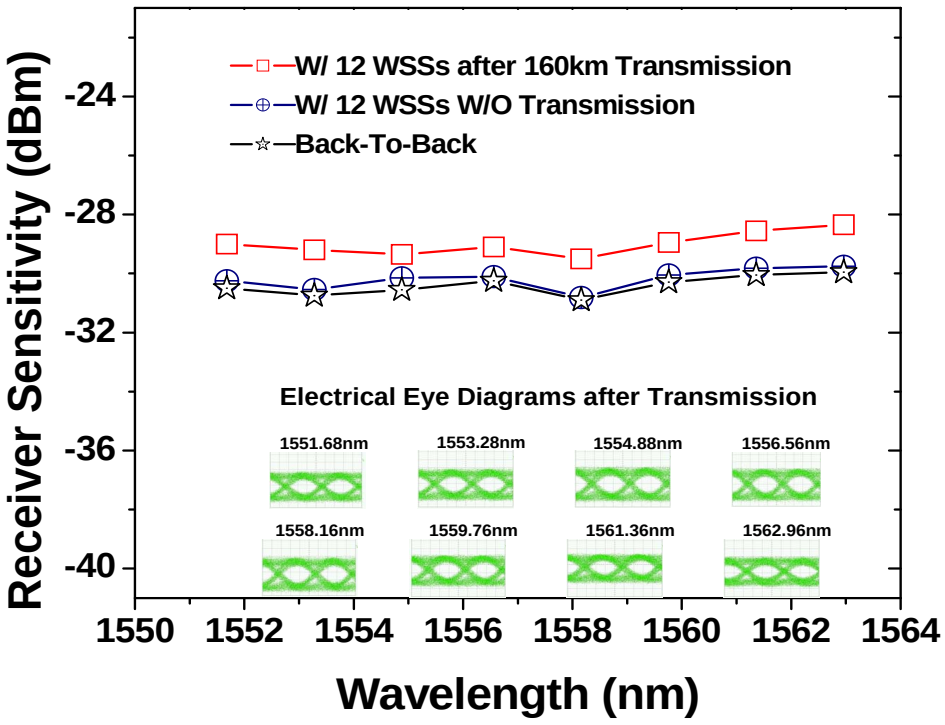

Figure 5.7: Receiver sensitivity and eye diagrams after transmission.

5.3 60-GHz millimeter-wave signals over 3 commercial ROADMs

Figure 5.8 depicts the experimental setup for super-broadband wireless signals over a ring access system with 3 cascaded ROADM nodes [132]. At the data source center, an optical transmitter at 1553.9 nm is modulated 2.5-Gb/s or 5-Gb/s data signals with a PRBS word length of $2^{31}-1$. The lightwave is then modulated by a LiNbO3 phase modulator (PM with 11v half-wave voltage) driven by a 30-GHz sinusoidal clock, which is generated by using 1:4 frequency multiplexer and a 7.5-GHz microwave source. The optical signal is then amplified by an EDFA to 6 dBm before transmission over 3-cascaded ROADM links. The optical spectrum of modulated signals after amplification is shown in Fig. 5.8 inset (a). Then, the modulated signals pass through the linear cascaded ROADMs (the structure includes 1x9 WSS as shown as inset (i)). Transmission is performed through 3 ROADM nodes and total 100-km SSMF with the dispersion coefficient of 16.7 ps/nm/km. the dispersion compensation fiber with total dispersion of 1650 ps and 15-dB loss is used to compensate fiber chromatic dispersion. The output power of each EDFA in the transmission link is around 5 dBm. The insertion loss of each WSS is around 5.5 dB for the transmission channel. The cumulative filtering shape of WSSs is shown in Fig. 5.8 inset (ii).

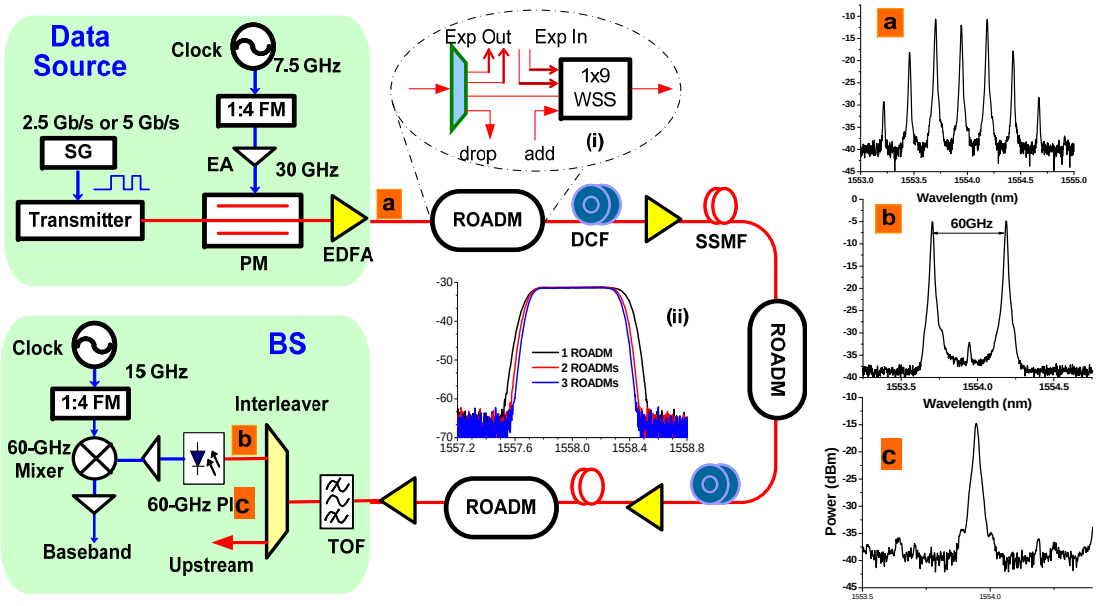

Figure 5.8: setup for 60-GHz ROF signals over 3-cascaded ROADMs. SG: signal generator.

At the BS, a 50/25 GHz optical interleaver with 35-dB channel isolation and two outputs is used to separate the optical carrier and the two sidebands. The optical spectrum of separated optical millimeter-wave and carrier is shown in Fig. 2 insets (b) and (c). It is clearly seen that the spacing between two peaks is 60 GHz, and all higher-order sidebands are suppressed while keeping first-order sidebands intact due to the matched filtering window of optical interleaver and cascaded WSSs. It is noted that the carrier is suppressed larger than 20 dB. Regarding the downlink connection, direct detection is made by a 60-GHz bandwidth PIN photodiode after a tunable optical filter with a bandwidth of 0.5 nm. The converted electrical millimeter-wave signal is then amplified by an electrical amplifier with 5-GHz bandwidth centered at 60 GHz. A 15-GHz clock is used in combination with a frequency multiplexer to produce 60-GHz electrical LO signal later mixed to down-convert the electrical signal to its baseband form.

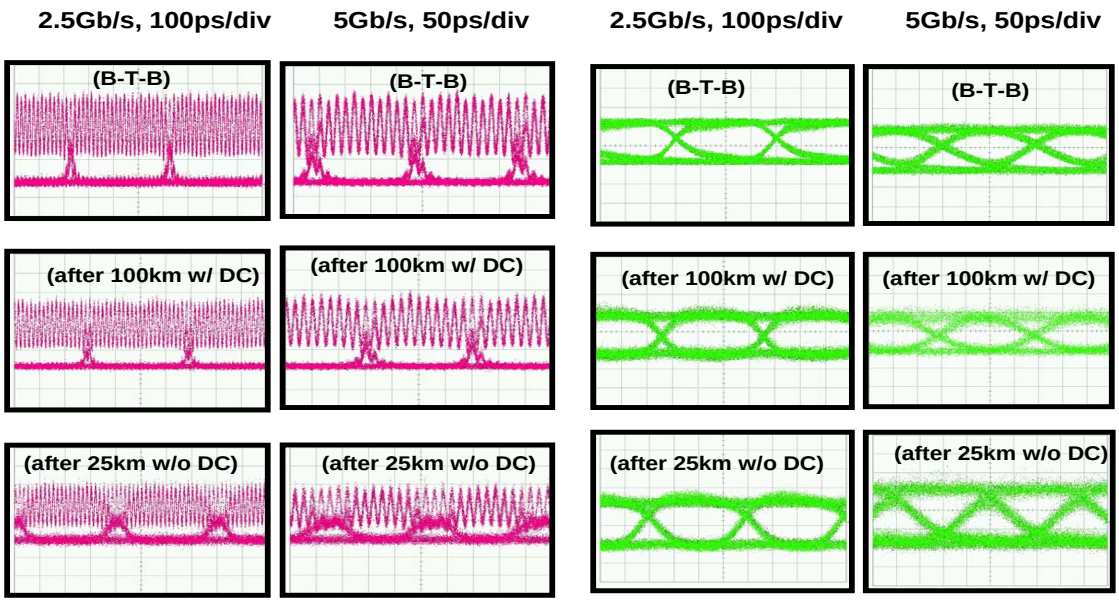

Figure 5.9: Eye diagrams evolution along the transmission link.

Figure 5.7 shows the optical and electrical eye diagrams of 2.5- and 5-Gb/s data signals. It is seen that the eyes are wide open despite 100-km SMF transmission. The measured BER curves in Fig. 5.8 show that the power penalty after 100-km SSMF transmission is less than 1.5 dB. The penalty mainly arises from the residual dispersion accumulation and ASE

noise from EDFA along optical links. The receiver sensitivity is high for both situations because of the use of optical pre-amplifier.

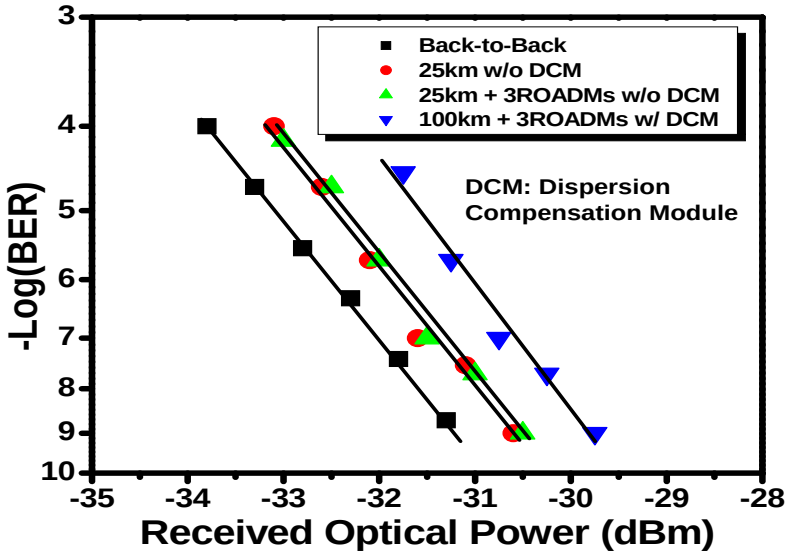

Figure 5.10: BER curves for all situations.

5.4 Chapter summary

Wireless networks typically show considerable dynamics in traffic load of the BSs because of the fluctuating density of mobile users in the radio cells. By allocating the network's communication resources to the BS according to their instantaneous traffic load, these resources can be more efficiently deployed. So, it is expected to use flexible ROADMs to realize dynamic optical routing, thus dynamically allocating the millimeter-wave carrier to the BSs with high traffic load.

In this chapter, we experimentally show the demonstration of 8x2.5-Gb/s WDM-ROF signals carried on 40-GHz millimeter-wave passing through linear cascaded 12 1x4 WSSs. We also successfully demonstrate super-broadband 60-GHz ROF signals over 3 cascaded ROADMs optical links. The 2.5/5-Gb/s signals are transmitted over 100-km SMF with less than 1.5-dB power penalty. These results show the transport feasibility of super-broadband wireless signals over optical millimeter-wave (40-60 GHz) for wide-area access networks using the WSS-based multiple ROADMs for increasing agility and flexibility.

CHAPTER VI

ROF SYSTEMS USING OFDM MODULATION FORMAT

Several methods for optical millimeter-wave signal generation and transmission are presented in the Chapter 2. However, only binary on-off keying (OOK) modulation format is used in all of these proposed schemes. Nonreturn-to-zero OOK (NRZ-OOK) is the simplest optical modulation format for intensity modulation and direct detection (IM-DD) optical transmission systems. For wireless applications, however, Orthogonal frequency division multiplexing (OFDM) has widespread use in wireless LANs, broadband access networks and in digital broadcasting. So, the integration of OFDM and optical-wireless techniques makes cost-effective and super-broadband wireless access possible. In this chapter, the experimental demonstrations of optical-wireless systems using OFDM modulation format are presented in microwave and millimeter-wave band in sections 6.2 and 6.3. Bandwidth record of radio signals on optical carriers is achieved for 6-m wireless transmission distance.

6.1 Introduction

OFDM technology [133] is considered the advanced modulation technique for future broadband wireless communications because it provides increased robustness against frequency-selective fading and narrowband interference. OFDM is also efficient in dealing with multi-path delay spread. OFDM is a multi-carrier transmission technique in which a high bit-rate digital stream is split into several narrowband channels at different frequencies (using sub-carriers). The sub-carriers are modulated by using Phase shift Keying (PSK) or Quadrature Amplitude Modulation (QAM) and are then carried on a high frequency microwave carrier (e.g. microwave or millimeter-wave). This is similar to conventional Frequency Division Multiplexing (FDM) or subcarrier multiplexing, except for the stringent requirement of orthogonality between the sub-carriers.

OFDM technology has been widely adopted in ADSL and RF-wireless systems such as IEEE 802.11a/g (Wi-Fi) and IEEE 802.16 (WiMAX). It is also used for wireless digital

audio and video broadcasting. The typical model for an OFDM system is shown in Fig. 6.1. At the transmitter of the OFDM system, data are apportioned in the frequency domain and an inverse fast Fourier transform (IFFT) is used to convert the data into the time domain. The IFFT produces a complex-valued time domain waveform containing a superposition of all of the sub-carriers. A cyclic prefix is added to each transmitted block after the IFFT, so that the relative delays between the received OFDM-subcarriers can be accommodated without destroying the orthogonality of the OFDM subcarriers [134]. In the receiver, an FFT is used to recover the original data.

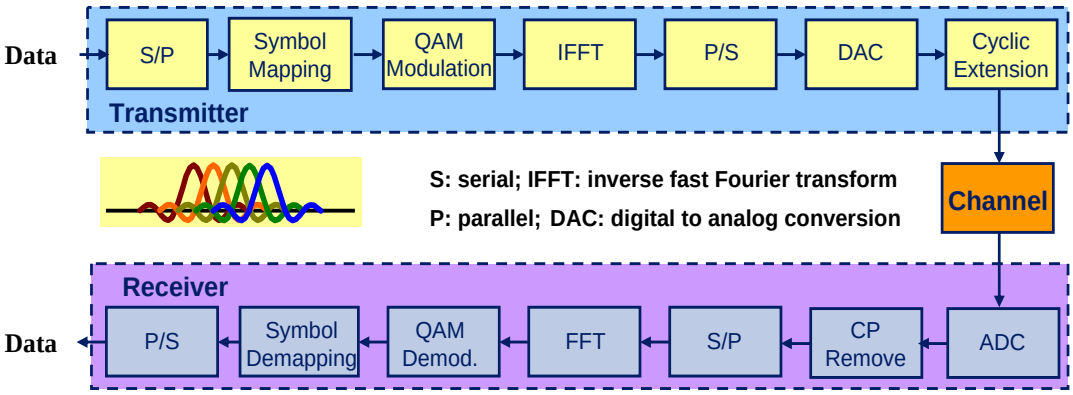

Figure 6.1: A block diagram of an OFDM system.

Recently, optical transmission systems employing OFDM have gained considerable research interest, as shown in Fig. 6.2, because OFDM can combat fiber chromatic dispersion and has the capability to use higher level modulation formats to increase spectral efficiency [135] [136]. In optical communications, optical OFDM was firstly demonstrated for multimode and free-space links [137], which both suffer from multipath. Optical OFDM systems in single mode fiber can be realized either with direct detection or with coherent detection [138]. Whereas direction detection is more suitable for cost-effective short-reach applications, the superior performance of cohere OFDM makes it an excellent candidate for long haul transmission systems. The sensitivity of cohere OFDM is superior to that of direct OFDM as direct OFDM requires half the optical power to be allocated for the transmission of the carrier [139].

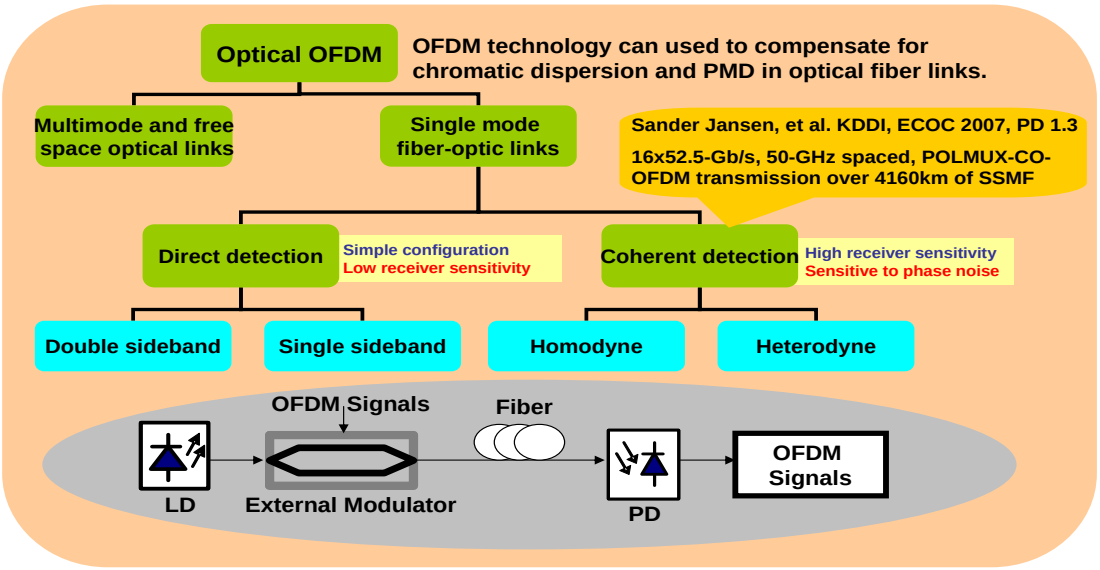

Figure 6.2: Optical OFDM research.

We have demonstrated that optical millimeter-wave can be generated and up-converted by using SCM technology and the interleaver at the BS. This scheme exhibits system configuration simplicity and furthermore provides full-duplex operation based on wavelength reuse. However, the transmission distance of optical millimeter-wave signals is still limited by the fiber chromatic dispersion. So, the combination of OFDM and ROF is naturally suitable for optical-wireless systems to extend the transmission distance over both fiber and air links. There are few papers related to OFDM-ROF links, most of them only showed the simulation results on 2.4/5-GHz wireless LAN or experimental results with very low-data rate [140] [141].

6.2 1-Gb/s OFDM signals over 80-km SMF

Figure 6.3 shows the schematic diagram of millimeter-wave OFDM-ROF system [142]. At the CO, the OFDM analog data and an RF clock at half of the LO frequency are mixed by using SCM technology. The mixed signals are applied to drive a LiNbO3 MZM to create first-order sidebands. After transmission over SMF, an interleaver is employed to separate the optical carrier from the first-order sidebands to generate optical millimeter-wave carrier at the BS. Then the boosted electrical millimeter-wave signal is down-converted through a mixer and retrieved by an OFDM receiver. The separated optical carrier is considered as

the continuous wave and directly modulated by the uplink data and sent back to the CO.

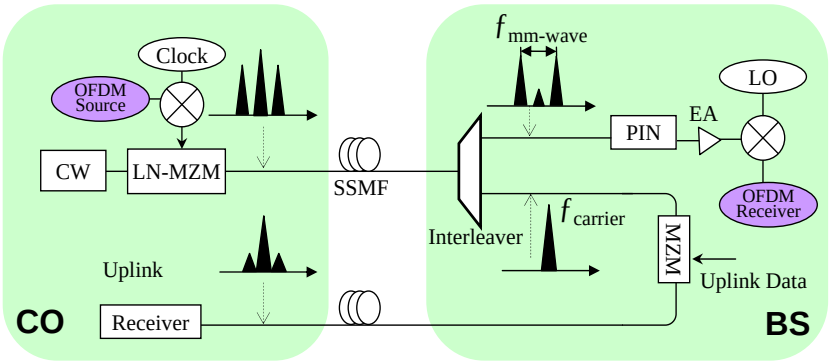

Figure 6.3: Optical OFDM research.

Figure 6.4 depicts the experimental setup of the OFDM-ROF system. At the optical transmitter side, a CW lightwave from a tunable laser at 1559.7 nm (5-MHz linewidth) is modulated by an MZM driven by the mixed OFDM analog signals.

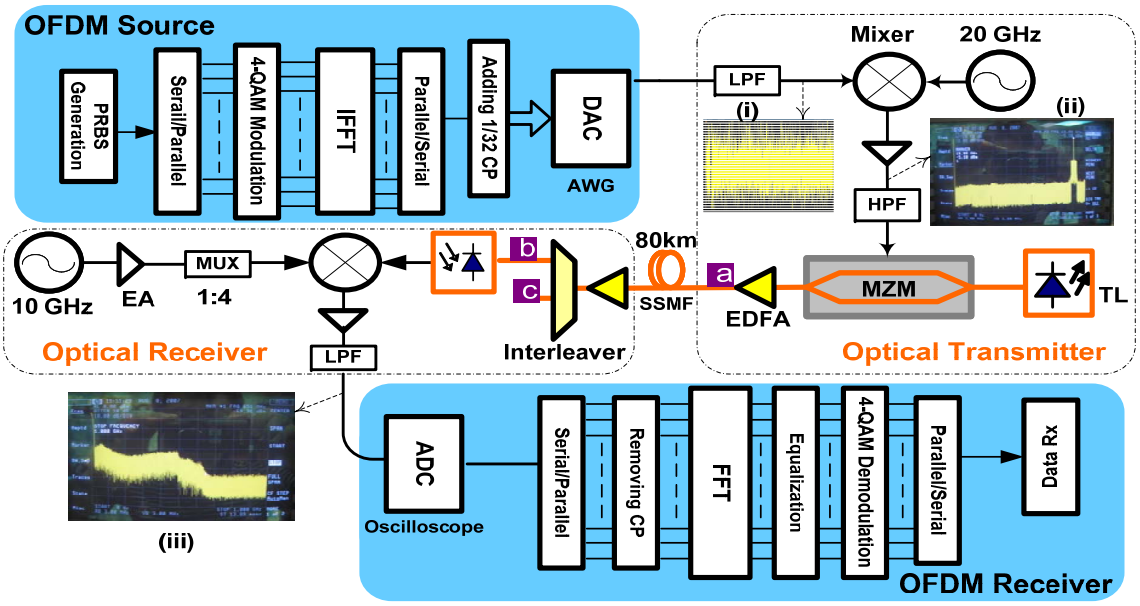

Figure 6.4: Experimental setup for an OFDM-ROF system at 1Gb/s on 40-GHz millimeter-wave carrier.

The 1-Gb/s OFDM baseband signals are generated offline with Matlab program. The FFT size is 256, where 201 subcarriers are mapped with a $2^{31} - 1$ PRBS bit data stream using 4-QAM encoding (QPSK), 54 subcarriers at high frequencies are set to zero for guard

channels and one subcarrier in the middle of the OFDM spectrum is set to zero for DC in baseband. 6.4-ns cyclic prefix (CP) is applied to resist chromatic dispersion. One preamble frame is added every 256 OFDM data frames for timing synchronization and channel equalization. Finally, the OFDM baseband signals are up-sampled 8 times for flatter channel response of the transmitter output signal before they are uploaded to a Tektronix AWG 7102 arbitrary waveform generator (AWG) operating at 10 GSample/s to produce 612.5MHz (1-Gb/s) bandwidth analog OFDM signals, which is shown in OFDM Source in Fig. 6.4 inset (i). The 1-Gb/s OFDM signals are mixed with a 20-GHz sinusoidal wave to realize SCM for the millimeter-wave signals and then used to drive the MZM. The electrical spectrum of mixed signal is shown in Fig. 5,4 inset (ii). The input power is 14 dBm before transmission over 80-km SMF.

At the optical receiver side, a 50/25-GHz optical interleaver with 35-dB channel isolation and two outputs is used to separate the optical carrier and the sub-carriers. The optical spectra of the modulated signal, separated optical carrier, and millimeter-wave signals are shown in Fig. 6.5 insets (a), (b), and (c), respectively. The carrier is suppressed larger than 20 dB. The optical eye diagram of the millimeter-wave OFDM signal is also shown in Fig. 6.5. The uplink transmission is similar to our previous bidirectional setup.

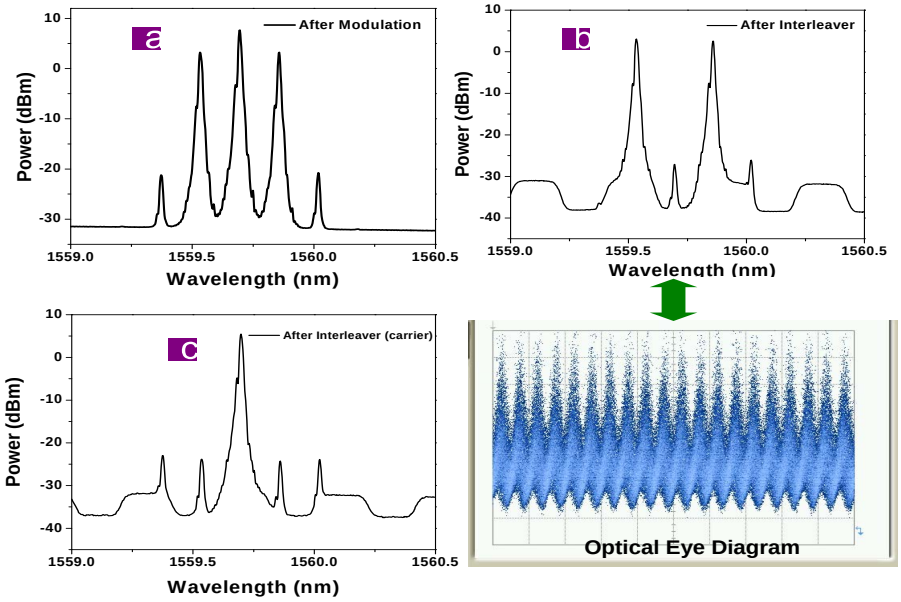

Figure 6.5: Optical spectra and eye diagram.

Regarding the downlink connection, direct detection is made by a 50-GHz bandwidth PIN photodiode. The converted electrical millimeter-wave signal is then amplified by an electrical amplifier with 10-GHz bandwidth centered at 40 GHz. A 10-GHz clock is used in combination with a frequency multiplier to produce 40-GHz electrical LO signal later mixed to down-convert the electrical signal to OFDM baseband form. The down-converted signals are sampled with a real-time digital oscilloscope (Tektronix TDS6154C) at 1.25 GSample/s. The received data are processed and recovered offline with a Matlab program as an OFDM receiver. The electrical spectrum of down-converted OFDM signals is shown in Fig. 6.5 inset (iii). The spectrum fluctuations for different frequency components arise from the nonlinear response of TL, MZM, and optical amplifier because of the large optical power.

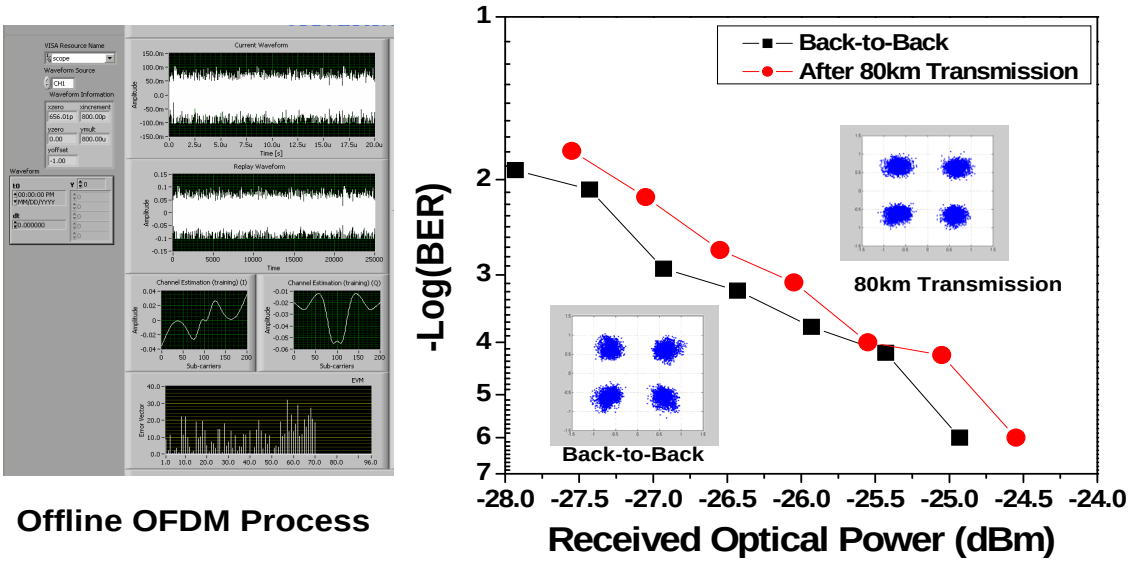

Figure 6.6: BER curves and constellation diagrams for B-t-B and 80-km transmission.

Figure 6.6 shows the BER curves of the B-t-B and 80-km SSMF transmission as a function of the received optical power. 1.17e6 cumulative bits are evaluated for both tests. Compared with the B-t-B case, it has less than 0.5-dB power penalty at the BER of 10^{-6}. The inset shows the constellation of the OFDM-ROF signal at the received power of -25 dBm. We found that the launched optical power to the MZM and SMF has the ineligible impact on the receiver sensitivity because of the link nonlinearity. Future work will focus on performance analysis of nonlinear distortion effects in WDM OFDM-ROF links. We

also measured 16-QAM signals on 40 and 18 GHz for SSB B-t-B systems. The constellation diagrams are shown in Fig. 6.7. 16-QAM OFDM signals on 40-GHz millimeter-wave carrier show worse performance even in the B-t-B situation.

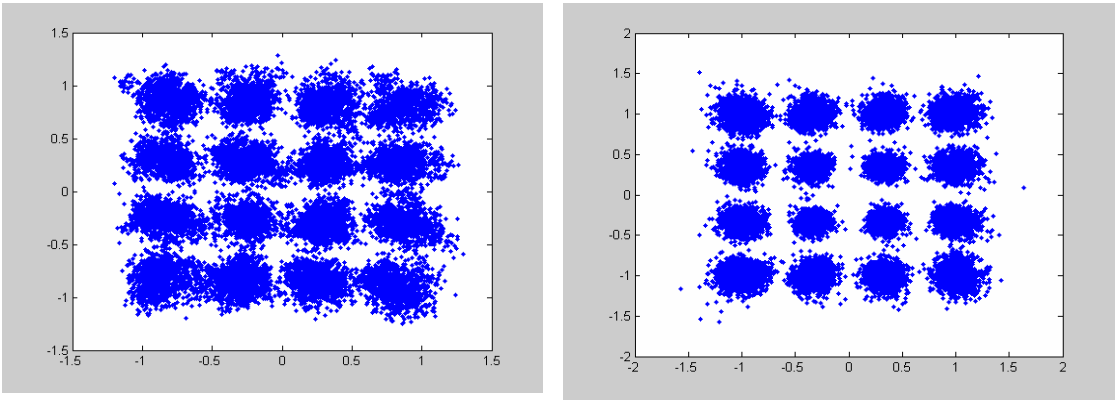

Figure 6.7: Constellation diagrams for 16-QAM signals.

6.3 16-Gb/s OFDM signals over 20-km SMF and 6-m air link

In this experiment, up-converted 16-Gb/s OFDM signals on 24-GHz microwave carrier over both 20-km SMF-28 and 6-m wireless distance are demonstrated with SSB modulation to overcome fiber dispersion effect [143]. This is so far a record bandwidth achieved by microwave photonics technique in ROF systems [144].

Figure 6.8 shows the experimental setup of the super-broadband OFDM-ROF system. The lightwave from a DFB laser at 1556.44 nm with the linewidth around 20 MHz is modulated by an intensity modulator driven by up-converted OFDM signals. The 16-Gb/s baseband OFDM signals are generated by an OFDM transmitter and then up-converted to 24 GHz to generate RF-OFDM signals via an electrical mixer. The OFDM baseband signal is generated offline and uploaded into a Tektronix AWG7102. The waveforms produced by the AWG are continuously output at a sample rate of 20 GHz (8Cbits DAC, 4-GHz bandwidth). QPSK encoding is used for symbol mapping, and 1.6-ns cyclic prefix per OFDM symbol is applied. The FFT size is 256, from which 200 channels are used for data transmission, 27 channels at high frequencies and 28 channels at low frequency are

set to zero for over-sampling, and one channel in the middle of the OFDM spectrum is set to zero for DC in the baseband. Ten training sequences are applied for each 150 OFDM-symbol frame in order to enable phase noise compensation. At the output of the AWG, a low-pass filter with 5-GHz bandwidth is used to remove the high-frequency components. The intensity modulator is driven by the RF-OFDM signals to create DSB optical signals. The bias and the power of the RF signals are carefully adjusted to obtain proper power ratio between the optical carrier and the first-order sideband signals. The optical spectrum after the intensity modulator is inserted in Fig. 6.8 inset (i). The power of the first-order sideband and the second-order sideband signal is 5 and 21 dB lower than that of the optical carrier, respectively.

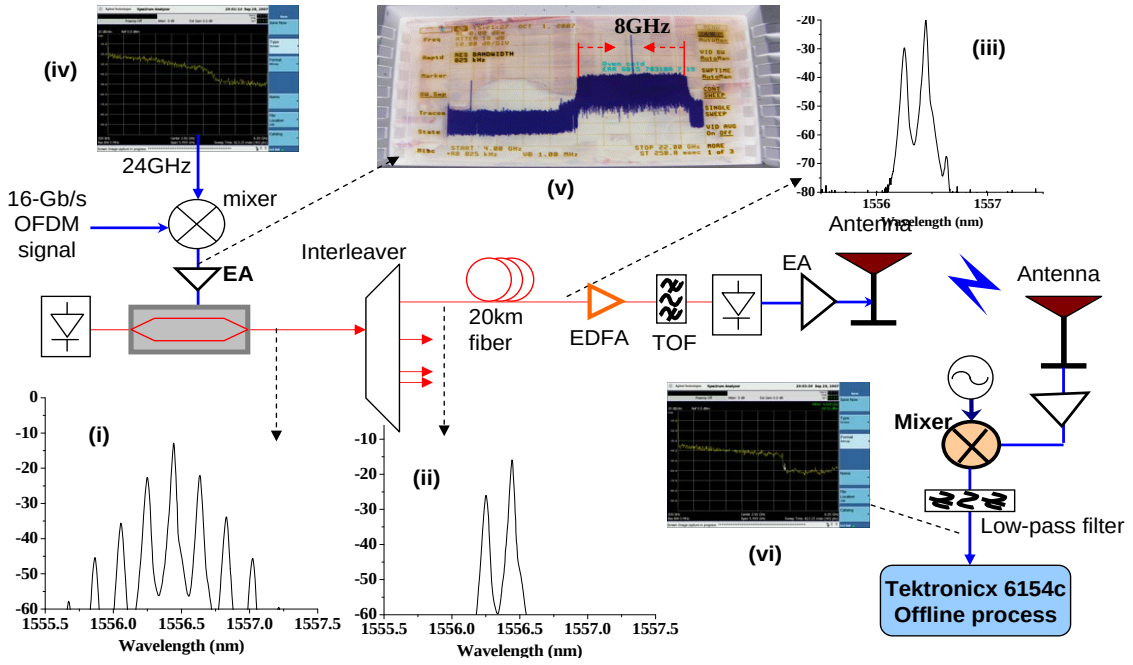

Figure 6.8: Experimental setup for 16-Gb/s OFDM wired transmission over 20-km SMF-28 and wireless transmission.

Then a 50/200-GHz optical interleaver with one input and four-output ports is employed to separate right first-order sideband from the optical carrier and the left first-order sideband to generate SSB-OFDM signals. The optical spectrum of the SSB-OFDM signals is shown in Fig. 6.8 inset (ii). The upper first-order sideband and other higher-order sidebands are fully suppressed. The SSB-OFDM signals are then launched into 20-km SMF-28 with an

input power of -11 dBm before the OFDM signals are detected by a high-speed PIN. The optical spectrum after transmission is shown in Fig. 6.8 inset (iii). A tunable optical filter with 3-dB bandwidth of 1 nm is used to suppress the ASE noise of the EDFA. The converted electrical signal is boosted by an electrical amplifier with 30-dBm saturation power before it is broadcasted through a double ridge guide antenna with a gain of 19.2 dBi at frequency range of 18 to 40 GHz. After wireless transmission, the signal is received by another identical antenna. The signal is down-converted through a mixer and time delay line using part of the incoming signal as the LO signal. The down-converted signals are sampled with a real-time oscilloscope (Tektronix 6154C) and processed offline. The electrical spectra of the original and down-converted signals are shown in Fig. 6.8 insets (iv) and (vi), respectively. The spectrum of the up-converted electrical signals is shown in Fig. 6.8 inset (v). It can be seen that signal-to-noise ratio of the high-frequency components of the OFDM signals in inset (vi) is little smaller, which leads to that the error of the subchannel at high frequency is large. The relatively weak response at high-frequency is caused by the imperfect response of the electrical devices, including the electrical amplifier, mixer, and antenna. The measured BER curves are shown in Fig. 6.9. The constellation figures are also inserted. One million bits are evaluated for all BER curves reported in this work. The main reason of the power penalty is the OSNR degradation arising from the 4.4-dB insertion loss of the fiber.

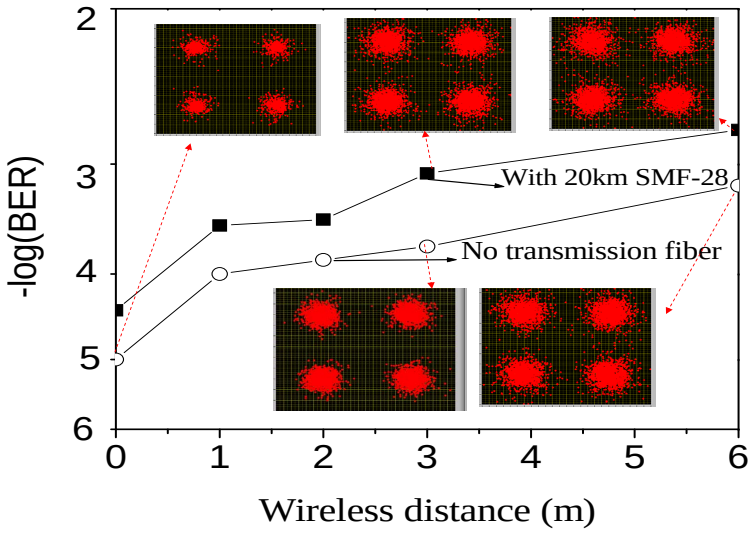

Figure 6.9: BER and constellation figures with or without transmission fiber and with different wireless distance.

6.4 Chapter summary

OFDM is the most promising modulation format for future optical-wireless access networks because it can mitigate the chromatic dispersion in the fiber as well as increasing the tolerance towards multi-path spreading. In this chapter, we show the experimental demonstrations of microwave and millimeter-wave OFDM-ROF systems with super-broadband optical-wireless signals. In the first experiment, 40-GHz optical millimeter-wave carriers are generated by using SCM and optical interleaver. 1-Gb/s OFDM data are successfully transmitted over 80-km SMF without dispersion compensation with less than 0.5-dB power penalty at a BER of 10^{-6}. In the second experiment, we demonstrate 16-Gb/s OFDM SSB signals transmission over 20-km SMF-28 fiber and 6-m wireless air distance. These results show the advantages of ROF systems using OFDM in terms of high dispersion tolerance and efficient spectrum utilization.

CHAPTER VII

OPTICAL-WIRELESS SYSTEM TESTBED DEMONSTRATION

In this chapter, the real video applications are implemented based on our developed technologies for optical millimeter-wave signal generation, transmission and processing in optical-wireless access systems. These video demonstration includes uncompressed standard-definition television (SDTV) and high-definition TV (HDTV) signals transmission over both optical fiber and air links.

7.1 Uncompressed SD/HDTV signals

The standards of HDTV and SDTV are both subsets of digital television systems. HDTV can provide high-quality video and audio entertainment than the SDTV which has different aspect ratios and formats in different parts of the world. For 4:3 aspect ratio in SDTV, the format containing 640 × 480 pixels is frequently used in those countries which follow the standard from National Television System Committee (NTSC), while the format of 720 × 576 pixels is used in the countries with Phase Alternating Line (PAL) standard. For the aspect ratio of 16:9, the 704 × 480 pixels format is used in NTSC countries, while 720 × 576 is used in PAL countries. In comparison with SDTV, HDTV has much higher resolution. There are two common formats: 1280 × 720 pixels in progressive scan mode (abbreviated 720p) and 1920 × 1080 pixels in interlace mode (abbreviated 1080i). Both of them are using 16:9 aspect ratios [145].

The three main standards defined by Society of Motion Picture and Television Engineers (SMPTE) for uncompressed HDTV and SDTV signal transmissions are SMPTE 292M, SMPTE 259M, and SMPTE 297M, respectively. SMPTE 292M defines how the video, audio, and data are transmitted in a serial manner over coaxial cable normally at 1.485-Gb/s, which is usually refer to as high-definition serial digital interface (HD-SDI). For example, in order to display high-quality video on a HDTV with the common 1080i resolution. The media server in the CO will need to transmit the video stream with 30

frames per second. Each frame has 1125 lines, each line has 2200 total pixels, each pixel is sampled by 10-bit A/D converter, and there are two channels Y and C to be transmitted. Therefore the line rate R_{HD} for HDTV video transmission can be calculated as follows

$$R_{HD} = 2200 \times 1125 \times 10 \times 30 \times 2 = 1.485 Gb/s. \tag{7.1}$$

Likewise, SMPTE 259M, which is called standard-definition serial digital interface (SD-SDI), is the standard for SDTV transmission over coaxial cables at lower data rate of 270-Mb/s. Equation (7.2) shows how the line rate is calculated for one of the 480i SDTV video display, which comprises 858 pixels per line, 525 lines per frame, 10 bits per pixel, 30 frames per second, and 2 transmission channels.

$$R_{SD} = 858 \times 525 \times 10 \times 30 \times 2 = 270 Mb/s. \tag{7.2}$$

7.2 Testbed demonstration

The designed testbed is shown in Fig. 7.1 [146]. At the CO, an analog-to-digital (A/D) converter is used to convert the analog video signal from a DVD player into the 270-Mb/s (SMPTE 259-M SDTV signal) or 1.485-Gb/s (SMPTE-292 HDTV signal) serial digital interface (SDI) signals to drive the MZM modulator for the baseband modulation.

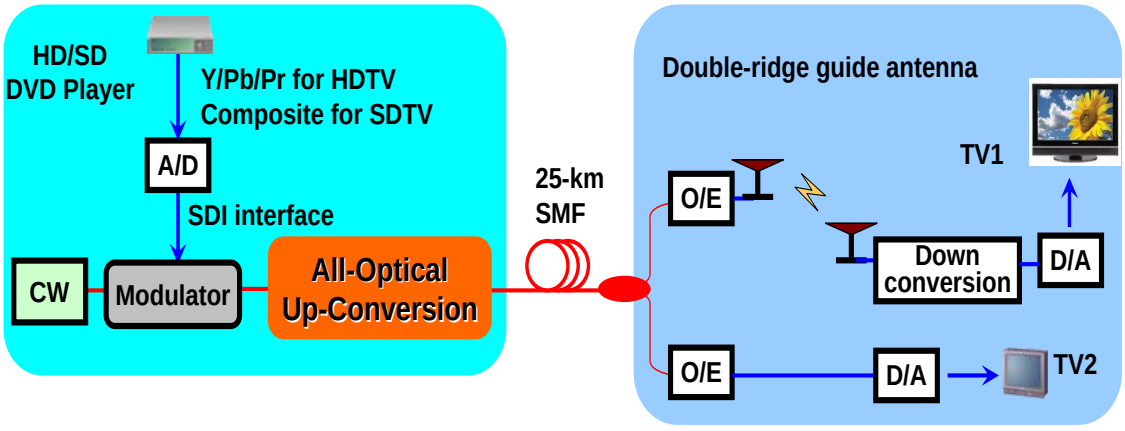

Figure 7.1: Testbed demonstration of SD/HDTV signals over optical-wireless systems.

Then, the modulated baseband signal is up-converted to millimeter-wave band using the

developed all-optical millimeter-wave generation methods. The millimeter-wave carriers at 35 GHz, 40 GHz, and 60 GHz are demonstrated based on the OCS scheme or the external phase modulation with subsequent optical filtering scheme. After transmission over 25-km SMF, the up-converted signal is sent to the BS. At the BS, the signal is split two parts for wireless and wired connections. For the wired part, O/E conversion is realized by using a low-frequency optical receiver. A digital-to-analog (D/A) converter is used to convert the SDI signal to the analog video signal for display on one TV. For the wireless part, O/E conversion is performed via a high-frequency photodetector. The converted electrical signal is then boosted by an RF low-noise electrical amplifier before it is broadcasted through a double ridge guide horn antenna. The received wireless signal from the other identical antenna is down-converted through a mixer and a LO signal. The down-converted signal is converted to analog video signal by another D/A converter and then displayed on a TV.

The photographs of the testbed and implementation environment are shown in Fig. 7.2, 7.3, and 7.4. To our knowledge, the is the first time showing uncompressed SD/HDTV signals over optical millimeter-wave wireless access systems.

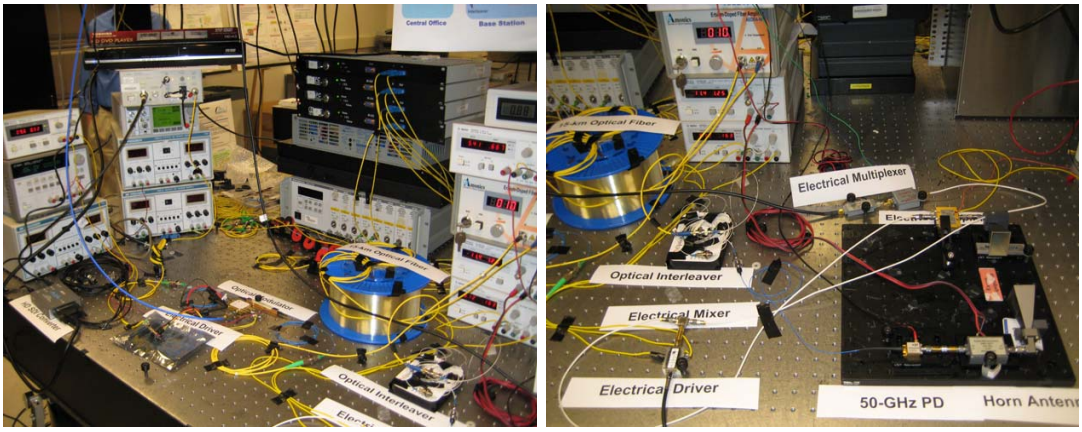

Figure 7.2: Testbed platform for the central office and base station.

Figure 7.3: The received videos on the SDTV and HDTV.

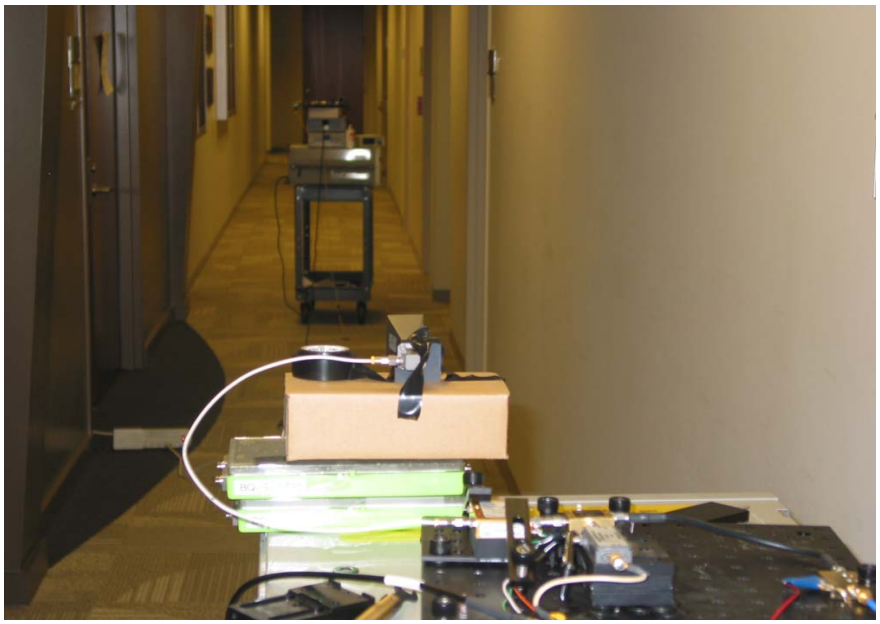

Figure 7.4: Testbed environment of office building hallway.

CHAPTER VIII

CONCLUSIONS

ROF-based optical-wireless access networks have been considered the most promising solution to increase the capacity, coverage, bandwidth, and mobility as well as decreasing cost for next-generation access networks. This hybrid system explore the converged benefits of the optical and wireless technology to serve both fixed and mobile end users.

Optical-wireless access utilizing millimeter-wave bands is an attractive way to provide higher signal bandwidth and overcome the congestion of lower-frequency bands. This is because large antenna resonance bandwidth and license-free spectrum are available for access communications. In such a system, all-optical generation, up-conversion, and transmission of high-quality millimeter-wave signals with a simple and reliable configuration are vital to successful deployment in real networks. Existing methods for optical millimeter-wave generation are not suitable for practical usefulness because of low-conversion efficiency, the requirement of high input optical power, nonlinear crosstalk effect in WDM situations, or polarization-sensitive drawbacks. In Chapter 2, six all-optical schemes for millimeter-wave up-conversion or mixing are proposed and experimentally demonstrated to solve these problems. These include the methods based on FWM and XPM in the HNL-DSF, the method based on XAM in an EAM, and the methods based on the OCS modulation or external phase modulation with optical filtering. The advantages and disadvantages of these generation and up-conversion technologies are compared based on experimental results. These results suggest that the optical millimeter-wave generation and up-conversion method based on external modulation (intensity and phase modulation) scheme shows practical advantages in terms of the low cost, simple system configuration, and high performance over long-distance transmission. These schemes will be the desirable candidates for downlink connection in full-duplex optical-wireless networks.

In addition to transparent transmission of optical millimeter-wave signals over optical

fiber, another critical issue in optical-wireless access networks is the full-duplex connection with a simple system configuration. Some schemes have been recently proposed. However, most of them only demonstrated uplink connections over short transmission distances at low frequency. The network architecture consisting of a single light source at the CO and the reuse of the downlink wavelength at the BS is an attractive solution for low-cost implementation as it requires no additional light source and wavelength management at the BS. In Chapter 3, There are three schemes that have been proposed for realizing full-duplex transmission based on wavelength reuse to avoid the need for the light source at the BS. These include up-converted DPSK for downstream and remodulated OOK for upstream, the OCS for downstream and reuse for upstream, and phase modulator with subsequent filter for downstream and directly modulated SOA for upstream. Among them, the system using one colorless SOA as both the amplifier and the modulator for the upstream signal is a practical solution for future optical-wireless access networks in terms of low cost and ease of maintenance.

Currently, wired and wireless services are separately provided by two independent physical networks. Wired networks based on FTTH access technologies provide huge bandwidth to users, but are not flexible enough to allow roaming connections. On the other hand, wireless networks offer mobility to users, but do not possess abundant bandwidth to meet the ultimate demand for multi-channel video services with HD quality. Therefore, seamless integration of wired and wireless services for future-proof access networks will lead to the convergence of ultimate high bandwidth for both fixed and mobile users in a single, low-cost transport platform. This can be accomplished by using our developed hybrid optical-wireless networks, which not only can transmit wireless signals at the BS over fiber, but also simultaneously provide the wired services to the end users. In Chapter 4, we have designed and demonstrated three super-broadband access platforms to deliver both wired and wireless services simultaneously via an optical fiber or air, and an order of magnitude larger access bandwidth than the state-of-the-art Wi-Fi systems can be provided. Our novel efficient techniques for generating and multiplexing millimeter-wave signals do not require expensive high-frequency electrical equipment. Moreover, baseband and millimeter-wave

signals can be easily separated and redistributed at the users' premises in our testbed. As a result, the single, practical optical-wireless access platform can provide future-proof information services to both stationary and mobile users.

Furthermore, to reduce the total cost and serve as many users as possible, the WDM is expected to seamlessly integrate with optical-wireless access networks. A network configuration using the OCS up to 32 channels has been proposed and experimentally demonstrated. The power penalty for all channels is less than 2 dB after 40-km SMF delivery. Meanwhile, ROADMs have become a standard part of long haul DWDM networks. Now, with the cost savings, ROADMs are expected to be deployed in metro and wide-area access networks to realize flexible optical routing in DWDM optical feeder networks. In Chapter 5, we have demonstrated the transport feasibility of super-broadband wireless signals over optical millimeter-wave (40-60 GHz) for wide-area access networks with multiple ROADMs for increasing agility and flexibility.

OFDM is the most promising modulation format for future optical-wireless access networks because it can mitigate the chromatic dispersion in the fiber as well as increasing the tolerance towards multi-path spreading. In Chapter 6, we have shown the experimental demonstrations of microwave and millimeter-wave OFDM-ROF systems with super-broadband optical-wireless signals. The experimental results show the advantages of ROF systems using OFDM in terms of high dispersion tolerance and efficient spectrum utilization. Using our developed technologies, we also successfully implements the testbed trial on the delivery of uncompressed 270-Mb/s SDTV and 1.485-Gb/s HDTV video signals over optical fiber and air links.

In this research, several key enabling technologies are identified and developed. However, there are many issues that still need to be addressed. The media access control (MAC) is a promising direction for future research. Although the analog nature of ROF links offers transparency for the transmission of the wireless protocol stack, the additional propagation delay introduced by the fiber in the end-to-end logical link connection limits the maximum fiber lengths that can be accommodated to guarantee sufficiently low latency for adequate protocol performance. Another research area would be the FDM design for optical-wireless

systems. OFDM is a good choice for wireless transmission, but the OFDM-ROF system has the stringent requirement of orthogonality between the sub-carriers. Since there are 7-GHz license-free spectrum, the traditional FDM can be used in the optical-wireless system to reduce the complexity of signal processing and increase the tolerance towards the frequency drift.

CHAPTER IX

CONTRIBUTIONS AND PUBLICATION TO DATE

Mr. Jia's graduate research has been focusing on leading-edge access networking technologies for delivering super-broadband (>1 Gb/s) symmetric wireless services over optical networks. He has pioneered optical millimeter-wave signal generation and system integration techniques for transmission of optical millimeter-wave over both fiber and air. He designed and demonstrated a super broadband access network testbed that seamlessly integrated a future-proof WDM PON and wireless access networks. He led a team, consisting of two graduate and one undergraduate students to demonstrate a powerful solution for future broadband access networks by increasing capacity and enhancing mobility as well as reducing cost in the access network. The most substantial of these contributions are the following:

- Developed six all-optical methods for millimeter-wave generation and up-conversion
- Designed 40/60-GHz optical-wireless architecture based on wavelength reuse
- Developed three technologies for simultaneously delivering wired and wireless services
- Designed ROADM-based systems for flexible optical routing and wireless control
- Established integrated testbed for SD/HDTV signals over fiber and air links

His PhD work has led to the following publications:

Journal Publications

- **Z. Jia**, J. Yu, Y.-T. Hsueh, A. Chowdhury, H.-C. Chien, J. Buck, G.-K. Chang, "Multi-band signal generation and dispersion-tolerant transmission based on photonic frequency tripling technology for 60-GHz radio-over-fiber systems," accepted by *IEEE Photon. Technol. Lett.*.

- J. Yu, **Z. Jia**, M.-F. Huang, M. Haris, P. N. Ji, T. Wang, G.-K. Chang, "Applications of 40-Gb/s chirp-managed laser in access and metro networks," submitted to *J. of Lightw. Technol.*.

- J. Yu, M.-F. Huang, **Z. Jia**, T. Wang, G.-K. Chang, "A novel scheme to generate single-sideband millimeter-wave signals by using low-frequency local oscillator signal," *IEEE Photon. Technol. Lett.*, vol.20, no.7, pp. 478-480, April 1, 2008.

- M.-F. Huang, J. Yu, **Z. Jia**, G.-K. Chang, "Simultaneous generation of centralized lightwaves and double/single sideband optical millimeter-wave requiring only low-frequency local oscillator signals for radio-over-fiber systems," to be published in *J. of Lightw. Technol.*.

- **Z. Jia**, J. Yu, G. Ellinas, G.-K. Chang, "Key enabling technologies for optical-wireless networks: optical millimeter-wave generation, wavelength reuse and architecture," *J. of Lightw. Technol.*, vol. 25, no.11, pp. 3452-3471, Nov. 2007.

- **Z. Jia**, J. Yu, A. Chowdhury, G. Ellinas, G.-K. Chang, "Simultaneous generation of independent wired and wireless services using a single modulator in millimeter-wave-band radio-over-fiber systems," *IEEE Photon. Technol. Lett.*, vol.19, no.20, pp. 1691-1693, Oct. 15, 2007.

- J. Yu, **Z. Jia**, T. Wang, G.-K. Chang, "Centralized lightwave radio-over-fiber system with photonic frequency quadrupling for high-frequency millimeter-wave generation," *IEEE Photon. Technol. Lett.*, vol.19, no.19, pp. 1499-1501, Oct. 1, 2007.

- **Z. Jia**, J. Yu, D. Boivin, M. Harris, G.-K. Chang, "Bi-directional ROF links using optically up-converted DPSK for downstream and re-modulated OOK for upstream," *IEEE Photon. Technol. Lett.*, vol.19, no.9, pp. 653-655, May 2007.

- **Z. Jia**, J. Yu and G.-K. Chang, "Chirp-managed directly-modulated DFB laser," *Recent Pat. on Eng.*, Bentham, vol.1, no.1, pp. 43-47, pp. 43-47, Feb. 2007.

- J. Yu, L. Xu, P. Ji, **Z. Jia**, Q. Yang, T. Wang, G.-K. Chang, "100-Gb/s packet signal generation with spectral efficiency larger than 1 bit/Hz/s," *IEEE Photon. Technol. Lett.*, vol.19, no.17, pp. 1310-1312, Sept. 1, 2007.

- J. Yu, O. Akanbi, Y. Luo, L. Zong, T. Wang, **Z. Jia**, G.-K. Chang, "Demonstration of a novel WDM passive optical network architecture with source-free optical network units," *IEEE Photon. Technol. Lett.*, vol.19, no.8, pp. 571-573, April 2007.

- J. Yu, **Z. Jia**, J. Yu, T. Wang, G.-K. Chang, "Novel ROF network architecture for providing wireless and wired broadband services," *Microwave Opt. Technol. Lett.*, vol.49, no.3, pp. 659-662, March 2007.

- J. Yu, **Z. Jia**, T. Wang, G.-K. Chang, "A novel radio-over-fiber configuration using optical phase modulator to generate an optical mm-wave and centralized lightwave for uplink connection," *IEEE Photon. Technol. Lett.*, vol.19, no.3, pp. 140-142, Feb. 2007.

- **Z. Jia**, J. Yu and G.-K. Chang, "A full-duplex radio-over-fiber system based on optical carrier suppression and reuse," *IEEE Photon. Technol. Lett.*, vol.18, no.16, pp. 1726-1728, Aug. 2006.

- J. Ma, J. Yu, C. Yu, **Z. Jia**, X. Sang, Z. Zhou, T. Wang and G.-K. Chang, "wavelength conversion based on four-wave mixing in high-nonlinear dispersion shifted fber using a dual-pump configuration," *J. of Lightw. Technol.*, vol.24, no.7, pp. 2851-2858, July 2006.

- J. Yu, **Z. Jia**, L. Xu, T. Wang, G.-K. Chang, "A DWDM optical mm-wave generation for ROF downstream link using optical phase modulator and optical inter-leaver," *IEEE Photon. Techno. Lett.*, vol.18, no.13, pp. 1418-1420, July 2006.

- G.-K. Chang, J. Yu, Y.-K. Yeo, A. Chowdhury, **Z. Jia**, "Enabling technologies for next generation optical core networks," *Proc. of IEEE*, vol. 94, no. 5, pp. 892-910, May 2006 (invited paper).

- J. Yu, **Z. Jia**, L. Yi, Y. Su, G.-K. Chang, T. Wang, "Optical millimeter wave generation or up-conversion using external modulators," *IEEE Photon. Technol. Lett.*, vol.18, no.1, pp. 265-267, Jan. 2006.

- **Z. Jia**, J. Yu and G.-K. Chang, "All-optical 16x2.5Gbits/s WDM signal simultaneous up-conversion based on XPM in an NOLM in ROF systems," *IEEE Photo. Technol. Lett.*, vol.17, no.12, pp. 2724-2726, Dec. 2005.

- J. Yu, **Z. Jia**, G.-K. Chang, "All-optical mixer based on cross-absorption modulation in EAM," I*EEE Photon. Technol. Lett.*, vol.17, no.11, pp. 2421-2423, Nov. 2005.

- J. Yu, J. Gu, X. Liu, **Z. Jia**, G.-K. Chang, "Seamless integration of an 8x2.5Gb/s WDM-PON and radio-over-fiber using all-optical up-conversion based on FWM," *IEEE Photo. Technol. Lett.*, vol.17, no.9, pp. 1986-1988, Sept. 2005.

Conference Presentations

- **Z. Jia**, J. Yu, Y.-T. Hsueh, H.-C. Chien, G.-K. Chang, "Demonstration of a symmetric bidirectional 60-GHz radio-over-fiber transport system at 2.5-Gb/s over a single 25-km SMF-28," *ECOC 2008*, Tu.3.F.5.

- H.-C. Chien, A. Chowdhury, **Z. Jia**, Y.-T. Hsueh, G.-K. Chang, "Long-reach, 60-GHz mm-wave optical-wireless access network using remote signal regeneration and upconversion," *ECOC 2008*, Tu.3.F.3.

- J. Yu, D. Qian, M.-F. Huang, **Z. Jia**, G.-K. Chang, T. Wang, "16Gbit/s radio OFDM signals over graded-index plastic optical fiber," *ECOC 2008*, P.6.16.

- **Z. Jia**, Y.-T. Hsueh, H.-C. Chien, A. Chowdhury, J. Yu, G.-K. Chang, "60-GHz signal generation and transmission in ROADM-based wide-area access systems," *OECC 2008* (invited paper).

- **Z. Jia**, J. Yu, L. Zong, G.-K. Chang, "Transport of 8x2.5-Gb/s wireless signals over optical millimeter wave through 12 straight-line WSSs and 160-km fiber for DWDM metro networks," *OFC/NFOEC 2008*, OMO3.

- J. Yu, J. Hu, D. Qian, **Z. Jia**, G.-K. Chang, T. Wang, "16Gbit/s Super Broadband OFDM-Radio-over-Fiber System," *OFC/NFOEC 2008*, OThP2.

- **Z. Jia**, J. Yu, D. Qian, G. Ellinas, G.-K. Chang, "Experimental demonstration for delivering 1-Gb/s OFDM signals over 80-km SSMF in 40-GHz radio-over-fiber access systems," *OFC/NFOEC 2008*, JWA108.

- J. Yu, **Z. Jia**, L. Zong, L. Xu, P. Ji, G.-K. Chang, T. Wang, "Labeled 100Gbit/s packet signals passing through 8 straight line OWSS nodes and 240km transmission fiber," *OFC/NFOEC 2008*, OThA1.

- G.-K. Chang, **Z. Jia**, J. Yu, A. Chowdhury, "Super broadband optical wireless access technologies," *OFC/NFOEC 2008*, OThD1 (invited paper).

- J. Yu, **Z. Jia**, P. Ji, T. Wang, G.-K. Chang, "40Gbit/s Centralized lightwave wavelength division multiplexed passive optical network," *OFC/NFOEC 2008*, OTuH8.

- **Z. Jia**, J. Yu, M.-F. Huang, R. L. Packham, G.-K. Chang, "Testbed demonstration and analysis for delivering dual services simultaneously in a single radio-over-fiber access platform." *MWP 2007*, Th-4.3.

- G.-K. Chang, J. Yu, **Z. Jia**, "Architectures and enabling technologies for super-broadband radio-over-fiber optical-wireless access networks," *MWP 2007* (invited paper).

- J. Yu, **Z. Jia**, T. Wang, G.-K. Chang, "Centralized lightwave radio-over-fiber system with high-frequency optical millimeter-wave generation by low-frequency and low-bandwidth optical and electrical devices," *MWP 2007*, Th-4.8.

- **Z. Jia**, J. Yu, A. Chowdhury, G. Ellinas, G.-K. Chang, "Simultaneous generation and delivery of independent wired and wireless services in radio-over-fiber systems using a single modulator," *ECOC 2007*, 3.3.2.

- M.-F. Huang, J. Yu, H.-C. Chien, A. Chowdhury, **Z. Jia**, J. Chen, S. Chi, and G.-K.

Chang, "A novel WDM PON using simultaneously generated DPSK and OOK centralized lightwaves for future multi-services in access networks." *ECOC 2007*, 10.6.4.

- J. Yu, L. Xu, P. N. Ji, **Z. Jia**, Q. Yang, T. Wang, G.-K. Chang, "100Gbit/s packet generation with spectral efficiency larger than 1bit/Hz/s by using optical carrier suppression and separation and vestigial sideband filtering techniques," *ECOC 2007*, 10.5.5.

- P. N. Ji, J. Yu, **Z. Jia**, T. Wang, X. Zheng, Y. Matsui, D. Mahgerefteh, K. McCallion, Z. F. Fan, and P. Tayebati, "Chirp-managed 42.8 Gbit/s transmission over 20 km standard SMF without DCF using directly modulated laser." *ECOC 2007*, 10.4.6.

- L. Kong, H.-C. Chien, A. Chowdhury, M.-F. Huang, Z. Jia, G.-K. Chang, "A novel bidirectional DWDM-PON using single light source for simultaneous download, upload and video selectcast services," *LEOS 2007*, ThW3.

- A. Chowdhury, **Z. Jia**, G.-K. Chang, R. Younce, "Novel 100Gbps Ethernet systems for next-generation metro transport and wide-area access networks using optical carrier suppression and separation technique," *IEEE/LEOS 2007 Summer Topical Meeting*, TuE1.2.

- **Z. Jia**, J. Yu, G. Ellinas, G.-K. Chang, "A novel full-duplex wavelength-reuse optical-wireless architecture with directly modulated SOA as upstream colorless amplified modulator," *OFC/NFOEC 2007*, OThM2.

- **Z. Jia**, J. Yu, G. Ellinas, G.-K. Chang, "Super-broadband access services delivery in optical-wireless networks," *OFC/NFOEC 2007*, NThB5.

- J. Yu, **Z. Jia**, T. Wang, G.-K. Chang, "Demonstration of a novel WDM-PON access network compatible with ROF system to provide 2.5Gb/s per channel symmetric data services," *OFC/NFOEC 2007*, OThM5.

- J. Yu, O. Akanbi, Y. Luo, L. Zong, **Z. Jia**, T. Wang, G.-K. Chang, "A novel WDM-PON architecture with centralized lightwaves in the OLT for providing triple play services," *OFC/NFOEC 2007*, OWS4.

- **Z. Jia**, J. Yu, Y.-K. Yeo, T. Wang and G.-K. Chang, "Design and implementation of a low cost, integrated platform for delivering super-broadband dual services simultaneously," *ECOC 2006*, Tu1.6.6.

- **Z. Jia**, J. Yu, G.-K. Chang, "A full-duplex radio-over-fiber system with 2.5Gbit/s data symmetric delivery over 40km SMF-28," *ECOC 2006*, Tu1.6.3.

- J. Yu, **Z. Jia**, L. Xu, T. Wang, G.-K. Chang, "A novel scheme to reduce physical layer interference in a DWDM radio-over-fiber network," *ECOC 2006*, P.148.

- **Z. Jia**, J. Yu, M. Haris, D. Boivin, G.-K. Chang, "A bi-directional radio-over-fiber system with all-optical up-converted DPSK for downstream and re-modulated OOK for upstream," *LEOS 2006*, TuV3.

- G.-K. Chang, **Z. Jia**, J. Yu, "Super broadband optical wireless over optical fiber network architecture," *LEOS 2006*, TuV1 (invited paper).

- G.-K. Chang, J. Yu, **Z. Jia** and J. Yu, "Novel optical-wireless access network architecture for simultaneously providing broadband wireless and wired services," *OFC/NFOEC 2006*, OFM1.

- J. Yu, G.-K. Chang, **Z. Jia**, L. Yi, Y. Su, T. Wang, "A ROF downstream link with optical mm-wave generation using optical phase modulator for providing broadband optical-wireless access service," *OFC/NFOEC 2006*, OFM3.

- **Z. Jia**, J. Yu and G.-K. Chang, "High-efficiency, all-optical wavelength conversion without spectrum inversion for optical switching networks," *LEOS 2005*, ThE3.

- J. Yu, **Z. Jia** and G.-K. Chang, "Seamless integration and large coverage delivery of 32x2.5Gbit/s DWDM signals in a radio-over-fiber network," *ECOC 2005*, Postdeadline Paper Th4.5.4.

- J. Yu, **Z. Jia**, Y.-K. Yeo, G.-K. Chang, "Spectrally non-inverting wavelength conversion based on FWM in HNL-DSF and its application in label switching optical network," *ECOC 2005*, P.032.

REFERENCES

[1] World Internet Usage Statistics News and World Population Stats, April, 2008. *http* : *//www.internetworldstats.com/stats.htm*.

[2] Cisco Systems, "Global IP Traffic Forecast and Methodology, 2006C2011," Jan. 2008.

[3] Cisco Systems, "The Exabyte Era," Jan. 2008.

[4] A. M. Odlyzko, "Internet traffic growth: Sources and implications," in *Proc. SPIE*: Optical Transmission systems and Equipment WDM Networking II, vol. 5427, pp.1-15, 2003.

[5] J. Mcdonough, "Moving standards to 100 Gbe and beyond," *IEEE Commun. Mag.*, vol45, no.11, pp.6-9, Nov. 2007.

[6] G.-K. Chang, A. Chowdhury, J. Yu, Z. Jia, R. Younce, "Next generation 100Gbit/s Ethernet Technologies," *APOC 2007*, Invited Paper, Wuhan China, November 2007.

[7] D. Chrissan, "Uni-DSLT: One DSL for universal service," *Texas Instruments White Paper* (Spay018), June 2004.

[8] T. Koonen, "Fiber to the home/fiber to the premises: what, where, and when?", *Proc. of IEEE*, vol. 94, no. 5, pp. 911-934, May 2006.

[9] C. Lee, W. V. Sorin, B. Y. Kim, "Fiber to the home using a PON infrastructure," *J. Lightw. Technol.*, vol. 24, no. 12, pp. 4568-4582, Dec. 2006.

[10] CableLabs, "Data Over Cable Service Interface Specifications DOCSIS 3.0, Physical Layer Specification," CM-SP-PHYv3.0-I05-070803, August, 2007.

[11] L. G. Kazovsky, W.-T. Shaw, D. Gutierrez, N. Cheng, S.-W. Wong, "Next-generation optical access networks," *J. Lightw. Technol.*, vol.25, no.11, pp.3428-3442, Nov. 2007.

[12] R. Bavey, J. Kani, F. Bourgart, K. McCammon, "Options for future optical access networks," *IEEE Commun. Mag.*, vol.44, no.10, pp.50-56, Oct. 2006.

[13] C. Bock, J. Prat, S. D. Walker, "Hybrid WDM/TDM PON using the AWG FSR and featuring centralized light generation and dynamic bandwidth allocation," *J. Lightw. Technol.*, vol. 23, no. 12, pp. 3981-3988, Dec. 2005.

[14] C. Lin, "Broadband Optical Access Networks and Fiber-to-the-Home, Systems Technologies and Deployment Strategies," *John Wiley and Sons, Ltd.*, 2006.

[15] X.Z. Qiu, Y.C. Yi, P. Ossieur, S. Verschuere, D. Verhulst, B. De Mulder, W. Chen, J. Bauwelinck, T. De Ridder, B. Baekelandt, C. Melange, J. Vandewege, "High performance burst-mode upstream transmission for next generation PONs," *Optical Fiber Communication, and Optoelectronic Exposition and Conference*, 2006.

[16] The Full Service Access Network (FSAN) Group. On-line available at *http* : *//www.fsanweb.org*.

[17] ITU-T. G.983 series: Broadband optical access systems based on Passive Optical Networks (PON). On-line available at *http* : *//www.itu.int/rec/T − REC − G/en*.

[18] ITU-T. G.984 series: Gigabit-capable Passive Optical Networks (PON). On-line available at *http* : *//www.itu.int/rec/T − REC − G/en*.

[19] IEEE 802.3 Ethernet Working Group. IEEE P802.3ah Ethernet in the First Mile. On-line available at *http* : *//www.ieee*802.*org*/3/*ah*/*index.html*.

[20] H.-C. Chien, M.-F. Huang, A. Chowdhury, J. Chen, S. Chi, G.-K. Chang, "A novel hybrid 10G/1G coexisted TDM-PON using central office controlled reflective transmitters for low-cost upstream 10G services," in *Proc. LEOS 2007*.

[21] J. Santos, J. Pedro, P. Monteiro, J. Pires, "Self-protected long-reach 10 Gbits/s EPONs based on a ring architecture," *J. Opt. Netw.*, vol. 7, no.5, pp.467-486, 2008.

[22] S.-J. Park, C.-H. Lee, K.-T. Jeong, H.-J. Park, J.-G. Ahn, K.-H. Song, "Fiber-to-the-home services based on wavelength-division-multiplexing passive optical network," *J. Lightw. Technol.*, vol. 22, no. 11, pp. 2582-2591, Nov. 2004.

[23] S.-M. Lee, K.-M. Choi, S.-G. Mun, J.-H. Moon, and C.-H. Lee, "Dense WDM-PON based on wavelength-locked Fabry-Perot laser diodes," *IEEE Photon. Technol. Lett.*, vol.17, no.7, pp.1579-1581, July 2005.

[24] C.Arellano, C. Bock, J. Prat, "RSOA-based optical network units for WDM-PON," in *Proc. OFC/NFOEC 2006*, OtuC1.

[25] L. Quinn, P. Mehta, A. Sicher, "Wireless communications technolgoy landscape," Dell White Paper, 2005.

[26] IEEE 801.15 WPAN Task Group 1 (TG1). IEEE 802.15.1 Standard for Wireless Personal Area Networks. On-line available at *http* : *//www.ieee*802.*org*/15/*pub*/*TG*1.*html*.

[27] IEEE 801.15 WPAN Task Group 3 (TG3). IEEE 802.15.3 Standard for High Rate Wireless Personal Area Networks. On-line available at *http* : *//www.ieee*802.*org*/15/*pub*/*TG*3.*html*.

[28] IEEE 801.15 WPAN Task Group 4 (TG4). IEEE 802.15.4 Standard for Low Rate Wireless Personal Area Networks. On-line available at *http* : *//www.ieee*802.*org*/15/*pub*/*TG*4.*html*.

[29] The Working Group for WLAN Standards. IEEE 802.11^{TM} Wireless Local Area Networks. On-line available at *http* : *//www.ieee*802.*org*/11/.

[30] Wi-Fi Alliance. On-line available at *http* : *//www.wi − fi.org/*.

[31] S. J. Vaughan-Nichols, "Achieving wireless broadband with WiMax," *Computer*, vol.37, no. 6, pp. 10-13, June 2004.

[32] IEEE 802.16 Working Group on Broadband Wireless Access Standards. IEEE 802.16 Wireless MAN Standard for Wireless Metropolitan Area Networks. On-line available at $http://ieee802.org/16/$.

[33] WiMAX Forum. On-line available at $http://www.wimaxforum.org/home/$.

[34] C. Andersson, "GPRS and 3G Wireless Applications," Wiley, 2001.

[35] S. K. Yong, "Multi gigabit wireless through millimeter wave in 60 GHz band," in *Proc. of Wireless Conference Asia*, Singapore, November 2005.

[36] S.-K. Yong, C.-C. Chong, "An overview of multigigabit wireless through millimeter wave technology: potentials and technical challenges," *EURASIP J. wirel. commun. netw.*, vol.2007, no.78907, pp. 1-10, 2007.

[37] N. Guo, R. Qiu, S. Mo, K. Takahashi, "60-GHz millimeter-wave radio: principle, technology, and new results,", *EURASIP J. wirel. commun. netw.*, vol.2007, no.68253, pp. 1-8, 2007.

[38] FCC, "First Report and Order," February 2002, On-line available at $http://hraunfoss.fcc.gov/edocspublic/$.

[39] J. Laskar, S. Pinel, D. Dawn, S. Sarkar, B. Perumana and P. Sen, "The next wireless wave is a millimeter wave," *Microw. J.*, vol.50, no.8, pp.22-35, August, 2007.

[40] K. Kitayama, "Architectural considerations of fiber radio millimeter wave wireless access systems," Fiber Integr. Opt. vol.19, pp. 167-186, 2000.

[41] WirelessHD, On-line available at $http://www.wirelesshd.org/$.

[42] P. Smulders, "Exploiting the 60-GHz band for local wireless multimedia access: prospects and future directions," *IEEE Commun. Mag.*, vol.40, no.1, pp. 140-147, Jan. 2002.

[43] D. Wake, "Trends and propects for radio over fiber picocells," *Proc. MWP 2002.*

[44] G.-K. Chang, Z. Jia, J. Yu, "Super broadband wireless over optical fiber network architecture," *Proc. LEOS 2006*, TuV1.

[45] W.I. Way, "Optical fibre-based microcelluar systems: an overview," *IEICE Trans. Commun.*, vol. E76-B, no.9, pp. 1078-1090, 1993.

[46] D. Wake, D. Johansson, D. G. Moodie, "Passive picocell - New in wireless network infrastructure," *Electron. Lett.*, vol.33, pp. 404-406, 1997.

[47] T. Nakasyotani, H. Toda, T. Kuri, K. Kitayama, "Wavelength-division-multiplexed millimeter-waveband radio-on-fiber system using a supercontinuum light source", *J. Lightw. Technol.*, vol. 24, no. 1, pp. 404-410, 2006.

[48] D. Wake, M. Webster, G. Wimpenny, K. Beacham, L. Crawford, "Radio over fiber for mobile communications", *MWP 2004.*

[49] A. J. Seeds, K. J. Williams, "Microwave photonics," *J. Lightw. Technol.*, vol. 24, no. 12, pp. 4628-4641, Dec. 2006.

[50] J. Yao, F. Zeng, Q. Wang, "Photonic generation of ultrawideband signals," *J. Lightw. Technol.*, vol. 25, no. 11, pp. 3219-3235, Nov. 2007.

[51] C. Lim, A. Nirmalathas, D. Novak, R. Waterhouse, G. Yoffe, "Millimeter-wave broadband fiber-wireless system incorporating baseband data transmission over fiber and remote LO delivery," *J. Lightw. Technol.*, vol. 18, no. 10, pp. 1355-1363, 2000.

[52] T. Kuri, K. Kitayama, Y. Ogawa, "Fiber-optic millimeter-wave uplink system incorporating remotely fed 60-GHz-band optical pilot tone," *IEEE Trans. on Microw. Theory and Tech.*, vol. 47, no. 7, pp. 1332-1337, 1999.

[53] L. Rosa, S. Selleri, G. Tartarini, P. Faccin, E. M. Fabbri, "Distortion performance prediction in multi-band radio over fiber systems exploiting direct laser modulation," *36th European Microwave Conference*, pp. 1292-1295, Sept. 2006.

[54] K. E. Razavi, P. A. Davies, "Millimetre wave generation by filtering the FM-IM spectra of a directly modulated DFB laser," *IEEE MTT-S Int. Microw. Symposium Digest*, vol.3, pp. 1707-1708, 1997.

[55] P. A. Rosher, M. K. Compton, A. D. Georgiou, "Dispersive consdierations in microwave optical systems," *IEE Colloquium on Microwave Optoelectronics*, London, UK, pp. 1-6, 1990.

[56] G. H. Smith, D. Novak, Z. Ahemd, "Overcoming chromatic-dispersion effects in fiber-wireless systems incorporating external modulators," *IEEE Trans. on Microw. Theory and Tech.*, vol. 45, no. 8, pp. 1410-1415, 1997.

[57] T. Kuri, K. Kitayam, A. Stohr, Y. Ogawa, "Fiber-optic millimeter-wave downlink system using 60GHz-band external modulation ," *J. Lightw. Technol.*, vol. 17, no. 5, pp. 799-806, 1999.

[58] B. Davies, J. Conradi, "Hybrid modulator structures for subcarrier and harmonic subcarrier optical single sideband," *IEEE Photon. Technol. Lett.*, vol. 10, no. 4, pp. 600-602, 1998.

[59] E. Vergnol, F. Devaux, D. Tanguy, E. Penard, "Integrated lightwave millimetric signle side-band source: design and issures," *J. Lightw. Technol.*, vol. 16, no. 7, pp. 1276-1284, 1998.

[60] K. Kitayama, T. Kuri, K. Onohara, T. Tamisaka, K. Murashima, "Dispersion effects of FBG filter and optical SSB fitlering in DWDM millimeter-wave fiber-radio systems," *J. Lightw. Technol.*, vol. 20, no. 8, pp. 1397-1407, 2002.

[61] R. P. Braun, G. Grosskopf, D. Rohde, F. Schmidt, "Low-phase noise millimeter-wave generation at 64 GHz and data transmission using optical sideband injection locking," *IEEE Photon. Technol. Lett.*, vol. 10, no. 5, pp. 728-730, 1998.

[62] L. N. Langley, M. D. Elkin, C. Edge, M. J. Wale, U. Gliese, X. Huang, A. J. Seeds, "Packaged semiconductor laser optical phase-locked loop (OPLL) for photonic generation, processing and transmission of microwave signals," *IEEE Trans. on Microw. Theory and Tech.*, vol. 47, no. 7, pp. 1257-1264, 1999.

[63] L. A. Johansson, A. J. Seeds, "Generation and transmission of millimeter-wave data-modulated optical signals using an optical injection phase-lock loop," *J. Lightw. Technol.*, vol. 21, no. 2, pp. 511-520, Feb. 2003.

[64] N. G. Walker, D. Wake, I. C. Smith, "Efficient millimeter-wave signal generation through FM-IM conversion in dispersion optical fiber links," *IEE Electron. Lett.*, vol. 28, no. 21, pp. 2027-2028, 1992.

[65] M. G. Larrode, A. M. J. Koonen, J. J. V. Olmos, "Overcoming modal bandwidth limitation in radio-over-multimode fiber links," *IEEE Photon. Technol. Lett.*, vol. 18, no. 22, pp. 2428-2430, 2006.

[66] B. Leesti, A. J. Zilkie, J. S. Aitchison, M. Mojahedi, R. H. Wang, T. J. Rotter, C. Yang, A. Stintz, and K. J. Malloy, "Broad-band wavelength up-conversion of picosecond pulses via four-wave mixing in a quantum-dash waveguide," *IEEE Photon. Technol. Lett.*, vol. 17, no. 5, pp. 1046-1048, May 2005.

[67] J.-H. Seo, Y.-K. Seo, and W.-Y. Choi, "Nonlinear characteristics of an SOA photonic frequency up-converter," *Int. Topical Meeting on Microwave Photonics*, pp. 109-112, Sept., 2003.

[68] H.-J. Song, J.-S. Lee and J.-I. Song, "Signal up-conversion by using a cross-phase-modulation in all-Optical SOA-MZI wavelength converter," *IEEE Photon. Technol. Lett.*, vol.16, no.2, pp. 593-595, Feb. 2004.

[69] O. Aso, M. Tadakuma, S. Namiki, "Four-wave mixing in optical fibers and its applications," *Furukawa Review*, 2000.

[70] J. Ma, J. Yu, C. Yu, Z. Jia, X. Sang, Z. Zhou, T. Wang, G.K. Chang, "wavelength conversion based on four-wave mixing in high-nonlinear dispersion shifted fiber using a dual-pump configuration," *J. Lightw. Technol.*, vol. 24, no. 7, pp. 2851-2858, July 2006.

[71] J. Yu, J. Gu, X. Liu, Z. Jia and G. K. Chang, "Seamless integration of an 8x 2.5Gb/s WDM-PON and Radio-Over-Fiber using all-optical up-conversion based on Raman-assisted FWM", *IEEE Photon. Technol. Lett*, vol. 17, no. 9, pp. 1986-1988, Sept. 2005.

[72] Z. Jia, J. Yu, G.-K. Chang, "High-efficiency, all-optical wavelength conversion without spectrum inversion for optical switching networks," *LEOS 2005*, ThE3.

[73] W. Wang, H. N. Poulsen, L. Rau, D. J. Blumenthal, "Regenerative 80-Gb/s fiber XPM wavelength converter using a hybrid Raman/EDFA gain-enhanced configuration," *IEEE Photon. Technol. Lett*, vol. 15, no. 10, pp. 1416-1418, Oct. 2003.

[74] D.A. Chestnut and J.R. Taylor, "Fibre optical wavelength-converter employing cross-phase modulation and low-threshold non-adiabatic Raman compression," *IEE Electron. Lett.*, vol. 39, no. 15, pp. 1133-1134, 2003.

[75] J. Yu, X. Zheng, C. Peucheret, A. T. Clausen, H. N. Poulsen, and P. Jeppesen, "All-optical wavelength conversion of short pulses and NRZ signals based on a nonlinear optical loop mirror", *J. Lightw. Technol.*, vol. 18, no. 7, pp. 1007-1017, 2000.

[76] W. Wang, H. N. Poulsen, L. Rau, H.-F. Chou, J. E. Bowers, D. J. Blumenthal, "Raman-enhanced regenerative ultrafast all-optical fiber XPM wavelength converter," *J. Lightw. Technol.*, vol. 23, no. 3, pp. 1105-1115, March 2005.

[77] Z. Jia, J. Yu, G.-K. Chang, "All-optical 16x2.5 Gbit/s WDM signals simultaneous up-conversion based on XPM in an NOLM in ROF systems," *IEEE Photon. Technol. Lett*, vol. 17, no. 12, pp. 2724-2726, Dec. 2005.

[78] C. Lim, M. Attygalle, A. Nirmalathas, D. Novak, R. Waterhouse, "Analysis of optical carrier-to-sideband ratio for improving transmission performance in fiber-radio links," *IEEE Trans. on Microw. Theory and Tech.*, vol. 54, no. 5, pp. 2181-2187, May 2006.

[79] P. S. Cho, D. Mahgerefteh, and J. Goldhar, "All-Optical 2R Regeneration and Wavelength Conversion at 20 Gb/s Using an Electroabsorption Modulator," *IEEE Photon. Technol. Lett.*, vol.11, no. 12, pp. 1662 -1664, Dec. 1999.

[80] K. Nishimura, R. Inohara, M. Usami, S. Akiba, "All-optical wavelength conversion by electroabsorption modulator," *IEEE J. Sel. Topics in Quantum Electronics*, vol. 11, no. 1, pp. 278 - 284, Jan. 2005.

[81] K. I. Kitayama and R. A. Grifin, "Optical downconversion from millimeter-wave to IF-Band over 50-km long optical fiber link using an electroabsorption modulator," *IEEE Photon. Technol. Lett.*, vol. 11, no. 2, pp. 287-289, Feb. 1999.

[82] J. Yu, Z. Jia, G.-K. Chang, "All-optical mixer based on cross-absorption modulation in electroabsorption modulator," *IEEE Photon. Technol. Lett.*, vol. 17, no. 11, pp. 2421-2423, Nov. 2005.

[83] M. Attygalle, C. Lim, G. J. Pendock, A. Nirmalathas, and G. Edvell, "transmission improvement in fiber wireless links using fiber Bragg gratings," *IEEE Photon. Technol. Lett.*, vol. 17, no. 1, pp. 190-192, Jan. 2005.

[84] A. Wiberg, P. Perez-Millan, M. V. Andres, P. A. Andrekson, P. O. Hedekvist, "Fiber-optic 40-GHz mm-wave link with 2.5Gb/s data transmission," *IEEE Photon. Technol. Lett.*, vol. 17, no. 9, pp. 1938-1940, Sept. 2005.

[85] G. H. Smith, D. Novak, Z. Ahmed, "Overcome chromatic-dispersion effects in fiber-wireless systems incorporating external modulators," *IEEE Trans. on Microw. Theory and Tech.*, vol. 45, no. 8, pp. 1410-1415, Aug. 1997.

[86] J. M. Fuster, J. Marti, J. L. Corral, V. Polo, F. Ramos, "Generalized study of dispersion-induced power penalty mitigation techniques in millimeter-wave fiber-optic links," *J. of Lightw. Technol.*, vol. 18, no. 7, pp. 933-940, July 2000.

[87] C. K. Sun, R. J. Orazi, S. A. Pappert, "Efficient microwave frequency conversion using photonic link signal mixing," *IEEE Photon. Technol. Lett.*, vol. 8, no. 1, pp. 154-156, Jan. 1996.

[88] J. Yu, Z. Jia, L. Yi, Y. Su, G.-K. Chang, T. Wang, "Optical millimeter-wave generation or up-conversion using external modulators," *IEEE Photon. Technol. Lett.*, vol. 18, no. 1, pp. 265-267, Jan. 2006.

[89] D. Wake, C. R. Lima, P. A. Davies, "Transmission of 60GHz signals over 100km of optical fiber using a dual-mode semiconductor laser," *IEEE Photon. Technol. Lett.*, vol. 8, no.4, pp. 578-580, April 1996.

[90] U. Gliese, S. Norskov, T. N. Nielsen, "Chromatic dispersion in fiber-optic microwave and millimeter-wave links," *IEEE Trans. Microw. Theory and Tech.*, vol. 44, no. 10, pp. 1716-1724 Oct. 1996.

[91] J. Yu, Z. Jia and G.-K. Chang, "Seamless integration and large coverage delivery of 32x2.5Gbit/s DWDM signals in a radio-over-fiber network," *ECOC 2005*, Postdeadline Paper Th4.5.4.

[92] G. Qi, J. Yao, et al., "Optical generation and distribution of continuously tunable millimeter-wave signals using an optical phase modulator," *J. Lightw. Technol.*, vol. 23, no. 9, pp. 2687-2695, Sept. 2005.

[93] J. Yu, Z. Jia, L. Xu, L. Chen, T. Wang, G.-K. Chang, "DWDM optical millimeter-wave generation for radio-over-fiber using an optical phase modulator and an optical interleaver," *IEEE Photon. Technol. Lett.*, vol. 18, no. 13, pp. 1418-1420, July 2006.

[94] R. Hui, B. Zhu, R. Huang, C. T. Allen, K. R. Demarest, D. Richards, "Subcarrier multiplexing for high-speed optical transmission," *J. Lightw. Technol.*, vol. 20, no. 3, pp. 417-427, March 2002.

[95] M. R. Phillips and T. E. Darcie, "Lightwave video transmission," in *Optical Fiber Telecommunications*, I. P. Kaminon and T. L. Koch, Eds. New York: Academic, 1997, vol. IIIA.

[96] A. Hirata, T. Kosugi, H. Takahashi, R. Yamaguchi, F. Nakajima, T. Furuta, H. Ito, H. Sugahara, Y. Sato, T. Nagatsuma, "120-GHz-band millimeter-wave photonic wireless link for 10-Gb/s data transmission," *IEEE Trans. Microw. Theory and Tech.*, vol. 54, no. 5, pp. 1937-1944, May 2006.

[97] T. Ismail, C. P. Liu, J. E. Mitchell, A. J. Seeds, X. Qian, A. Wonfor, R. V. Penty, I. H. White, "Transmission of 37.6-GHz QPSK wireless data over 12.8-km fiber with remote millimeter-wave local oscillator delivery using a bi-directional SOA in a full-duplex system with 2.2-km CWDM fiber ring architecture," *IEEE Photon. Technol. Lett.*, vol. 17, no. 9, pp. 1989-1991, Sep. 2005.

[98] F. Giannetti, M. Luise, R. Reggianni, "Mobile and personal communication in the 60GHz band: a survey," *Wirless Personal Communications*, vol. 10, pp. 207-243, 1999.

[99] H. Ogawa, D. Polifko, S. Banba, "Millimeter wave fiber optics systems for personal radio communication," *IEEE Trans. Microw. Theory and Tech.*, vol. 40, pp. 2285-2293, 1992.

[100] M.G. Larrode, A.M.J .Koonen, J.J.V. Olmos, A. Ng'Oma, "Bidirectional radio-over-fiber link employing optical frequency multiplication," *IEEE Photon. Technol. Lett.*, vol. 18, no. 1, pp. 265-267, Jan. 2006.

[101] W. W. Hu, K. Inagaki, T. Tanaka, T. Ohira, A. Xu, "High SNR 50 GHz radio-over-fibre uplink system by use of low biased Mach-Zehnder modulator technique," *Electon. Lett.*, vol.42, no.9, pp.550-551, April 2006.

[102] J.-H. Seo, C.-S. Choi, Y.-S. Kang, Y.-D. Chung, J. Kim, W.-Y. Choi, "SOA-EAM frequency up/down-converters for 60-GHz bi-directional radio-on-fiber systems," *IEEE Trans. Microw. Theory Tech.*, vol.54, no.2, pp. 959-966, Feb. 2006.

[103] P. J. Winzer, R.-J. Essiambre, "Advanced optical modulation format," *Proc. of the IEEE*, vol.94, no.5, pp.952-985, May 2006.

[104] Z. Jia, J. Yu, D. Boivin, M. Harris, G.-K. Chang, "Bi-directional ROF links using optically up-converted DPSK for downstream and re-modulated OOK for upstream," *IEEE Photon. Technol. Lett.*, vol.19, no.9, pp. 653-655, May 2007.

[105] Z. Jia, J. Yu, M. Haris, D. Boivin, G.-K. Chang, "A bi-directional radio-over-fiber system with all-optical up-converted DPSK for downstream and re-modulated OOK for upstream," *LEOS 2006*, TuV3.

[106] Z. Jia, J. Yu, G.-K. Chang, "A full-duplex radio-over-fiber system with 2.5Gbit/s data symmetric delivery over 40km SMF-28," *ECOC 2006*, Tu1.6.3.

[107] Z. Jia, J. Yu and G.-K. Chang, "A full-duplex radio-over-fiber system based on optical carrier suppression and reuse," *IEEE Photon. Technol. Lett.*, vol.18, no.16, pp. 1726-1728, Aug. 2006.

[108] J. Yu, Z. Jia, T. Wang, G.-K. Chang, "A novel radio-over-fiber configuration using optical phase modulator to generate an optical mm-wave and centralized lightwave for uplink connection," *IEEE Photon. Technol. Lett.*, vol.19, no.3, pp. 140-142, Feb. 2007.

[109] Z. Jia, J. Yu, G. Ellinas, G.-K. Chang, "A novel full-duplex wavelength-reuse optical-wireless architecture with directly modulated SOA as upstream colorless amplified modulator," *OFC/NFOEC 2007*, OThM2.

[110] J.-H. Moon, K.-M. Choi, S.-G. Mun, and C.-H. Lee, "Effects of back-reflection in WDM-PONs based on seed light injection," *IEEE Photon. Technol. Lett.*, vol.19, no.24, pp. 2045-2047, Dec. 2007.

[111] G.-K. Chang, J. Yu, Z. Jia, J. Yu, "Novel optical-wireless access network architecture for simultaneously providing broadband wireless and wired services," *OFC/NFOEC 2006*, OFM1.

[112] Z. Jia, J. Yu, Y.-K. Yeo, T. Wang and G.-K. Chang, "Design and implementation of a low cost, integrated platform for delivering super-broadband dual services simultaneously," *ECOC 2006*, Tu1.6.6.

[113] A. Martinez, V. Polo, and J. Marti, "Simultaneous baseband and RF optical modulation scheme for feeding wireless and wireline heterogeneous access network," *IEEE Trans. Microw. Theory Technol.*, vol. 49, no. 10, pp. 2018C2024, Oct. 2001.

[114] Z. Jia, J. Yu, M.-F. Huang, R. L. Packham, G.-K. Chang, "Testbed demonstration and analysis for delivering dual services simultaneously in a single radio-over-fiber access platform." *MWP 2007*, Th-4.3.

[115] T. Kamisak, T. Kuri, K. Kitayama, "Simultaneous modulation and fiber-opti transmission of 10-Gb/s baseband and 60-GHz-band radio signals on a single wavelength," *IEEE Trans. Microw. Theory Tech.*, vol. 49, no. 10, pp. 2013-2017, Oct. 2001.

[116] K. Ikeda, T. Kuri, K. Kitayama, "Simultaneous three-band modulation and fiber-optic transmission of 2.5-Gb/s baseband, microwave-, and 60-GHz-band signals on a single wavelength," *J. Lightw. Technol.*, vol. 21, no.12, pp. 3194-3202, Dec. 2003.

[117] M. Bakaul, A. Nirmalathas, C. Lim, D. Novak, R. Waterhouse, "Hybrid multiplexing of multiband optical access technologies towards an integrated DWDM network," *IEEE Photon. Technol. Lett.*, vol. 18, no.21, pp. 2311-2313, Nov. 2006.

[118] C.-T. Lin, J. Chen, P.-C. Peng, C.-F. Peng, W.-R. Peng, B.-S. Chiou, S. Chi, "Hybrid optical access network integrating fiber-to-the-home and radio-over-fiber systems," *IEEE Photon. Technol. Lett.*, vol. 19, no.8, pp. 610-612, April 2007.

[119] C. Lim, A. Nirmalathas, D. Novak, R. Waterhous, G. Yoffe, "Millimeter-wave broadband fiber-wireless system incorporating baseband data transmission over fiber and remote LO delivery," *J. Lightw. Technol.*, vol. 18, no.10, pp. 1355-1363, Oct. 2000.

[120] Z. Jia, J. Yu, A. Chowdhury, G. Ellinas, G.-K. Chang, "Simultaneous generation of independent wired and wireless services using a single modulator in millimeter-wave-band radio-over-fiber systems," *IEEE Photon. Technol. Lett.*, vol.19, no.20, pp. 1691-1693, Oct. 15, 2007.

[121] Z. Jia, J. Yu, A. Chowdhury, G. Ellinas, G.-K. Chang, "Simultaneous generation and delivery of independent wired and wireless services in radio-over-fiber systems using a single modulator," *ECOC 2007*, 3.3.2.

[122] C. Lim, A. Nirmalathas, K.-L. Lee, D. Novak, and R. Waterhouse, "Intermodulation distortion improvement for fiber-radio applications incorporating OSSB+C modulation in an optical integrated-access environment," *J. Lightw. Technol.*, vol. 25, no.6, pp.1602-1612, June 2007.

[123] J. Yu, M.-F. Huang, Z. Jia, T. Wang, and G.-K. Chang, "A novel scheme to generate single-sideband millimeter-wave signals by using low-frequency local oscillator signal," *IEEE Photon. Technol. Lett.*, vol. 20, no.7, pp. 478-480, April 2008.

[124] A. Wiberg, B. -E. Olsson, P. O. Hedekvist, and P. A. Andrekson, "Dispersion-tolerant millimeter-wave photonic link using polarization-dependent modulation," *J. Lightw. Technol.*, vol. 25, no.10, pp. 2984-2991, Oct. 2007.

[125] C. Lim, A. Nirmalathas, D. Novak, R. Waterhouse, "Capacity analysis for WDM fiber-radio backbones with star-tree and ring architecture incorporating wavelength interleaving," *J. Lightwave Technol.*, vol. 21, no. 12, pp.3308-3314, 2003.

[126] Infonetics Research, "ROADM evolves: should you be paying attention?" *white paper*, 2006.

[127] M. Kuznetsov, N. M. Froberg, S. R. Henion, H. G. Rao, J. Korn, K. A. Rauschenbach, E. H. Modiano and V. W. S. Chan, "A next-generation optical regitional access network," *IEEE Commun. Mag.*, pp. 66-72, Jan. 2000.

[128] Y. J. Chen, "Different aspects and design considerations of PLC based ROADM/WSS," *OFC/NFOEC 2007*, Anaheim.

[129] L. Zong, X. Huang, T. Wang, P. Ji, O. Matsuda, M. Cvijetic, "A novel tunable DeMUX/MUX solution for WSS-based ROADM and WXC Nodes," *OFC/NFOEC 2006*, NThE2.

[130] B. Clouet, B. Le Guyader, S. Lobo, F. Merlaud, J. C. Simon, T. Ducellier, "Cascadability study of 16 1x9 wavelength selective switches with 5x52.6 Gb/s CS-RZ channels," *ECOC 2005*, We4.P.117.

[131] Z. Jia, J. Yu, L. Zong, G.-K. Chang, "Transport of 8x2.5-Gb/s wireless signals over optical millimeter wave through 12 straight-line WSSs and 160-km fiber for DWDM metro networks," *OFC/NFOEC 2008*, OMO3.

[132] Z. Jia, Y.-T. Hsueh, H.-C. Chien, A. Chowdhury, J. Yu, G.-K. Chang, "60-GHz signal generation and transmission in ROADM-based wide-area access systems," *OECC 2008*.

[133] R. Prasad, OFDM for Wireless Communications Systems, *Artech House Publication*, 2004.

[134] J.G. Proakis and M. Salehi, Essentials of Communications Systems Engineering, Chapter 11, *Prentice Hall*, 2005.

[135] S. L. Jansen, I. Morita, N. Takeda, H. Tanaka, "20-Gb/s OFDM transmission over 4,160-km SSMF enabled by RF-pilot tone phase noise compensation," *OFC 2007*, PDP 15.

[136] A. J. Lowery, L. B. Du, and J. Armstrong, "Performance of optical OFDM in ultralong-haul WDM lightwave systems," *J. Lightwave Technol.*, vol. 25, no. 1, pp.131-138, Jan. 2007.

[137] B. J. Dixon, R. D. Pollard, and S. Iezekiel, "Orthogonal frequencydivision multiplexing in wireless communication systems with multimode fiber feeds," *IEEE Trans. Microw. Theory Tech.*, vol. 49, no. 8, pp. 1404-1409, Aug. 2001.

[138] W. Shieh, X. Yi, and Y. Tang, "Transmission experiment of multi-gigabit coherent optical OFDM systems over 1000 km SSMF fibre," *Electron. Lett.*, vol. 43, no. 3, pp. 183-184, 2007.

[139] S. L. Jansen, I. Morita, T. C. W. Schenk, N. Takeda, and H. Tanaka, "Coherent optical 25.8-Gb/s OFDM transmission over 4160-km SSMF," *J. Lightwave Technol.*, vol. 26, no. 1, pp.6-15, Jan. 2008.

[140] H. Sasa, T. Niiho, K. Tanaka, K. Utsumi and S. Morikura, "Radio-over-fiber transmission performance of OFDM signal for dual-band wireless LAN systems," *MWP 2003*, pp. 139-142.

[141] A. Kim, Y. Joo and Y. Kim, "60GHz wireless communication systems with radio-over-fiber links for indoor wireless LANs," *IEEE Trans. Consum. Electron.*, vol. 50, no. 2, pp.517-520, 2004.

[142] Z. Jia, J. Yu, D. Qian, G. Ellinas, G.-K. Chang, "Experimental demonstration for delivering 1-Gb/s OFDM signals over 80-km SSMF in 40-GHz radio-over-fiber access systems," *OFC/NFOEC 2008*, JWA108.

[143] J. Yu, J. Hu, D. Qian, Z. Jia, G.-K. Chang, T. Wang, "16Gbit/s Super Broadband OFDM-Radio-over-Fiber System," *OFC/NFOEC 2008*, OThP2.

[144] G.-K. Chang, Z. Jia, J. Yu, A. Chowdhury, "Super broadband optical wireless access technologies," *OFC/NFOEC 2008*, OThD1.

[145] National Telecommunications and Information Administration (NTIA) (Feb. 2006). PUBLIC LAW 109-171: Digital Television Transition and Public Safety. On-line available at $http://www.ntia.doc.gov/otiahome/dtv/index.html$

[146] Z. Jia, J. Yu, G. Ellinas, G.-K. Chang, "Key enabling technologies for optical-wireless networks: optical millimeter-wave generation, wavelength reuse and architecture," *J. of Lightw. Technol.*, vol. 25, no.11, pp. 3452-3471, Nov. 2007.

VITA

Zhensheng Jia was born in Tianjin, China, in 1976. He received the B.E. and M.S.E degree in Physical Electronics and Optoelectronics from the Electronic Engineering Department, Tsinghua University, Beijing, China, in 1999 and 2002, respectively. His master thesis dealt with optical label processing technologies in optical label swapping networks. From 2002 to 2004, he worked as a Research Engineer on transport and access networks in the Optical System and Network Lab, China Telecom Beijing Research Institute (CTBRI), where he was responsible for DWDM systems over ultra-long haul optical links in China Telecom's optical backbone networks.

In August 2004, Jia joined the Optical Networking Research Group in the School of Electrical and Computer Engineering at Georgia Institute of Technology, where he has conducted research toward the Ph.D. degree in the field of super-broadband optical-wireless access networks. He spent two summer internships working on the projects of the design of the chirp-controlled direct modulated transmitter and optical equalizers for metro optical links at NEC Laboratories, America in summer 2006 and 2007. He has been author or co-author of over 50 peer-reviewed journal articles and conference papers. He also serves as an active reviewer for *IEEE Photonics Technology Letters*, *IEEE/OSA Journal of Lightwave Technology*, *IEEE Microwave and Wireless Components Letters*, *IET Optoelectronics*, *Optical Express*, and *Optics Communications*.

Jia's research results have been featured in Georgia Tech Research News in March 2006, and have been selected as one of four Scientific Highlights of *OFC/NFOEC 2008*. His work has been recognized with the *IEEE/LEOS 2007 Graduate Student Fellowship Award*, awarded by the IEEE Lasers and Electro-Optics Society, *2008 Bor-Uei Chen Memorial Scholarship Award*, awarded by Photonics Society of Chinese-Americans, and *2008 ECE Graduate Research Assistant Excellence Award*, awarded by School of Electrical and Computer Engineering, Georgia Institute of Technology.